2012

Kinetic Studies on Lactonization of Quinone Propionic Acid Derivatives for the Development of Redox Responsive Liposomes

K. L. Iresha Sampathi Perera
Louisiana State University and Agricultural and Mechanical College, kperer4@lsu.edu

KINETIC STUDIES ON LACTONIZATION OF QUINONE PROPIONIC ACID DERIVATIVES FOR THE DEVELOPMENT OF REDOX RESPONSIVE LIPOSOMES

A Thesis

Submitted to the Graduate Faculty of the
Louisiana State University and
Agricultural and Mechanical College
in partial fulfillment of the
requirements for the degree of
Master of Science

In

The Department of Chemistry

by
K. L. Iresha Sampathi Perera
B.S., University of Colombo, 2008
August 2012

This thesis is dedicated to my parents

ACKNOWLEDGEMENTS

I take immense pleasure in thanking my advisor Professor Robin L. McCarley, for his valuable guidance, patience and time through my entire period of graduate studies at Louisiana State University. Without his close guidance, I would not have completed my graduate studies at LSU. It is a huge privilege for me to work under such an elite professor. I also thank my graduate advisory committee, Professor Graca Vicente and Professor John Pojman for being a part of my graduate committee and being so generous in devoting their valuable time for my queries.

I would like to thank McCarley research group for their invaluable support. The group has been a source of friendship as well as good advice. I wish each and every one of you the very best in your future endeavors. To Dr. Elizabeta Mitran and Dr. Fabiana Mendoza, thank you for proof-reading my documents and offering me valuable advice. I will always remember your encouraging words. My acknowledgement would be incomplete without a word on Dr. Sreelatha Balamurugan. I am utterly grateful to her for sharing ideas and prior experience on the research which made my uphill task much easier. You are like a second mom to me.

I am also grateful to the Department of Chemistry for providing me unrestricted facilities during my entire course of study. I would like to convey my sincere gratitude to Dr. W. Dale Treleaven and Dr. Thomas Weldegheorghis for helping me with NMR studies.

I take this opportunity to convey my special thanks to Pramuditha Abhayawardhana, Waruna Jinadasa, Chamini Karunarathna, Udaya Rodrigo, Benson Edgawa, and Indika Galapothdeniya for motivating me and supporting me in my academic life as well as in my personal life. I am truly fortunate to be around such great friends during my stay at LSU. I wish that you all may achieve success in everything you do in future.

Finally, my humble gratitude to my parents and my husband for being excessively supportive and standing by me at every step of the way. This whole journey would not have been possible without your love and support.

TABLE OF CONTENTS

DEDICATION……...ii

ACKNOWLEDGEMENT ……....iii

LIST OF TABLES ……....vii

LIST OF FIGURES ……....viii

LIST OF SCHEMES ……....x

LIST OF ABBREVIATIONS AND SYMBOLS ……....xi

ABSTRACT. ……....xiv

CHAPTER 1. INTRODUCTION 1
1.1 Research Goals and Aims .... ……...1
1.2 Nanoparticle Drug Delivery Systems ... ……..3
1.2.1 Motivation ..... ……3
1.2.2 Types of Engineered Nanoparticles in Drug delivery……... 5
1.3 Rate Enhancement in Trimethyl-lock induced lactonization 8
1.3.1 Applications of the Trimethyl-lock System……. 10
1.4 Redox-Responsive Quinone Trimethyl-lock Liposome Delivery System..... 12
1.5 References..... 15

CHAPTER 2. SYNTHESIS AND CHARACTERIZATION OF QUINONE COMPOUNDS 20
2.1 Syntheses..... 20
2.1.1 Chemicals and General Methods..... 20
2.2 Synthetic Routes 20
2.3 Experimental Details..... 21
2.3.1 Synthetic Procedures for compounds 2a-f, 4, 5 and 7..... 21
2.4 Summary 25
2.5 Spectral Data..... 26
2.6 References..... 37

CHAPTER 3. KINETIC STUDIES ON LACTONIZATION OF QUINONE PROPIONIC ACID AMIDE DERIVATIVES BY ^{1}H NMR FOR DEVELOPMENT OF REDOX-ACTIVE LIPOSOMES 38
3.1 Introduction..... 38
3.2 Experimental Section……42
3.2.1 Materials..... 42
3.2.2 Sodium Dithionite ($Na_2S_2O_4$) Purification..... 42
3.2.3 Deuterated Buffer Preparation 43

3.2.4 Instrumentation 43
3.2.4.1 Nuclear Magnetic Resonance Spectroscopy (NMR) 43
3.2.5 General Procedure for Sample Preparation 43
3.2.5.1 D_2O as Solvent 43
3.2.5.2 DMSO-D_2O as Solvent 44
3.3 Results and Discussion 44
3.3.1.1 Effect of Functional Group 44
3.3.1.2 Effect of Organic Solvents 52
3.3.1.3 Effect of Temperature 54
3.3.1.4 Effect of Buffer Conditions 55
3.3.2 Lactonization Behavior of Q_{Me}-COOH 57
3.3.3 Lactonization Behavior of Other Q_{Me}-Amide Derivatives 60
3.4 Conclusion 67
3.5 References 69

CHAPTER 4. CONCLUSIONS AND OUTLOOK 72
4.1 Summary 72
4.2 Conclusion 74
4.3 Outlook 74
4.4 References 75

VITA 77

LIST OF TABLES

Table 3.1 Kinetic results for Q_{Me}-ETA lactonization in D_2O medium at different temperatures. Only one replicate obtained in each case 55

Table 3.2 Kinetic data for Q_{Me}-ETA lactonization in 0.1 M phosphate buffer conditions 57

Table 3.3 Summary of kinetic Evaluation. 68

LIST OF FIGURES

Figure 1.1 Mechanism of Q-DOPE liposome destabilization (representation by Dr. N. H. Carrier) 13

Figure 1.2 Calcein release profiles (normalized) of various Q-DOPE liposomes as determined by fluorescence emission spectroscopy (λ_{ex}=490 nm, λ_{em} = 515 nm). Each trace represents the typical release behavior observed for each Q-DOPE liposome composition 14

Figure 3.1 Amide derivative of trimethyl-lock quinone propionic acid 41

Figure 3.2 Parent lipid structures a) Q-DOPE b) Q-AQM-DOPE used for liposome formation 41

Figure 3.3 Ferrocene salt, internal standard used for ^{1}H NMR experiments 42

Figure 3.4 Time-dependent Q_{Me}-ETA (3.8×10^{-3} M) lactonization in pure D_2O by ^{1}H NMR. The signals at δ 2.85 ppm and 4.20–4.50 ppm are associated with the internal 45

Figure 3.5 Confirmation of Q_{Me}-lactone (4.8×10^{-3} M) precipitation in pure D_2O by ^{1}H NMR. The signals at δ 2.85 ppm and 4.20–4.50 ppm are associated with the internal standard 46

Figure 3.6 Kinetic evaluations of Q_{Me}-ETA lactonization in pure D_2O medium 47

Figure 3.7 Time-dependent Q_{Br}-ETA (3.16×10^{-3} M) lactonization in pure D_2O by ^{1}H NMR. The signals at δ 2.85 ppm and 4.20–4.50 ppm associated with the internal standard 48

Figure 3.8 Time-dependent Q_{NMe}-ETA (3.80×10^{-3} M) lactonization in pure D_2O by ^{1}H NMR. The signals at δ 3.00 ppm and 4.30–4.60 ppm associated with the internal standard 48

Figure 3.9 Time-dependent Q_{NPr}-ETA (3.02×10^{-3} M) lactonization in pure D_2O by ^{1}H NMR. The signals at δ 3.00 ppm and 4.30–4.60 ppm associated with the internal standard. The signals denoted as asterisks indicate the residual solvents that remain from the purification. 49

Figure 3.10 Time-dependent Q_H-ETA (4.7×10^{-3} M) lactonization in pure D_2O by ^{1}H NMR. The signals at δ 2.85 ppm and 4.20–4.50 ppm associated with the internal standard. Asterisk (*****) and (**x**) represent the increasing and decreasing signals respectively 50

Figure 3.11 Spectral comparison of Q_H-ETA in (a) $CDCl_3$ and (b) D_2O medium. Asterisk (*) at 4.65ppm in spectrum (b) represents the noise peak 51

Figure 3.12 Spectral comparison of Q_H-COOH in (a) $CDCl_3$ and (b) D_2O medium.....52

Figure 3.13 Time-dependent Q_{Me}-ETA lactonization in a 5:2 mixture of DMSO: D_2O by ^1H NMR in the absence of internal standard. (*) denotes the impurities from medium.....53

Figure 3.14 Time-dependent Q_{Me}-ETA (1.7×10^{-2} M) lactonization in a 5:2 mixture of DMSO: D_2O by ^1H NMR in the presence of internal standard. Both (*) & (x) denote the impurities from medium 53

Figure 3.15 Kinetic evaluations of Q_{Me}-ETA lactonization in a 5:2 mixture of DMSO:D_2O.....54

Figure 3.16 Kinetic evaluations of Q_{Me}-ETA lactonization in D_2O medium at a) 10 °C (3.6×10^{-3} M), b) 25°C (3.8×10^{-2} M), and c) 35 °C (4.3×10^{-2} M) 56

Figure 3.17 Kinetic evaluation of Q_{Me}-ETA lactonization in 0.1 M, pD 7.41 phosphate buffer medium; three replicates are shown. 58

Figure 3.18 Kinetic evaluation of Q_{Me}-ETA lactonization in 0.1 M, pD 7.21 phosphate buffer medium; three replicates are shown. 59

Figure 3.19 Time-dependent Q_{Me}-COOH (4.3×10^{-3} M) lactonization in D_2O medium by ^1H NMR. The signals at δ 3.00 ppm and 4.30–4.60 ppm associated with the internal standard….....60

Figure 3.20 Time dependent Q_{Me}-COOH (4.7×10^{-3} M) lactonization in 0.1 M phosphate buffer at pD 7.41 by ^1H NMR. The signals at δ 3.00 ppm and 4.30–4.60 ppm associated with the internal standard… 61

Figure 3.21 Time-dependent, Q_{Me}-NMeBnOH (4.1×10^{-3} M) lactonization in a 5:2 mixture of DMSO: D2O medium by ^1H NMR in the absence of internal standard….....62

Figure 3.22 Time-dependent Q_{Me}-NN (2.4×10^{-3} M) lactonization in a 5:2 mixture of DMSO: D_2O medium by a) ^1H NMR region of 0.00– 5.50 ppm b) region of 7.50–9.75 ppm… 64

Figure 3.23 Spectral variations of Q_{Me}-MeETA in different solvents A) DMSO, B) $CDCl_3$, and C) D_2O… 65

Figure 3.24 Time-dependent Q_{Me}-NMeETA (1.3×10^{-3} M) lactonization in pure D_2O medium by ^1H NMR. The signals at δ 2.90 ppm and 4.20–4.45 ppm associated with the internal standard 66

Figure 3.25 Kinetic evaluation of Q_{Me}-MeETA (1.3×10^{-3} M) lactonization in pure D_2O medium 66

LIST OF SCHEMES

Scheme 1.1 Mechanism of ortho-hydroxycinnamic acid lactonization 8

Scheme 1.2 Schematic representation of lactonization for quinone propionic acid derivatives 10

Scheme 2.1 Synthesis of succinimidyl ester of *N*-methylamino quinone propionic acid 20

Scheme 2.2 Synthesis of quinone propionic acid ethanolamine derivatives 21

Scheme 2.3 Synthesis of quinone propionic acid 4-(*N*-methylamino)phenol derivative 21

Scheme 3.1 General mechanism of trimethyl-lock quinone lactonization. 40

Scheme 3.2 Possible degradation routes of Q_H-ETA in aqueous condition in the absence of a reducing agent 50

Scheme 3.3 Mechanism of Q_{Me}-NN disconnection after reduction 63

LIST OF ABBREVIATIONS AND SYMBOLS

APIs	Active pharmaceutical ingredients
FDA	Food and Drug Administration
PEG	Poly(ethylene glycol)
MPS	Mononuclear phagocyte system
ADME	Absorption, Distribution, Metabolism, and Excretion
RES	Reticuloendothelial system
IgG	Immunoglobulin G
C3b	Complement component 3.
HIV	Human immunodeficiency virus
DNA	Deoxyribonucleic acid
CMC	Critical micelle concentration
EPR	Enhanced Permeation and Retention (effect)
$sPAL_2$	Secretory phospholipase A_2
MMP	Matrix metalloproteinase
PPI	Poly(propylene imine)
DOPE	Dioleoylphosphatidylethanolamine
Q-DOPE	Quinone-dioleoylphosphatidylethanolamine
hNQO1	Human NAD(P)H:quinone oxidoreductase type 1
HT29	Colorectal adenocarcinoma cells
A549	Adenocarcinomic human alveolar basal epithelial cells
L_α	Lamellar phase
H_{II}	Hexagonal phase

Q_{Me}-DOPE	Methyl-substituted Q-DOPE
Q_{Br}-DOPE	Bromine-substituted Q-DOPE
Q_{nPrNH}-DOPE	*N*-(Propyl)amino-substituted Q-DOPE
Q_{H}-DOPE	Hydrogen-substituted Q-DOPE
TLC	Thin layer chromatography
ESI	Electrospray ionization
ESI-MS	Electrospray ionization-mass spectrometry
L1210, P338	Murine leukemia
A431	Human squamous cell carcinoma
BT-474	Human breast cell carcinoma
Q-ETA	Quinone-ethanolamine
Q-MeETA	Quinone-methylethanolamine
Q-NMeBnOH	Quinone-methylaminophenol
NMR	Nuclear magnetic resonance
^{1}H NMR	Proton Nuclear magnetic resonance
Q-AQM-DOPE	Quinone-azaquinonemethide-dioleoylphosphatidylethanolamine
d_6-DMSO	Deuterated dimethylsulfoxide
MeOH	Methanol
Q_{Me}-ETA	Methyl-substituted Q-ETA
Q_{Br}-ETA	Bromine-substituted Q-ETA
Q_{NMe}-ETA	*N*-(Methyl)amino-substituted Q-ETA
Q_{H}-ETA	Hydrogen-substituted Q-ETA
Q_{NPr}-ETA	*N*-(Propyl)amino-substituted Q-ETA

Q_{Me}-ETA_{Tet}	Tetrahedral intermediate of methyl-substituted Q-ETA
Q_H-COOH	Hydrogen-substituted quinone propionic acid
CV	Cyclic voltammetry
k	Rate constant
$t_{1/2}$	Half-life
Q_{Me}-COOH	Methyl-substituted quinone propionic acid
Q_{Me}-NMeBnOH	Methyl-substituted Q-NMeBnOH
Q_{Me}-MeETA	Methyl-substituted Q-MeETA
HOAC	Acetic acid
NHS	*N*-hydroxysuccinimide
DCC	Dicyclohexylcarbodiimide
THF	Tetrahydrofuran
DCM	Dichloromethane
DIEA	*N*,*N*-Diisopropylethylamine
DMF	Dimethylformamide
EtOAC	Ethylacetate
HATU	*O*-(7-Azabenzotriazol-1-yl)-*N,N,N′,N′*-tetramethyluronium hexafluorophosphate

ABSTRACT

Stimuli-responsive liposome systems that utilize endogenous triggers of tumor microenvironment have generated great attention in recent drug delivery research. Among such formulations, redox-responsive liposomes seem highly promising for cancer treatment due to their potential to release high drug concentrations upon reduction (by reductase enzymes).

The research described in this thesis involved the evaluation of kinetics of trimethyl-lock quinone propionic acid reduction and lactonization, which accounts for payload release from trimethyl-lock quinone propionic acid-decorated liposomes. To achieve the ultimate goal of this research, several trimethyl-lock quinone propionic acid-based amide compounds were synthesized and characterized. Kinetic studies were carried out with ^{1}H NMR spectroscopy under different experimental conditions, and time-resolved ^{1}H NMR spectra were used to evaluate the kinetic rate constant (k) and half-life time ($t_{½}$) values for the lactonization (cyclization) reaction.

Upon reduction, five different quinone ring-substituted quinone propionic acid-ethanolamine derivatives have shown distinct cyclization rates, representing the influence of ring substituent on lactonization. Tertiary amides, and organic solution conditions, slow down the cyclization process, whereas buffer conditions and higher temperature enhanced the trimethyl-lock lactonization. The outcome of this research can be utilized to optimize redox-responsive trimethyl-lock quinone propionic acid based liposomes, as well as other effective target delivery systems, in order to achieve efficient payload release.

CHAPTER 1
INTRODUCTION

1.1 Research Goals and Aims

The goal of this research is an investigation of the kinetics associated with the reduction and lactonization of trimethyl-lock quinone propionic acid derivatives for potential application in liposome drug delivery systems. In particular, kinetics of quinone reduction followed by its lactone formation with different amide structures, as well as substituents on the quinone ring, under various experimental conditions (temperature, pH, buffer, and solvent) will be investigated.

After the discovery of spontaneous formation of closed bilayered structures of phospholipids in aqueous medium by Alec Bangham, liposomes have developed enormously due to their versatile supramolecular architecture.[1-3] They have piqued an extensive interest during the last decades as a pharmaceutical carrier because of their attractive biological properties, such as biocompatibility, low toxicity, biodegradability, and amphiphilicity.[3] In addition, their amphiphilic architecture provides the opportunity to enclose both hydrophobic and hydrophilic active pharmaceutical ingredients (API).[1] In 1995, the U.S. Food and Drug Administration (FDA) approved the first liposomal drug formulation, Doxil, doxorubicin encapsulated in poly(ethyleneglycol), PEG, liposomes, for the treatment of Kaposi sarcoma and eventually it was accepted for ovarian, and metastatic breast cancers.[1,4] Since then, several liposomal drug formulations were developed and introduced to the market. To date, 11 liposomal drug formulations have been clinically accepted and 6 more are under clinical evaluation.[4] Moreover, liposomal applications are well established in several other areas, including gene delivery, sensors, immunoassays, microfluidics, and separations etc.[2,5-7]

At present, conventional liposomes are used in some therapeutic applications, but their utility is problematic due to their instability, inefficient drug accumulation, and harmful toxic side effects to normal healthy tissues.[8] Furthermore, they encounter fast elimination from the blood stream and are captured by the mononuclear phagocyte system (MPS) before entering the target site.[1,9] In order to thwart these issues, research has been moved a long way to develop novel liposomal frameworks which can be optimized to have an efficient targeting and payload release. To date, several new liposomes have been developed, but they still carry limitations, such as stability and toxicity. Nevertheless, efforts continue to be made to optimize these systems.[1,3,10]

One possible method that can be used to achieve selective targeting and efficient drug accumulation involves the development of stimuli-responsive liposomal system by using environmental triggers that are prominent at the targeted site of delivery. In response to the internal stimulus, they are expected to release their cargo in a selective and controllable manner, thereby improving drug efficacy and minimizing side effects.[1,3,8,11,12] To date, the McCarley research group has developed a redox-triggerable liposome system based on a trimethyl-lock quinone propionc acid attached to a lipid. This liposome system dissembles upon reduction of the trigger moiety (quinone) that provokes the subsequent lipid detachment to release of liposome payload to the external environment.[8,11,12] However, the kinetics of trigger disintegration from the lipid remains unexplored under different buffer, pH, solvent, and temperature conditions.

The first aim of this research is the synthesis of model trimethyl-lock quinone propionic acid-amide derivatives for kinetic studies. The potential of quinone reduction, as well as the rate of amide cleavage from the model compounds, are assumed to be similar to corresponding quinone-lipids in liposomes since the distance to any functional moiety at the end of the propionic acid

side chain is far off from the quinone head group to have any electronic impacts.[11] However, investigating how the different substituents on the quinone ring affect the kinetics of trigger cleavage is essential. Therefore, different types of quinone propionic acid-amide derivatives were synthesized and characterized.

The second aim of this research is to investigate the lactonization kinetics of trimethyl-lock quinone propionic acid-amide derivatives under different environmental conditions. In response to that, influence of temperature, solvent, and buffer conditions were studied. The reduction and lactonization of the compounds were followed by ^{1}H NMR spectroscopy upon addition of a chemical reducing agent, sodium dithionite ($Na_2S_2O_4$), under anaerobic conditions.

The encapsulated cargo of the liposome will be delivered with the activation of the quinone via either chemical or enzymatic reduction, making possible to use liposomes made up of lipids processing a specific quinone trimethyl-lock head group as reagent carriers. The findings here contribute to the development of a redox-responsive liposomal formulation having a favorable kinetic payload release profile under appropriate environmental conditions.

1.2 Nanoparticle Drug Delivery Systems

1.2.1 Motivation

An exciting new direction in drug delivery is the development of biocompatible and biodegradable pharmaceutical carriers capable of precise drug release to a specified target at a given time.[9,13] One possible approach is the miniaturization of the delivery systems through advances in nano-biotechnology.[14] So far, various nanoscaled pharmaceutical drug delivery devices have been developed and are in diverse stages of investigation to meet up the challenges in drug delivery. [9,14-16]

Nanoscaled drug carriers are "integrated functionalized nanostructures" having fascinating properties due to their "spatial and temporal organization, coordination and regulation of action of individual components."[9] They can be optimized so as to alter their pharmacokinetics, such as favorable absorption, distribution, metabolism, and excretion (ADME) compared to free drug. Due to their diminutive size and high surface-to-volume ratios, their rates of dissolution are enhanced and are able to penetrate across the capillaries into cells to permit the efficient accumulation.[9,14,15] Moreover, opzonization of these with opsonins such as fibrinogen, IgG ant, and protein C3b prevents the rapid clearance by the reticuloendothelial system (RES). Thus thereby promoted active or passive targeting.[9] These properties increase the therapeutic agent's stability and pharmacokinetics, while reducing the harmful side effects to healthy cells.

Most of the recent research focus toward the nanoparticulate pharmaceutical carriers in order to apply for challenging, long-lasting diseases such as HIV, cancer, and diabetes.[14] Among these, cancer gains greater attention because of its complex nature of treatment. Current therapies for cancer are not universally effective due to lower therapeutic index and poor selection between healthy and cancer cells. One of the most promising tactics to overcome this challenge is the use of nanocarriers where chemotherapeutic agent is encapsulated and is then dissembled at the tumor site, which thereby improves site-specific toxicity.[14] In addition, Cui and co-workers have reported a nanoparticulate vaccine delivery system wherein peptide antigen is encapsulated for immunization. Even though this methodology provides attractive platform for other biologicals such as peptides, proteins, and DNA, its *in vivo* potential still needs to be evaluated.[17 14]

1.2.2 Types of Engineered Nanopartcles in Drug Delivery

The immense interest has surrounded the area of new delivery systems based on the state-of-the-art nanotechnology owing to the emerging development of nanotechnology in the past few decades.[14] They are considered as smart candidates for transporting therapeutic agents to the targeted sites.[14] To date, a variety of nanoengineered drug delivery systems are available, and only a few selected systems are discussed here.

Polymeric nanoparticles are either nanospheres or nanocapsules depending on their structure and offer distinct advantages over other nano-systems in terms of efficiency and effectiveness.[9,15] They are highly stable and able to deliver therapeutic agents at a higher concentration due to their variable surface charge.[15] "Drug encapsulation and absorption, biodistribution pattern, elimination, and drug release are affected by various factors, including polymer composition, hydrophobicity, surface charge, biodegradation profile of the nanoparicles".[15] In order to achieve the desired biodistribution, most of them are modified with different targeting moieties such as PEG molecules, folic acids, avidin, and biotin, etc. Some known polymers used to prepare these types of nanoparticles are: poly(D, L-lactide), poly(lactide-co-glicolide), poly(cyanoacrylates), poly(anhydride) etc.[9] These are potential drug carriers for cancer, diabetes, transplant rejection and schizophrenia therapies. [9,14,15]

Polymer drug conjugates and polymeric micelles are other forms of nanoscale polymeric structures that are stable under biological environments. Polymer drug conjugates are hybrid architectures that merge a bioactive agent with a water-soluble polymer (natural or synthetic) in a covalent manner to ensure proper transport to the desired site. Once it goes to the targeted site, the polymer-drug link dissembles, and the active form of the drug is released into the medium.[9] Polymeric micelles are typically formed by amphiphilic block copolymers (20–50 nm), which

are comprised of a hydrophobic core and a hydrophilic corona. They are highly stable, biodegradable, biocompatible, and possess a small consistent size distribution, extending their circulation time in the blood stream.[9] Furthermore, polymeric micelles possess very low critical micelle concentration (CMC) and are susceptible for active targeting via modifications.[9,18,19]

Dendrimers are compact artificial macromolecules, composed of a central core, internal branches, and end groups in a symmetric three dimensional architecture. This unique organization allows creating a controlled, mono-dispersed, nano-sized sphere that possesses a hydrophobic interior with multiple attachment sites.[15,20] This feature facilitates bioactive agents to be chemically attached or encapsulated or physically adsorbed on to the dendrimer surface according to its application.[9] So far they have been used to carry a number of low molecular weight drugs (5-fluorouracyl and nifedipine), DNA, and imaging agents (gadolinium) for the diagnosis and treatment of cancer.[9]

Liposomes are extremely versatile, self-closed structures formed by one or more concentric lipid bilayers with a hydrophilic interior and a hydrophobic exterior.[1,2] The hydrophobic lipid bilayers provide room for the hydrophobic active pharmaceutical ingredients (APIs), while the aqueous interior can host hydrophilic APIs. They offer several advantages over other nano-carriers due to their size, amphiphilic nature, and molecular framework, and are also the first nanocarrier which came into the market.[1,11,21] Liposomes can entrap a wide variety of API as well as larger doses of them due to their micro to nanometer size. The encapsulation protects APIs from destructive entities inside the body and facilitates delayed release which is advantageous for minimizing the toxic effects and maximizing the therapeutic index.[5]

Liposome research has been progressed extensively from first-generation to third-generation materials in the last few decades.[9] The conventional or first-generation liposomes protect their

payload from degradation, while allowing for passive targeting to tissues or organs (spleen, bone marrow, liver). However, their higher uptake by the reticuloendothelial system (RES) that leads to their removal from the blood circulation system led research towards the second generation of liposomes, which are primarily obtained by inclusion of a protective polymer, poly(ethylene glycol), to the liposomal composition. [9] Consequently, stable, long-circulating "stealth" liposomes have been developed and have an increased accumulation at the pathological sites via the enhanced permeability and retention effect (EPR).[3,9,22] This effect is beneficial for chemotherapy[23] because liposomes need to reach and stay for an extended time period at the tumor sites in order to achieve proper drug release. As a result, liposome research had as its preliminary focus on cancer treatment, and the U.S. FDA approved the first chemotherapeutic liposomal drug formulation, Doxil, in1995 for the treatment of Kaposi sarcoma, ovarian, and metastatic breast cancers.[1,4] DaunoXome and Myocet are other commercially-available chemotherapeutic liposomal formulations, while some are still at different stages of clinical evaluations.[4,9,24]

Subsequently, liposomal research has been pioneered to include targeting moieties which are responsible for cell targeting, as well as higher drug accumulation at the desired site.[3] Targeting agents, such as monoclonal antibodies, growth factors, glycoproteins, and ligands, can be attached either to the bilayer surface or distal ends of the PEG-lipid chains. However, studies have shown that the targeting ligands at the end of PEG chains are more preferred.[3,9] Recently, liposome technology was upgraded to stimuli-responsive systems which involve programmed delivery of liposomal contents via specific stimulus at the targeted site.[3] The stimulus can be either exogenous (radiation, temperature) or endogenous (pH and enzyme).[25] Construction of these formulations, typically achieved by designing a lipid bilayer with a triggerable

functionality or subunit that is responsible for destabilizing the bilayer, upon induction of the appropriate stimulus.[11,12,25] So far, several numbers of stimuli-responsive liposomes have been engineered using radiation,[26,27] enzymes,[28,29] pH,[30] metal ions[31] and heat[32,33] as stimuli. However, the use of endogenous stimuli are highly favorable because it offers "local control over payload delivery".[12] On that note, the use of certain over-expressed enzymes at pathological sites provides an opportunity for their use as an internal stimulus, thereby resulting in programmed site-specific drug delivery.[11] Consequently, several liposomal formulations based on tumor selective enzymes, such as secretory phospholipase A2 ($sPAL_2$)[34] and matrix metalloproteinases (MMP–2 and MMP–9)[35-37] have been studied.

1.3 Rate Enhancement in Trimethyl-lock induced lactonization

In 1959, Cohen and Schmir observed that the ortho-hydroxyhydrocinnamic acid compounds undergo facile imtramolecular cyclization in order to form their corresponding lactone derivatives.[38] After this initial observation, researchers investigated the reaction extensively. Cohen and Milstien conducted their preliminary study with a series of ortho-hydroxyhydrocinnamic acids (**1**) containing both electron donating and electron withdrawing groups at the 5′ position (Scheme 1).[39,40]

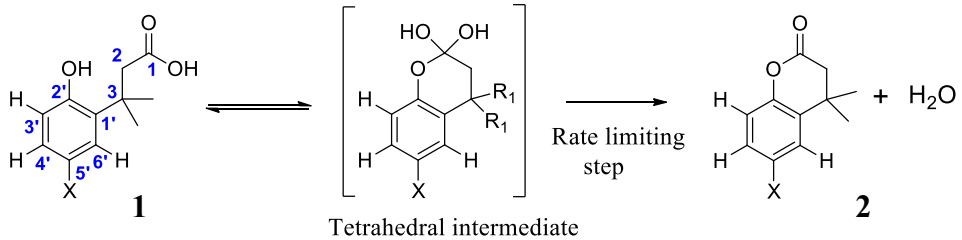

$X = OH, OCH_3, C_2H_6, H, F, Cl, NO_2, N(CH_3)_3^+$

Scheme 1.1: Mechanism of ortho-hydroxyhydrocinnamic acid lactonization.

In weakly acidic conditions, the reaction proceeded at medium rates, while it was catalyzed by both acidic and basic buffer components. Catalysis was concurrent and independent, but not concerted. From the kinetic results (from the linear free energy relationship data), researchers concluded that the reaction proceeds through a tetrahedral intermediate, wherein breakage of the tetrahedral intermediate is key to the rate limiting step.[39,40]

Subsequent studies that involved a variety of structurally distinct ortho-hydroxyhydrocinnamic acid compounds also confirmed the breakage of the tetrahedral intermediate as the rate determining step, and it was found to follow pseudo-first-order kinetics.[40-43] Moreover, it was observed that introduction of methyl substitution on 3, 3′, 4′, and 6′ positions had a significant effect on rate of lactonization, and were 10^{10}-10^{11} times as fast as unsubstituted hydroxyhydrocinnamic acid under buffer catalysis. For example, the reaction was found to have a half life of 6 s at pH 7 and temperature 30 °C.[40,41,43,44] Additionally, rate data revealed that the tetrahedral intermediate is more sensitive to acid catalysis compared to base catalysis in the rate-determining step.[41] This finding reveals the significance of the surrounding methyl groups, and in an attempt to explain the outcome, the concept of the "trimethyl-lock" or "stereopopulation control" has been developed.[41,44] The trimethyl-lock effect arises from the unique interlocking arrangement of the gem-dimethyls and single methyl at 3 and 6′ positions(Scheme 1), and the explanation of the outcomes states that "the effect is attributed to a unique interlocking of methyl groups, which produces a severe conformational restriction of the side chain and ground-sate geometry highly favorable to formation of the transition state".[41] The results, as well as Cohen's explanation, attained much interest, and many experimental (crystallographic and spectroscopic) and theoretical works were conducted to verify the rate enhancement.[40,45-47] As a result, different explanations emerged, and from empirical force-field

model calculations, it was argued that conventional steric strain relief is the dominant factor compared to stereopopulation control.[11,47]

In addition, later work by Caswell and Schmir determined that the lactonization rates for these compounds were overestimated, [42] and thus, Cohen later on revised the value 10^{10}-10^{11} as 10^{5}.[48] These values were compatible with rate values obtained from other trimethyl-locked related systems.[48] Furthermore, kinetic studies on ortho-hydroxyhydrocinnamic acids possessing different substituents at the 6′ position have shown different rates of lactonization, indicating the importance of the size of the substituent for accelerated lactonization;[49] thus it was concluded that steric strain relief is the major factor for trimethyl-lock induced lactonization.

1.3.1 Applications of the Trimethyl-lock System

After those pioneering observations (above), research has progressed toward the utilization of trimethyl-lock induced lactonization to other relevant applications. Because the parent trimethyl-lock ortho-hydroxyhydrocinnamic acid is highly reactive, scientists modified the parent structure for further applications. As a result, a variety of trimethyl-lock quinone propionic acids and their amide or ester derivatives have been developed.[50-53] Upon reduction, the quinone is converted to the hydroquinone which then undergoes intramolecular lactonization to release alcohols or amines to the medium (Scheme 2). So far, several trimethyl-lock quinone propionic acid-based systems have been introduced, but only a few selected systems are discussed here.

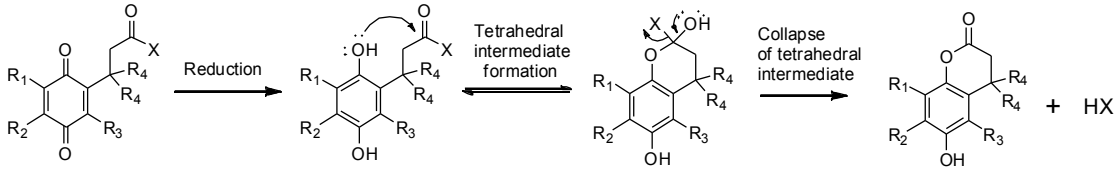

X = OR, NR_1R_2

Scheme1.2: Schematic representation of lactonization for quinone propionic acid derivatives.

The development of new prodrug systems that can utilize the tumor microenvironment as a stimulus for release of an active form of a given drug is a topic of current interest.[54] One possible methodology to accomplish this target is the derivatization of the drug with a trimethyl-lock quinone proionic acid to form their ester or amide derivatives. For example with cancer, this arrangement is highly beneficial because it increases the drug's (cytotoxic agent's) stability thereby decreasing its toxic side effects before reaching the tumor site.[54] When it enters the site, the tumor hypoxic environment facilitates prodrug bioreductive activation through the presence of overexpressed reductase enzymes, and as a result intramolecular lactonization of thrimethyl-lock quinone propionic amide occurs to release the cytotoxic agent to the surroundings.[54] Chikhale *et al.* followed this approach to selectively deliver the methyl ester of melphalan and acivicin to tumor site. In addition, they investigated the stability and efficiency of drug release via structural modification of the parent quinone ring.[50-52] So far, several prodrug systems have been reported for chemotherapy based on this methodology.[54-56]

In 1999, Wang and coworkers developed a redox-sensitive resin linker, based on a trimethyl-lock quinone propionic acid, for solid phase synthesis of *C*-terminally modified peptides where, the linker was disintegrated through mild reduction conditions.[57] Described in another paper published by Lin's group, is a trimethyl-lock quinone latent flurophore system based on rhodamine 110 for possible cancer cell imaging. The system was targeted for DT Diaphorase, an oxidoreductase that is overexpressed in certain cancer cells and is able to generate or release fluorescently active rhodamine 110 dye.[58] Silvers and McCarley went on to greatly improve latent fluorophores for cancer diagnosticis by developing a single-trigger probe based on a trimethyl-lock quinone propionic acid-rhodamine.[59]

Mrksich and Hodneland created a novel dynamic electroactive monolayer system on gold surfaces capable of selectively liberating immobilized ligands under electro-chemical control. The ligand, biotin, is attached to the alkanethiolate through a quinone propionic ester. Application of a reducing electrochemical potential to the gold surface causes quinone reduction, and after lactonization, biotin is released. This new class of self-assembled monolayer system is important for development of tailored structures for both mechanistic and experimental studies in cell biology.[60]

In 2005, the McCarley research group initiated use of trimethyl-lock quinone propionic acids for stimuli-sensitive systems. As a first step, they established the new redox-sensitive symmetric poly(propylene imine), PPI, dendrimer system, containing trimethyl-lock quinone propionic acids as peripheral groups.[61,62] Secondly, in 2007, they developed redox-responsive aggregates by using trimethyl-lock quinone propionic acid-modified amphiphilic molecules.[63] Both systems were dissembled upon redox activation and were able to release their entrapped cargo in an efficient manner. Currently, the McCarley research group is extending this concept to develop new liposomal formulations.

1.4 Redox-Responsive Quinone Trimethyl-lock Liposome Delivery System

In 2008, the McCarley research group extended the use of trimethyl-lock quinone propionic acids to develop a novel stimuli-responsive liposome system.[12] This system, which is currently under its optimizing stages, utilizes dioleoylphosphatidylethanolamine (DOPE) lipids with trimethyl-lock quinone propionic acid attached as head groups (Q-DOPE). Liposomes are targeted for human NAD(P)H:quinone oxidoreductase (hNQO1) enzyme, that is overexpressed in certain cancerous cells (A549, HT29). The development of such a stimuli-sensitive liposome

system is highly beneficial, because it offers potential "local control over payload release" upon redox stimulus.[8,11,12]

The overall structure of the liposome to function as a smart pharmaceutical carrier is permitted by the specific role played by each component of the Q-DOPE system. The process of liposome destabilization is attributable to the lipid's lamellar-to-inverted hexagonal (L_α-H_{II}) phase transition,[8,11,12] that occurs as a result of a three-step mechanism (Figure 1.1).

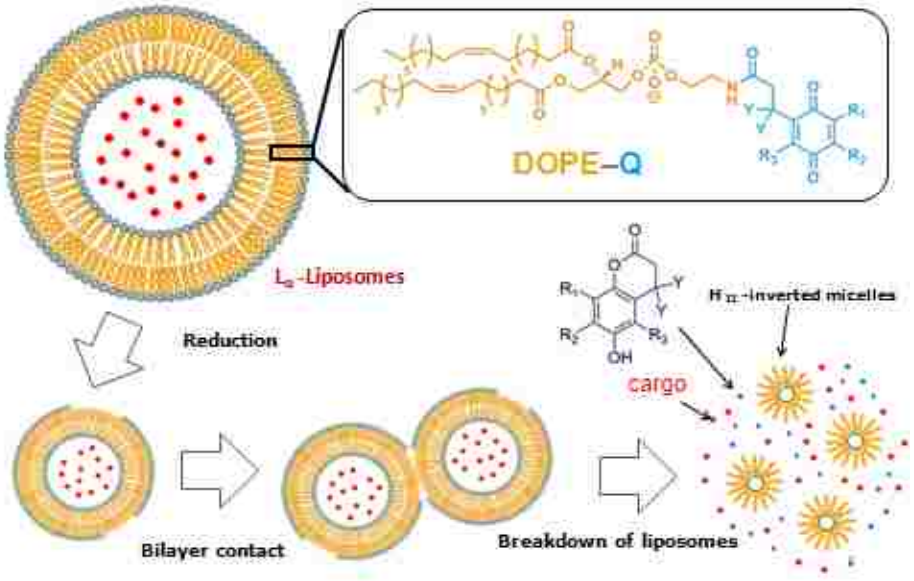

$R_1 = CH_3$, nPrNH, Br, H

R_2, R_3, Y = CH_3

Figure 1.1: Mechanism of Q-DOPE liposome destabilization (representation by Dr. N. H. Carrier).

Initial reduction of the quinone ring initiates head group removal from the lipid via lactonization. Then, the exposed lipids in the bilayers of the liposomes experience inter liposomal electrostatic interactions, leading to apposed bilayer fusion. This fusion induces destabilization in the bilayer, resulting in the L_α-H_{II} phase transition that causes removal of contents to the external environment. Owing the L_α-H_{II} transition, the lipids rearrange to a stable

cone-shaped inverted miceller structure to minimize their electrostatic attraction between positively charged amine and the negatively charged phosphate groups (Figure 1).[11]

Recently, Nicole Carrier from the McCarley research group synthesized a family of redox-responsive quinone-dioleoylphosphatidylethanolamine liposomes, by varying the functionality at the 3′ position of the quinone head group (Q_{Me}-DOPE, Q_{Br}-DOPE, Q_{nPrNH}-DOPE, Q_{H}-DOPE). The payload release kinetics were studied using fluorescence spectroscopy under anaerobic conditions.[11] Following injection of chemical reducing agent ($Na_2S_2O_4$), liposomes were destabilized, and the entrapped calcein was released at different rates (Figure 2). Quantitatively, Q_{Br}-DOPE showed faster release profile while Q_{H}-DOPE revealed slower release. The Q_{nPrNH}-DOPE and Q_{Me}-DOPE revealed almost similar medium rate release profile.[11] This observation points to the fact that quinone head group lactonization plays a major role in liposomal payload release kinetics. Therefore, investigation of lactonization kinetics of trimethyl-lock quinones is paramount importance in order to achieve efficient liposomal payload release.

.

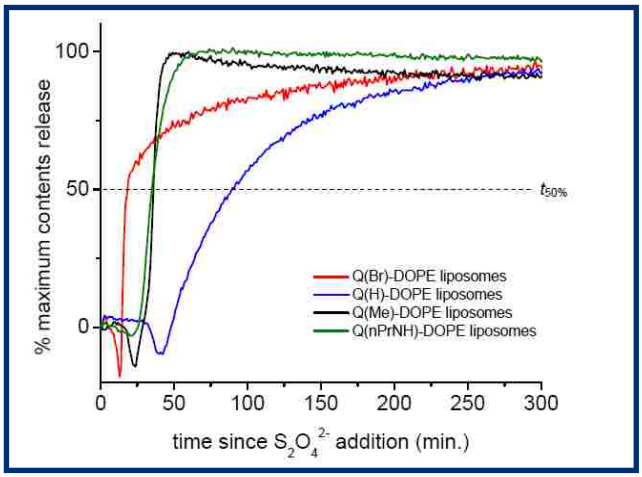

Figure 1.2: Calcein release profiles (normalized) of various Q-DOPE liposomes as determined by fluorescence emission spectroscopy (λ_{ex}=490 nm, λ_{em} = 515 nm). Each trace represents the typical release behavior observed for each Q-DOPE liposome composition[11]

1.5 References

(1) Torchilin, V. P. Recent advances with liposomes as pharmaceutical carriers. *Nature Reviews Drug Discovery* **2005**, *4*, 145-160.

(2) Jesorka, A.; Orwar, O. Liposomes: Technologies and Analytical Applications. *Annual Review of Analytical Chemistry* **2008**, *1*, 801-832.

(3) Sawant, R. R.; Torchilin, V. P. Liposomes as 'smart' pharmaceutical nanocarriers. *Soft Matter* **2010**, *6*, 4026-4044.

(4) Zhang, L.; Gu, F. X.; Chan, J. M.; Wang, A. Z.; Langer, R. S.; Farokhzad, O. C. Nanoparticles in Medicine: Therapeutic Applications and Developments. *Clincal Pharmacology and Therapeutics* **2008**, *83*, 761-769.

(5) Edwards, K. A.; Baeumner, A. J. Liposomes in analyses. *Talanta* **2006**, *68*, 1421-1431.

(6) Vreeland, W. N.; Locascio, L. E. Using Bioinspired Thermally Triggered Liposomes for High-Efficiency Mixing and Reagent Delivery in Microfluidic Devices. *Analytical Chemistry* **2003**, *75*, 6906-6911.

(7) Corradini, D.; Mancini, G.; Bello, C. Use of liposomes as a dispersed pseudo-stationary phase in capillary electrophoresis of basic proteins. *Journal of Chromatography A* **2004**, *1051*, 103-110.

(8) Forsythe, J. Kinetics and Mechanisms of Release by Redox-Active Liposomes in Drug Delivery. Ph.D Dissertation, Louisiana State University, Baton Rouge, LA. 2011.

(9) Leucuta, S. E. Nanotechnology for Delivery of Drugs and Biomedical Applications. *Current Clinical Pharmacology* **2010**, *5*, 257-280.

(10) Dutta, R. C. Drug Carriers in Pharmaceutical Design: Promises and Progress. *Current Pharmaceutical Design* **2007**, *13*, 761-769.

(11) Carrier, N. H. Redox-Active Liposome Delivery Agents with Highly Controllable Stimuli-Responsive Behavior. Ph.D Dissertation, Louisiana State University, Baton Rouge, LA. 2011.

(12) Ong, W.; Yang, Y.; Cruciano, A. C.; McCarley, R. L. Redox-Triggered Contents Release from Liposomes. *Journal of the American Chemical Society* **2008**, *130*, 14739-14744.

(13) Kiparissides, C.; Kammona, O. Nanoscale carriers for targeted delivery of drugs and therapeutic biomolecules. *The Canadian Journal of Chemical Engineering* **2012**, *9999*, 1-14.

(14) Yih, T. C.; Al-Fandi, M. Engineered nanoparticles as precise drug delivery systems. *Journal of Cellular Biochemistry* **2006**, *97*, 1184-1190.

(15) Marcato, P. D.; Duran, N. New Aspects of Nanopharmaceutical Delivery Systems. *Journal of Nanoscience and Nanotechnology* **2008**, *8*, 2216-2229.

(16) Vladimir P, T. Multifunctional nanocarriers. *Advanced Drug Delivery Reviews* **2006**, *58*, 1532-1555.

(17) Cui Z; Han S ; Padinjaree D; L, H. Immunsotimulation mechanism of LPD nanoparticles as a vaccine carrier. *Molecular Pharmaceutics* **2005**, *2*, 22 -28.

(18) Torchilin, V. P. Micellar nanocarriers: pharmaceutical perspectives. *Pharmaceutical Research* **2007**, *24*, 1-16.

(19) Torchilin, V. P. Targeted polymeric micelles for delivery of poorly soluble drugs. *Cellular and Molecular Life Sciences* **2004**, *61*, 2549-2559.

(20) Flomenbom, O.; Amir, R. J.; Shabat, D.; Klafter, J. Some new aspects of dendrimer applications. *Journal of Luminescence* **2005**, *111*, 315-325.

(21) Kaasgaard, T.; Andresen, T. L. Liposomal cancer therapy: exploiting tumor characteristics. *Expert Opinion on Drug Delivery* **2010**, *7*, 225-243.

(22) Gabizon, A.; Catane, R.; Uziely, B.; Kaufman, B.; Safra, T.; Cohen, R.; Martin, F.; Huang, A.; Barenholz, Y. Prolonged circulation time and enhanced accumulation in malignant exudates of doxorubicin encapsulated in polyethylene-glycol coated liposomes. *Cancer research* **1994**, *54*, 987-992.

(23) Li, S.-D.; Huang, L. Stealth nanoparticles: high density but sheddable PEG is a key for tumor targeting. *Journal of Controlled Release* **2010**, *145*, 178-181.

(24) Zang, H. B.; Wang, G. J.; Yang, H. A. Drug Delivery Systems forDifferential Release in Combination Theraphy. *Expert Opinion Drug Delivery* **2011**, *8*, 171-190.

(25) Andresen, T. L.; Jensen, S. S.; Jørgensen, K. Advanced strategies in liposomal cancer therapy: Problems and prospects of active and tumor specific drug release. *Progress in Lipid Research* **2005**, *44*, 68-97.

(26) Subramaniam, R.; Xiao, Y.; Li, Y.; Qian, S. Y.; Sun, W.; Mallik, S. Light-mediated and H-bond facilitated liposomal release: the role of lipid head groups in release efficiency. *Tetrahedron Letters* **2010**, *51*, 529-532.

(27) Jin-Ye, W.; Qing-Fen, W.; Jian-Ping, L.; Qiu-Shi, R.; Yu-Lu, W.; Xin-Ming, L. Photo-Sensitive Liposomes: Chemistry and Application in Drug Delivery. *Mini Reviews in Medicinal Chemistry* **2010**, *10*, 172-181.

(28) Elegbede, A. I.; Banerjee, J.; Hanson, A. J.; Tobwala, S.; Ganguli, B.; Wang, R.; Lu, X.; Srivastava, D. K.; Mallik, S. Mechanistic Studies of the Triggered Release of Liposomal

Contents by Matrix Metalloproteinase-9. *Journal of the American Chemical Society* **2008**, *130*, 10633-10642.

(29) Sarkar, N.; Banerjee, J.; Hanson, A. J.; Elegbede, A. I.; Rosendahl, T.; Krueger, A. B.; Banerjee, A. L.; Tobwala, S.; Wang, R.; Lu, X.; Mallik, S.; Srivastava, D. K. Matrix Metalloproteinase-Assisted Triggered Release of Liposomal Contents. *Bioconjugate Chemistry* **2007**, *19*, 57-64.

(30) Budker, V.; Gurevich, V.; Hagstrom, J. E.; Bortzov, F.; Wolff, J. A. pH-sensitive, cationic liposomes: A new synthetic virus-like vector. *Nature Biotechnology* **1996**, *14*, 760-764.

(31) Davis, S. C.; Szoka, F. C. Cholesterol Phosphate Derivatives: Synthesis and Incorporation into a Phosphatase and Calcium-Sensitive Triggered Release Liposome. *Bioconjugate Chemistry* **1998**, *9*, 783-792.

(32) Kenji, K. Thermosensitive polymer-modified liposomes. *Advanced Drug Delivery Reviews* **2001**, *53*, 307-319.

(33) Koning, G. A.; Eggermont, A. M.; Lindner, L. H.; ten Hagen, T. L. Hyperthermia and thermosensitive liposomes for improved delivery of chemotherapeutic drugs to solid tumors. *Pharmaceutical Research* **2010**, *27*, 1750-1754.

(34) Andresen, T. L.; Jensen, S. S.; Kaasgaard, T.; Jorgensen, K. Triggered activation and release of liposomal prodrugs and drugs in cancer tissue by secretory phospholipase A2. *Current Drug Delivery* **2005**, *2*, 353-362.

(35) Terada, T.; Iwai, M.; Kawakami, S.; Yamashita, F.; Hashida, M. Novel PEG-matrix metalloproteinase-2 cleavable peptide-lipid containing galactosylated liposomes for hepatocellular carcinoma-selective targeting. *Journal of Controlled Release* **2006**, *111*, 333-342.

(36) Sarkar, N. R.; Rosendahl, T.; Krueger, A. B.; Banerjee, A. L.; Benton, K.; Mallik, S.; Srivastava, D. K. "Uncorking" of liposomes by matrix metalloproteinase-9. *Chemical Communications* **2005**, 999-1001.

(37) Banerjee, J.; Hanson, A. J.; Gadam, B.; Elegbede, A. I.; Tobwala, S.; Ganguly, B.; Wagh, A. V.; Muhonen, W. W.; Law, B.; Shabb, J. B.; Srivastava, D. K.; Mallik, S. Release of Liposomal Contents by Cell-Secreted Matrix Metalloproteinase-9. *Bioconjugate Chemistry* **2009**, *20*, 1332-1339.

(38) Schmir, G. L.; Cohen, L. A.; Witkop, B. The Oxidative Cleavage of Tyrosyl-Peptide Bonds. I. Cleavage of Dipeptides and Some Properties of the Resulting Spirodienone-lactones. *Journal of the American Chemical Society* **1959**, *81*, 2228-2233.

(39) Milstien, S.; Cohen, L. A. Concurrent general-acid and general-base catalysis of esterification. *Journal of the American Chemical Society* **1970**, *92*, 4377-4382.

(40) Amsberry, K. L. Development of Amine Prodrugs Which Utilize Hydroxy Amide Lactonization. Ph.D. Dissertation, University of Kansas, Lawrence, KS. 1990.

(41) Milstien, S.; Cohen, L. A. Stereopopulation control. I. Rate enhancement in the lactonizations of o-hydroxyhydrocinnamic acids. *Journal of the American Chemical Society* **1972**, *94*, 9158-9165.

(42) Caswell, M.; Schmir, G. L. Formation and hydrolysis of lactones of phenolic acids. *Journal of the American Chemical Society* **1980**, *102*, 4815-4821.

(43) Milstien, S.; Cohen, L. A. Rate Acceleration by Stereopopulation Control: Models for Enzyme Action. *Proceedings of the National Academy of Sciences* **1970**, *67*, 1143-1147.

(44) Berglund, R. A. Bioreductive Heterosubstituted Quinne Antitumor Drug Delivery Agents. Ph.D. Dissertation, University of Massachusetts, 1987.

(45) Karle, J. M.; Karle, I. L. Correlation of reaction rate acceleration with rotational restriction. Crystal-structure analysis of compounds with a trialkyl lock. *Journal of the American Chemical Society* **1972**, *94*, 9182-9189.

(46) Danforth, C.; Nicholson, A. W.; James, J. C.; Loudon, G. M. Steric acceleration of lactonization reaction: an analysis of "stereopopulation control". *Journal of the American Chemical Society* **1976**, *98*, 4275-4281.

(47) Winans, R. E.; Wilcox, C. F. Comparison of stereopopulation control with conventional steric effects in lactonization of hydrocoumarinic acids. *Journal of the American Chemical Society* **1976**, *98*, 4281-4285.

(48) Borchardt, R. T.; Cohen, L. A. Stereopopulation control. II. Rate enhancement of intramolecular nucleophilic displacement. *Journal of the American Chemical Society* **1972**, *94*, 9166-9174.

(49) King, M. M.; Cohen, L. A. Stereopopulation control. VII. Rate enhancement in the lactonization of 3-(o-hydroxyphenyl)propionic acids: dependence on the size of aromatic ring substituents. *Journal of the American Chemical Society* **1983**, *105*, 2752-2760.

(50) Gharat, L.; Visser, P.; Brummelhuis, M.; Guiles, R.; Chikhale, P. Reductive activation of conformationally-constrained, anticancer drug delivery systems. *Medicinal Chemistry Research* **1998**, *8*, 444-456.

(51) Weerapreeyakul, N.; Visser, P.; Brummelhuis, M.; Laxmikant, G.; Chikhale, P. J. Reductive and bioreductive activation is controlled by electronic properties of substituents in conformationally-constrained anticancer drug delivery systems. *Medicinal Chemistry Research* **2000**, *10*, 149-163.

(52) Weerapreeyakul, N.; Hollenbeck, R. G.; Chikhale, P. J. Stability of bioreductive drug delivery systems containing melphalan is influenced by conformational constraint and electronic properties of substituents. *Bioorganic & Medicinal Chemistry Letters* **2000**, *10*, 2391-2395.

(53) Weerapreeyakul, N.; Anorach, R.; Khuansawad, T.; Yenjai, C.; Isaka, M. Synthesis of bioreductive esters from fungal compounds. *Chemical and Pharmaceutical Bulletin* **2007**, *55*, 930-935.

(54) Blanche, E. A.; Maskell, L.; Colucci, M. A.; Whatmore, J. L.; Moody, C. J. Synthesis of potential prodrug systems for reductive activation. Prodrugs for anti-angiogenic isoflavones and VEGF receptor tyrosine kinase inhibitory oxindoles. *Tetrahedron* **2009**, *65*, 4894-4903.

(55) Amsberry, K.; Borchardt, R. Amine Prodrugs Which Utilize Hydroxy Amide Lactonization. I. A Potential Redox-Sensitive Amide Prodrug. *Pharmaceutical Research* **1991**, *8*, 323-330.

(56) Volpato, M.; Abou-Zeid, N.; Tanner, R. W.; Glassbrook, L. T.; Taylor, J.; Stratford, I.; Loadman, P. M.; Jaffar, M.; Phillips, R. M. Chemical synthesis and biological evaluation of a NAD(P)H:quinone oxidoreductase-1–targeted tripartite quinone drug delivery system. *Molecular Cancer Therapeutics* **2007**, *6*, 3122-3130.

(57) Zheng, A.; Shan, D.; Wang, B. A Redox-Sensitive Resin Linker for the Solid Phase Synthesis of C-Terminal Modified Peptides. *The Journal of Organic Chemistry* **1998**, *64*, 156-161.

(58) Huang, S.-T.; Lin, Y.-L. New Latent Fluorophore for DT Diaphorase. *Organic Letters* **2005**, *8*, 265-268.

(59) Silvers, W. C.; Payne, A. S.; McCarley, R. L. Shedding light by cancer redox-human NAD(P)H:quinone oxidoreductase 1 activation of a cloaked fluorescent dye. *Chemical Communications* **2011**, *47*, 11264-11266.

(60) Hodneland, C. D.; Mrksich, M. Biomolecular Surfaces that Release Ligands under Electrochemical Control. *Journal of the American Chemical Society* **2000**, *122*, 4235-4236.

(61) Ong, W.; McCarley, R. L. Redox-driven shaving of dendrimers. *Chemical Communications* **2005**, 4699-4701.

(62) Ong, W.; McCarley, R. L. Chemically and Electrochemically Mediated Release of Dendrimer End Groups. *Macromolecules* **2006**, *39*, 7295-7301.

(63) Yang, Y. Develpoment of New Stimuli-Responsive Vesicles Using a Novel Surfactant. Ph.D Dissertation, Louisiana State University, Baton Rouge, LA, 2011.

CHAPTER 2
SYNTHESIS AND CHARACTERIZATION OF QUINONE COMPOUNDS

2.1 Syntheses

2.1.1 Chemicals and General Methods

All the chemicals were purchased from Sigma-Aldrich, Acros Organic, or TCI America and used as received. Flash chromatography was conducted using a Biotage FlashMaster Personal Chromatography system with SPE ISOLUTE FLASH Silica II columns (pore size 60 Å, diameter 40-63μm, disposable). Reactions were followed by TLC on precoated silica plates (60 Å, F_{254}, EMD Chemicals Inc) and were visualized by UV lamp (UVGL-25, 254/365 nm). ^{1}H NMR spectra were recorded with either Bruker AV-Liquid-400 MHz or Bruker DPX 400MHz spectrometers. ESI-mass spectra were collected using an Agilent Technologies 6210 ESI-TOF LC/MS instrument with 90% acetonitrile as solvent.

2.2 Synthetic Routes

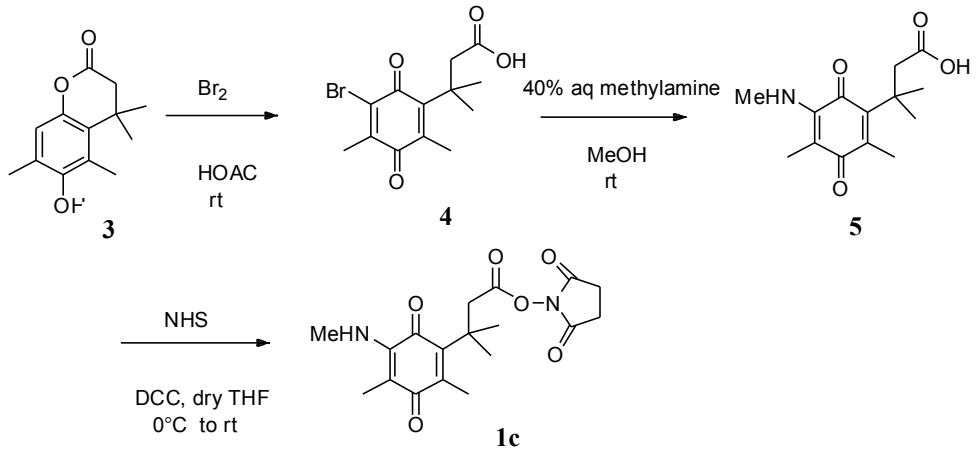

Scheme 2.1: Synthesis of succinimidyl ester of *N*-(methyl)amino quinone propionic acid.

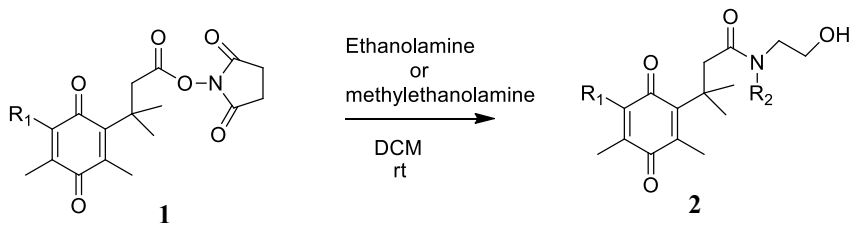

1 **2**

1 a) $R_1 = CH_3$	2 a) $R_1 = CH_3$ $R_2 = H$	(72%)
b) $R_1 = Br$	b) $R_1 = Br$ $R_2 = H$	(70%)
c) $R_1 = NMeH$	c) $R_1 = NMeH$ $R_2 = H$	(55%)
d) $R_1 = NPrH$	d) $R_1 = NPrH$ $R_2 = H$	(64%)
e) $R_1 = H$	e) $R_1 = H$ $R_2 = H$	(43%)
f) $R_1 = CH_3$	f) $R_1 = CH_3$ $R_2 = CH_3$	(59%)

Scheme 2.2: Synthesis of quinone propionic acid ethanolamine derivatives.

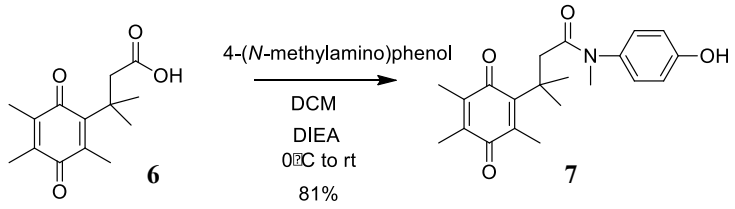

6 **7**

Scheme 2.3: Synthesis of quinone propionic acid 4-(*N*-methylamino)phenol derivative.

2.3 Experimental Details

The compounds **1a, b, d, e**, **3 and 6** were previously synthesized by members of our group, and purity of these were checked by ^{1}H NMR before used.[1] The References for the synthetic procedures are cited at the end of each procedure.

2.3.1. Synthetic Procedures for compounds 2a-f, 4, 5 and 7

(4). Lactone **3** was dissolved (0.690 g, 3.14 mmol) with stirring in 26 mL of glacial acetic acid. To this solution, Br_2 (0.35 mL, 6.81mmol) in 4.2 mL of HOAc was added slowly at room temperature. After 15 hours, the resulting mixture was diluted with 150 mL of water and

extracted with DCM (3 × 30 mL). The combined organic extracts were washed with water (2 × 20 mL) and next with saturated $NaHCO_3$ (5 × 20 mL). Then the bicarbonate extracts were made acidic by adding 30% HCl (15 mL) and the resulting solution was extracted with DCM (3 × 30 mL). These organic extracts were washed with water (50 mL), dried with $MgSO_4$, and concentrated to give a yellow oil (0.88 g, 89%). The crude oil was directly used for amination reaction without further purification. ^{1}H NMR ($CDCl_3$) δ 1.46 (s, 6H, geminal CH_3), 2.18 and 2.20 (s, 3H, CH_3), 3.04 (s, 2H, CH_2).[1,2]

(5). Bromo acid **4** (0.580 g, 1.85 mmol) was dissolved in 16 mL of MeOH and 40% aqueous methylamine (225μL, 6.42 mmol) was added with stirring at room temperature. The system was tightly stoppered, and the reaction was continued for 48 hours. Next the mixture was diluted to 250 mL with water. After dilution, 20 mL of 5% HCl solution was added. The resulting solution was extracted with EtOAc (3 × 70 mL), and the combined organic extracts were washed with 140 mL of saturated NaCl solution. The solution was dried over $MgSO_4$, and solvent was removed with the use of a rotary evaporator to give a red-purple oil. The crude oil was purified by silica column using hexanes/ethylacetate/acetic acid (14:6:1) as eluent. Concentration of the major red fraction afforded a red-purple oil, which was taken up in 50 mL of DCM and washed with water (2 × 40 mL) to remove the acetic acid. Next the DCM layer was dried over $MgSO_4$ and solvent was removed with a rotary evaporator to give a red-purple oil (0.26 g, 53%). ^{1}H NMR ($CDCl_3$) δ 1.45 (s, 6H, gem CH_3), 2.07 (s, 3H, quinone CH_3), 2.20 (s, 3H, quinone CH_3), 2.99 (s, 2H, CH_2), 3.11 (s, 3H, N-methyl CH_3), 5.15 (broad peak, N-methyl H). HRMS (ESI) *m/z* $[M+H]^+$, calculated = 266.1392, observed = 266.1387; 1.88 ppm error.[1,2]

(1c). Dicyclohexylcarbodiimide (0.095g, 0.436 mmol) was added to a solution of quinone propionic acid **5** (0.103g, 0.389 mmol) and *N*-hydroxysuccinimide (0.054 g, 0.426 mmol) in 25

mL of dry THF at 0 °C. The mixture was continuously stirred for 24 hours under argon. The remained solution was filtered to remove the dicyclohexylurea, evaporated using a rotary evaporator, and then treated with 10 mL of EtOAc. The corresponded solution was filtered again. This sequence was repeated for four times to remove the unreacted dicyclohexylurea. The solvent was removed with rotary evaporator, and the red crude material was purified on silica column using dichloromethane/ethylacetate (14:1) as eluent to give 55 mg (39%) of red solid. *The purified product was contaminated but used for the synthesis of **2c**. ^{1}H NMR ($CDCl_3$) δ 1.57 (s, 6H, geminal CH_3), 2.07 (s, 3H, CH_3), 2.22 (s, 3H, CH_3), 2.72 (s, 4H, CH_2), 2.80 (s, 2H, CH_2), 3.25 (s, 3H, CH_3), 5.30 (broad peak, N-methyl H). HRMS (ESI) *m/z* $[M+H]^+$, calculated = 363. 1556, observed = 363.1592; 9.91 ppm error.[1,2]

(2a). In a typical procedure, ethanolamine (0.044 g, 0.72 mmol) was added dropwise to a solution of **1a** (0.111 g, 0.320 mmol) in dichloromethane (12 mL). The mixture was stirred for 15 hours at room temperature under inert environment. The reaction mixture was diluted with DCM and filtered to remove the white solid that appeared in the middle of the reaction. Solvent was evaporated using a rotary evaporator and the crude mixture was purified on silica column using ethylacetate/dichloromethane (1:1) as eluent. Finally solvent was evaporated to give a 68 mg of yellow solid (72%). ^{1}H NMR ($CDCl_3$) δ 1.45 (s, 6H, gem CH_3), 1.96 (s, 3H, quinone CH_3), 1.98 (s, 3H, quinone CH_3), 2.14 (s, 3H, quinone CH_3), 2.86 (s, 2H, CH_2), 3.35(t, 2H, ethanolamine-CH_2), 3.65 (t, 2H, ethanolamine-CH_2), 5.81 (broad peak, ethanolamine H). HRMS (ESI) *m/z* $[M+H]^+$, calculated = 294.1705, observed = 294.1568; 46.57 ppm error.[3]

(2b) Starting material **1b** was used to synthesize **2b** and it was synthesized and purified following the same steps utilized in procedure **2a**. Yield 70%. ^{1}H NMR ($CDCl_3$) δ 1.47 (s, 6H, gem CH_3), 2.17 (s, 6H, 2 × quinone CH_3), 2.88 (s, 2H, CH_2) 3.34 (t, 2H, ethanolamine-CH_2),

3.67 (t, 2H, ethanolamine-CH_2), 5.84 (broad peak, ethanolamine H). HRMS (ESI) *m/z* $[M+H]^+$, calculated = 358.0654, observed = 358.0650; 1.12 ppm error. [3]

(2c). Starting material **1c** was used to synthesize **2c** and it was synthesized and purified following the same steps utilized in procedure **2a**. Yield 55%. ^{1}H NMR ($CDCl_3$) δ 1.44 (s, 6H, gem CH_3), 2.05 (s, 3H, quinone CH_3), 2.18 (s, 3H, quinone CH_3), 2.80 (s, 2H, CH_2), 3.11 (s, 3H, N-methyl CH_3), 3.36 (t, 2H, ethanolamine-CH_2), 3.69 (t, 2H, ethanolamine-CH_2). HRMS (ESI) *m/z* $[M+Na]^+$, calculated = 331.1634, observed = 331.1640; 1.81 ppm error.[3]

(2d). Starting material **1d** was used to synthesize **2d** and it was synthesized and purified following the same steps utilized in procedure **2a**. Yield 64%. ^{1}H NMR ($CDCl_3$) δ 0.97 (t, 3H, propyl CH_3), 1.44 (s, 6H, gem CH_3), 1.58 (m, 2H, CH_2*CH_2*CH_3), 2.01 (s, 3H, quinone CH_3), 2.17 (s, 3H, quinone CH_3), 2.79 (s, 2H, CH_2), 3.33–3.39 (m, 2H, N*CH_2*CH_2CH_3+2H, N*CH_2*CH_2OH), 3.64 (t, 2H, ethanolamine-CH_2), 5.79 (broad peak, ethanolamine H), 5.81 (broad peak, N-propyl H). HRMS (ESI) *m/z* $[M+H]^+$, calculated = 337.2127, observed = 337.2219; 27.28 ppm error. [3]

(2e). Starting material **1e** was used to synthesize **2e** and it was synthesized and purified following the same steps utilized in procedure **2a**. Yield 43%. ^{1}H NMR ($CDCl_3$) δ 1.46 (s, 6H, gem CH_3), 2.00 (s, 3H, quinone CH_3), 2.18 (s, 3H, quinone CH_3), 2.88 (s, 2H, CH_2), 3.34 (t, 2H, ethanolamine-CH_2), 3.66 (t, 2H, ethanolamine-CH_2), 6.51 (s, H, quinone H) 5.81 (broad peak, ethanolamine H). HRMS (ESI) *m/z* $[M+H]^+$, calculated = 280.1549, observed = 280.1551; 0.71 ppm error. [3]

(2f). Methylethanolamine (0.049 g, 0.66 mmol) was added dropwise to a solution of **1f** (101.70 mg, 0.293 mmol) in dichloromethane (12 mL). The mixture was stirred for 15 hours at room temperature under inert conditions. The reaction mixture was diluted with DCM and filtered. Solvent was evaporated using a rotary evaporator and the crude mixture was purified on silica

column using ethylacetate/dichloromethane (2:1) as eluent. Finally solvent was evaporated to give a 53 mg of yellow solid (59%). ^{1}H NMR ($CDCl_3$) δ 1.45 (s, 6H, gem CH_3), 1.92 (s, 3H, quinone CH_3), 1.94 (s, 3H, quinone CH_3), 2.14 (s, 3H, quinone CH_3), 2.86 (s, 2H, CH_2), 3.02 and 3.06 (2×s, 3H, *N*-methylethanolamine CH_3), 2.70, 3.46, 3.70, 3.81 (*N*-methylethanolamine CH_2). HRMS (ESI) *m/z* $[M+H]^+$, calculated = 308.1862, observed = 308.1871; 2.92 ppm error.[3]

(7). 4-(methylamino)phenol (0.109 g, 0.885 mmol) was dissolved with stirring in 10 mL of DMF. To this solution, quinone acid **6** (0.207 mg, 0.827 mmol) in 5 mL of DMF was added at 0°C. HATU (0.308 mg, 0.812 mmol) and DIEA (161μL, 0.975 mmol) were added to the reaction mixture sequentially, and the mixture was gradually warmed to room temperature overnight. Next, the solution was extracted with EtOAc (3 × 20 mL) and combined organic extracts were washed with saturated NaCl (2 × 20 mL) solution. The solution was dried over $MgSO_4$ and solvent was removed with the use of rotary evaporator to give a yellow solid. The crude solid was purified by silica gel column using hexanes/ethylacetate (2:5) as eluent. Solvent was evaporated to yield 238 mg (81%) of yellow solid.

^{1}H NMR ($CDCl_3$) δ 1.31 (s, 6H, gem CH_3), 1.96 (s, 3H, quinone CH_3), 2.00 (s, 3H, quinone CH_3), 2.17 (s, 3H, quinone CH_3), 2.75 (s, 2H, CH_2), 3.12 (s, 3H, N-methyl CH_3), 6.87–7.08 (d, 4H, benzene H,). HRMS (ESI) *m/z* $[M+H]^+$, calculated = 356.1862, observed = 356.1858; 1.12 ppm error.

2.4 Summary

A series of seven different simple quinone propionic acid amide derivatives (**2a–f** and **7**) were synthesized by varying the amide structure or substituents on the parent quinone ring. All quinone propionic acid amide derivatives were obtained in good yield and were characterized by

^{1}H NMR and ESI-MS techniques for subsequent reduction and lactonization kinetic studies (see chapter 3).

2.5 Spectral Data

^{1}H NMR data for compound 4

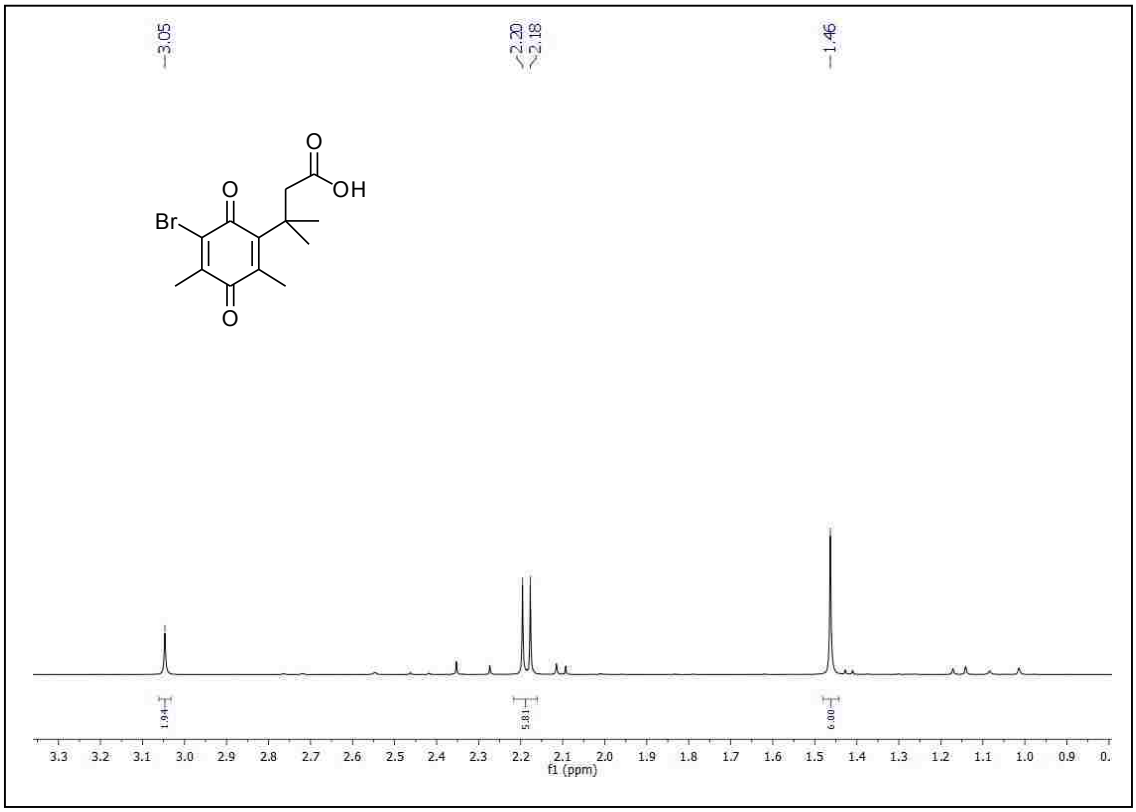

^{1}H NMR data for compound 5

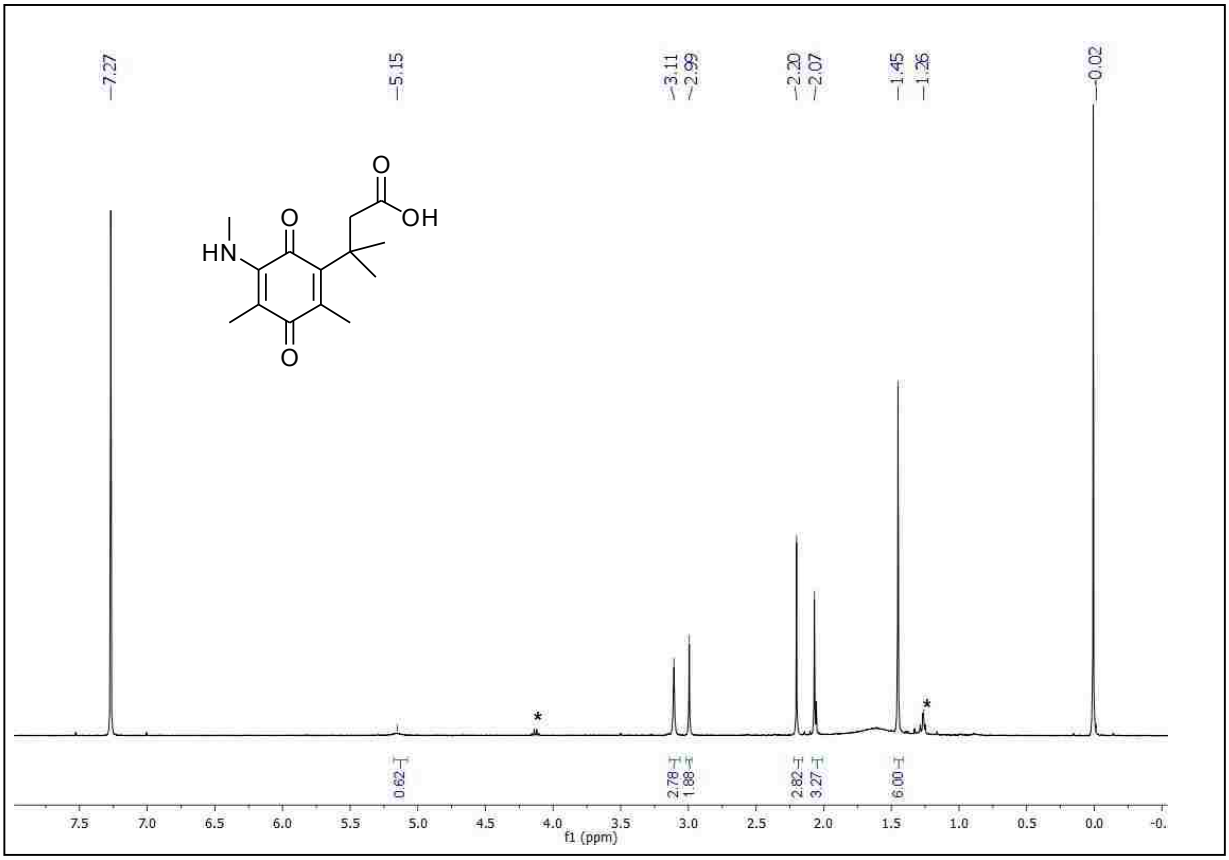

HR-ESI-ToF-MS data compound 5

^{1}H NMR data for compound 1c (contaminated product)

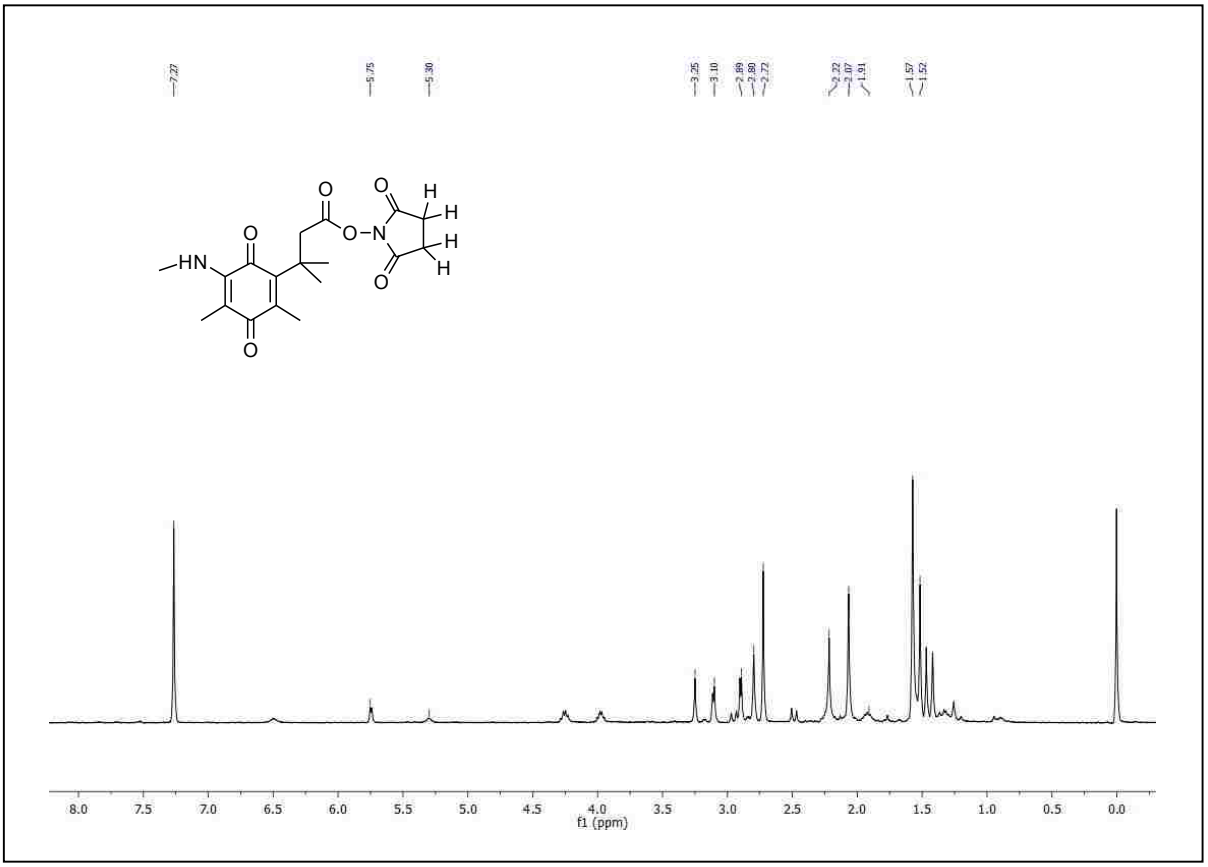

HR-ESI-ToF-MS data compound 1c

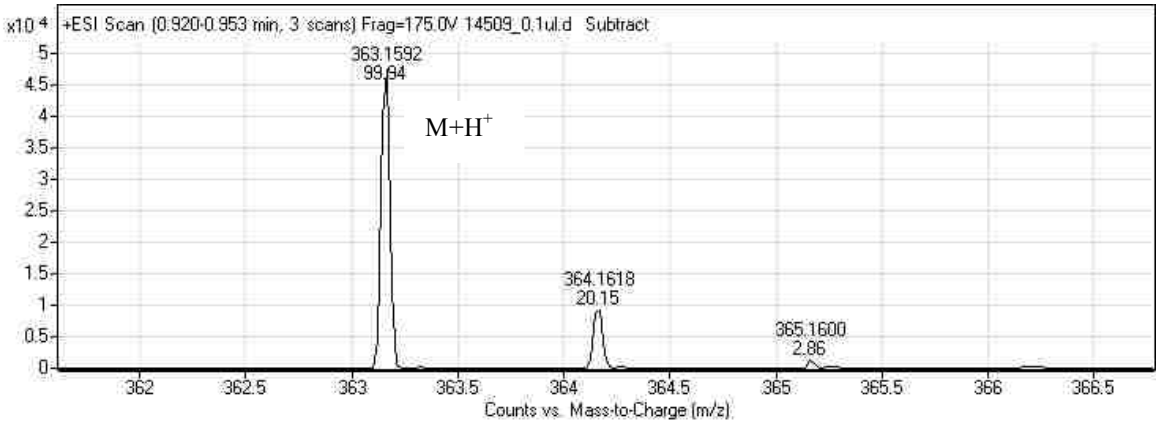

^{1}H NMR data for compound 2a

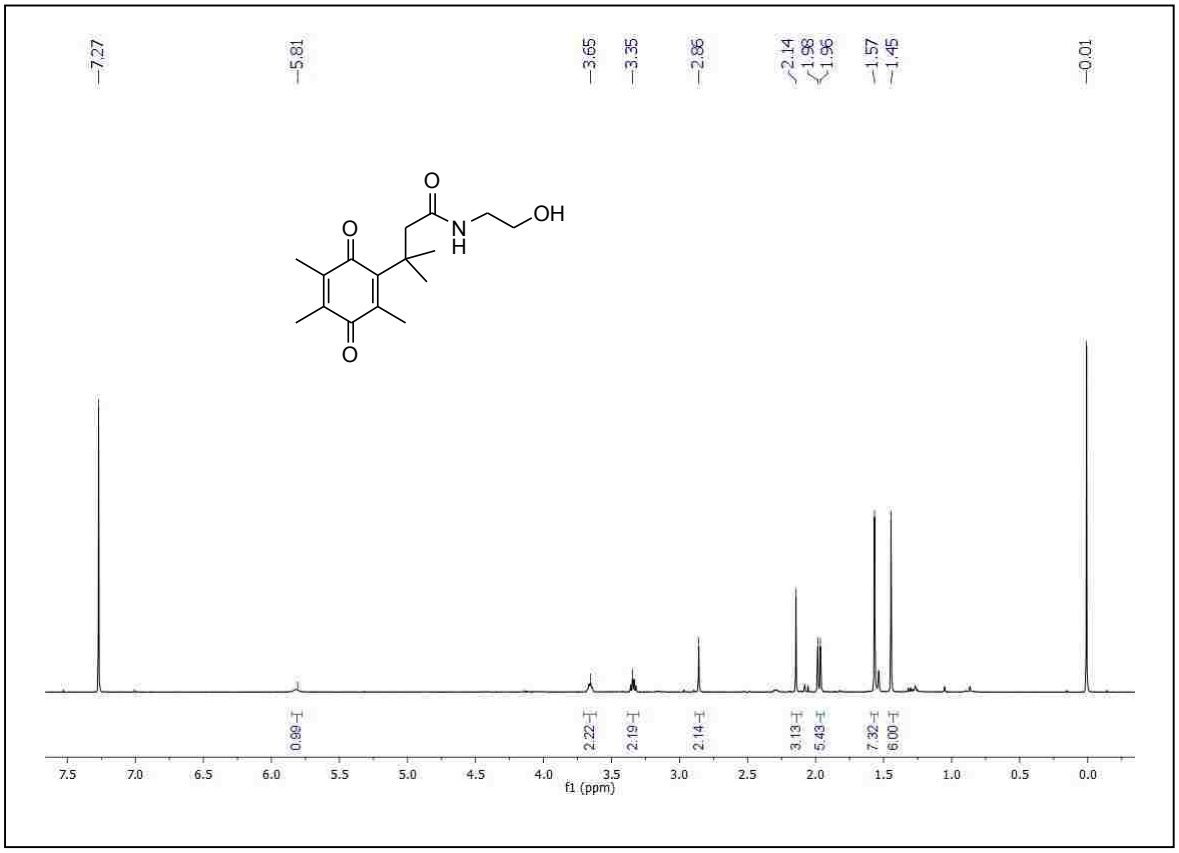

HR-ESI-ToF-MS data compound 2a

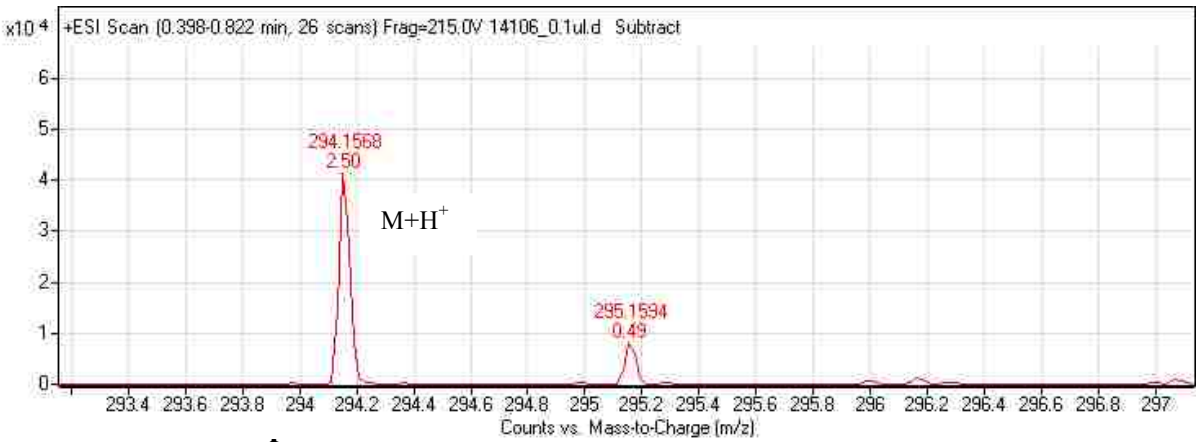

1

^{1}H NMR data for compound 2b

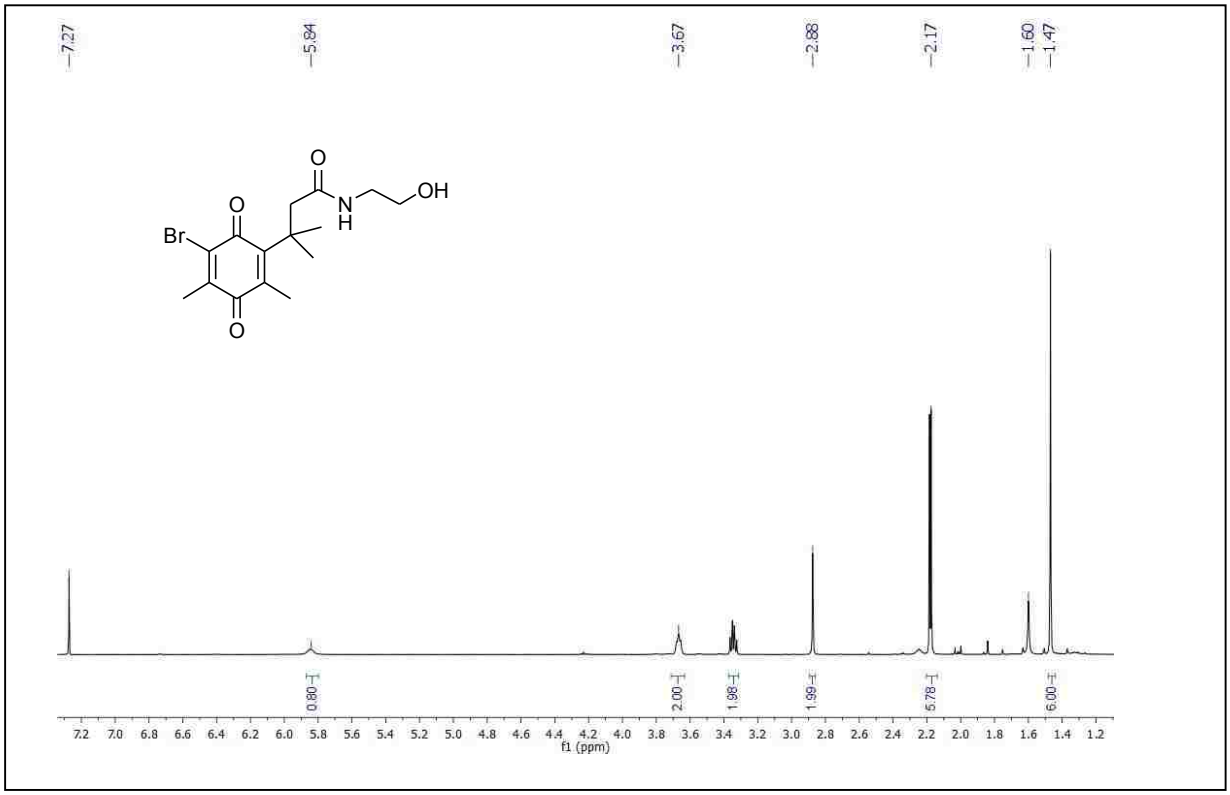

HR-ESI-ToF-MS data compound 2b

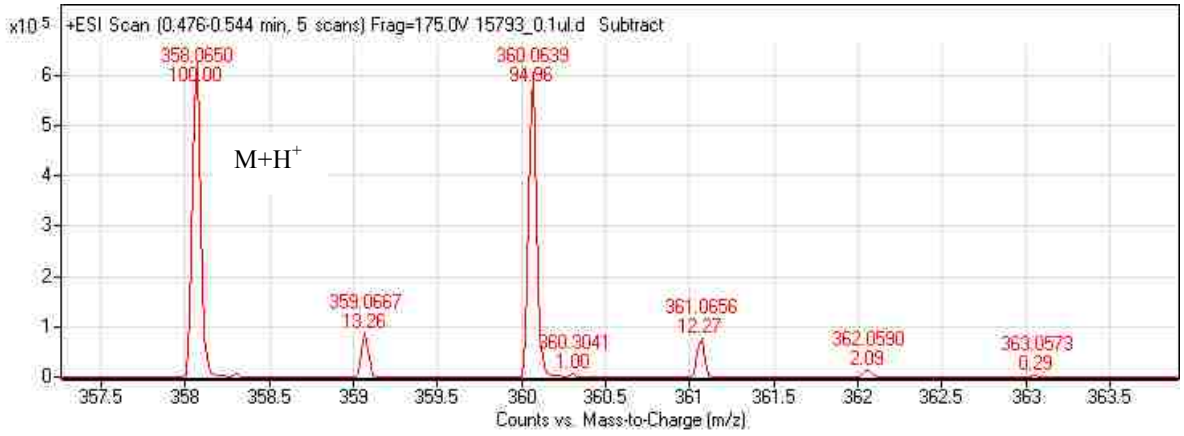

^{1}H NMR data for compound 2c

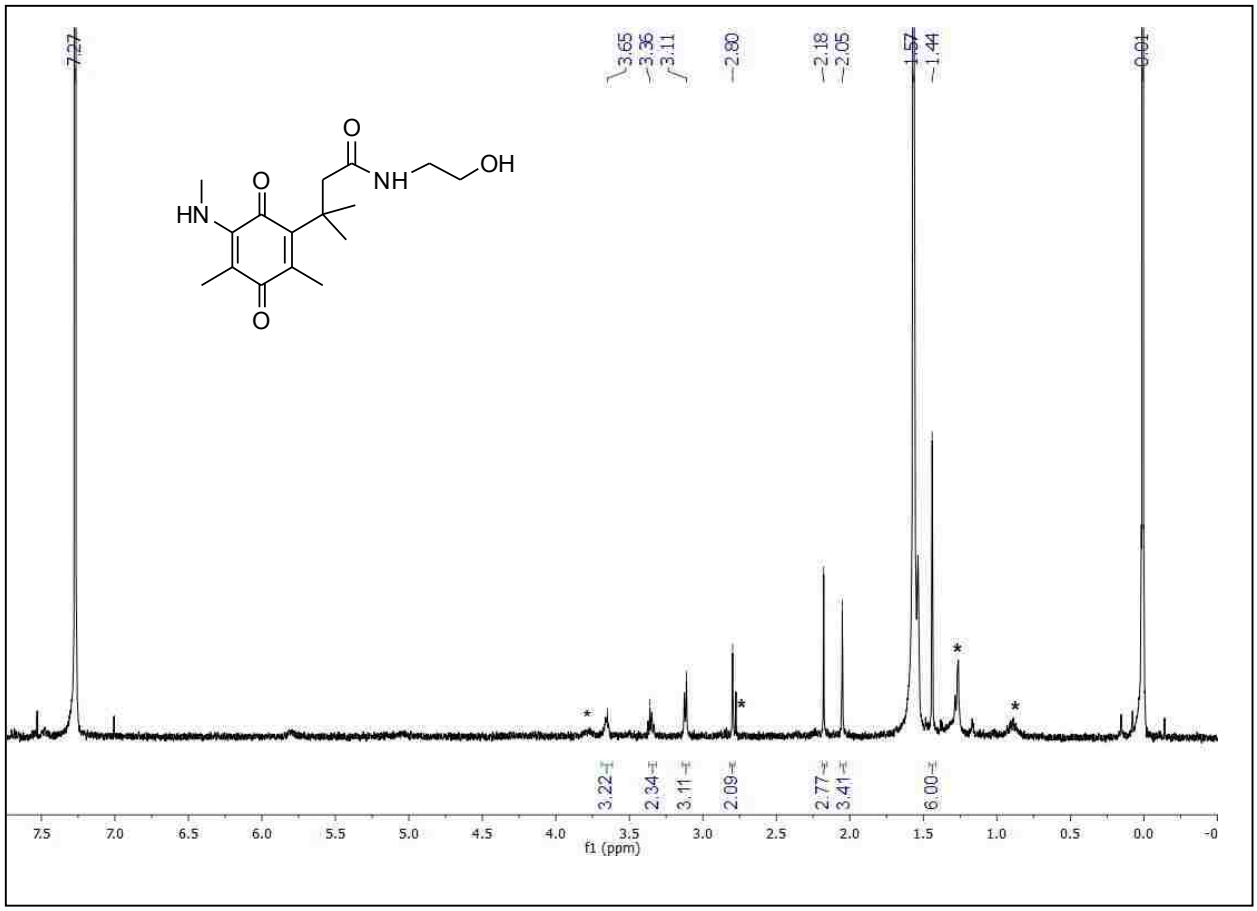

HR-ESI-ToF-MS data compound 2c

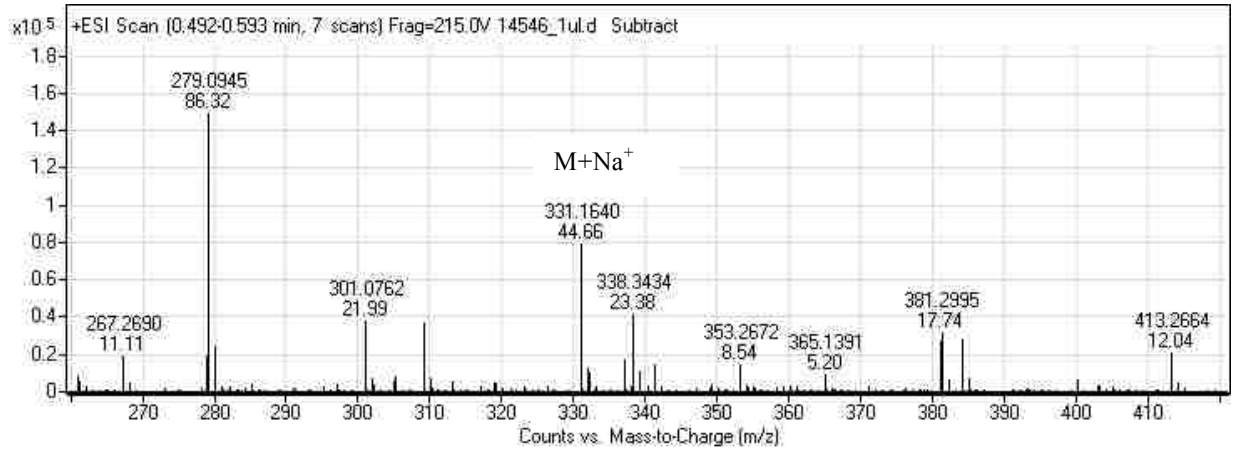

^{1}H NMR data for compound 2d

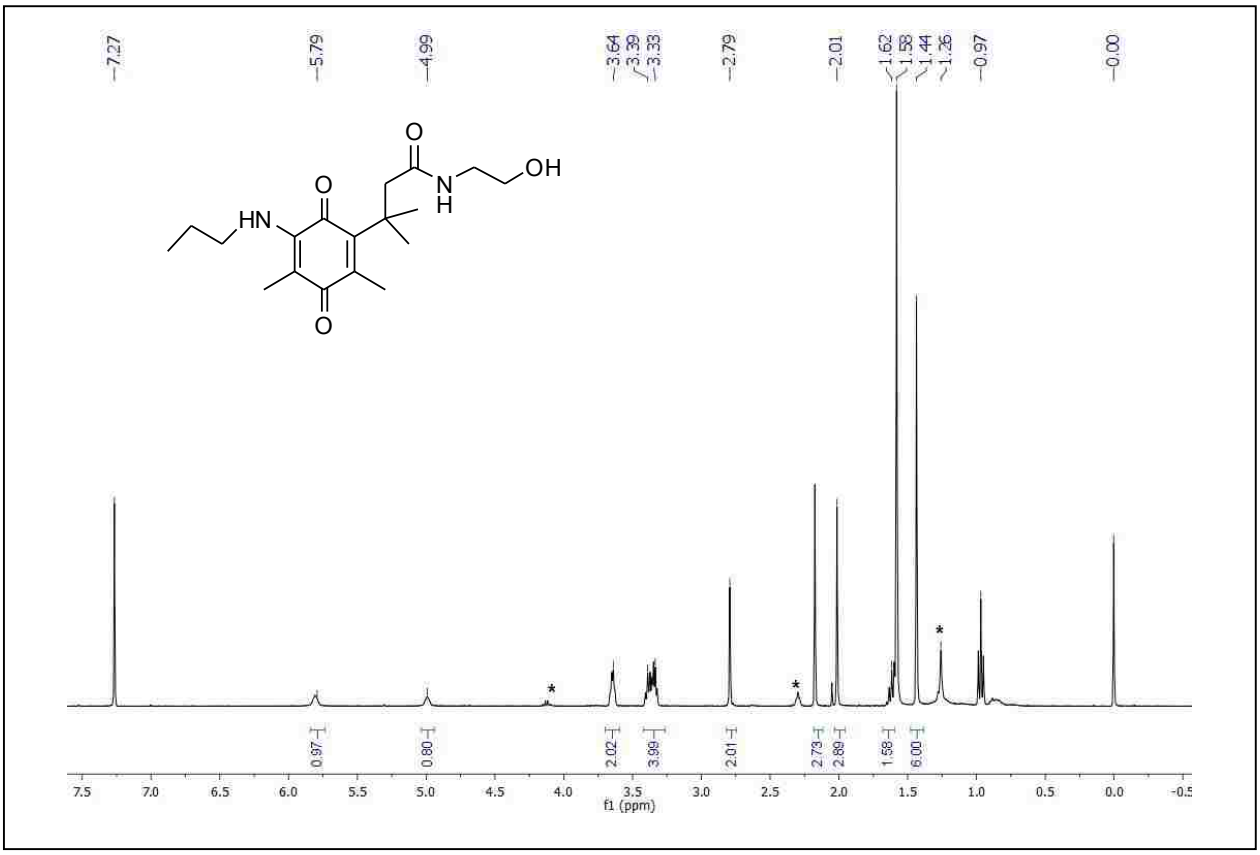

HR-ESI-ToF-MS data compound 2d

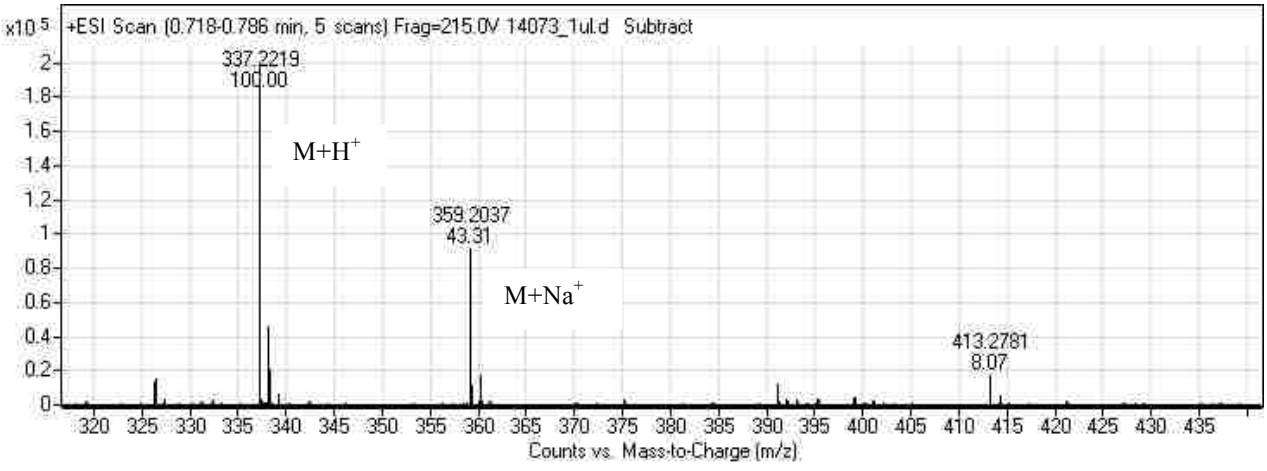

^{1}H NMR data for compound 2e

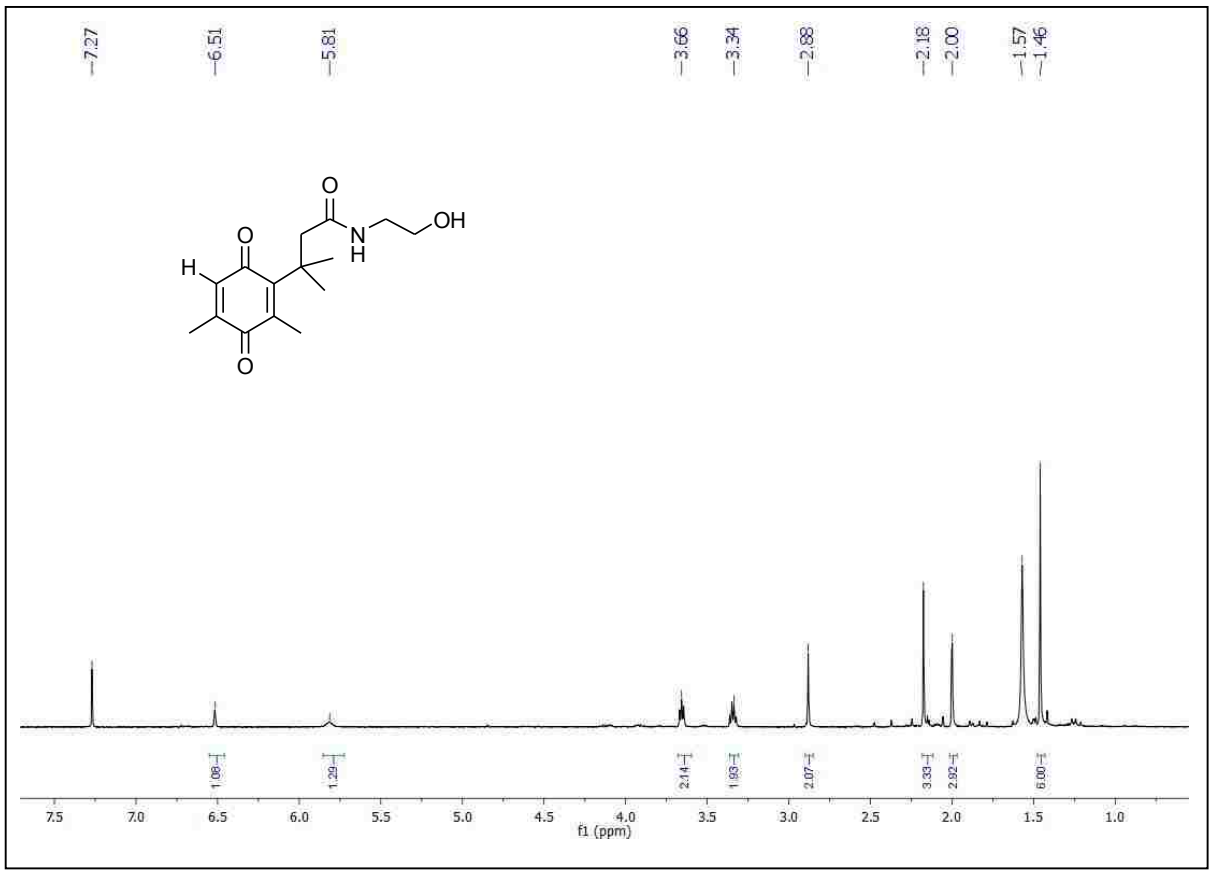

HR-ESI-ToF-MS data compound 2e

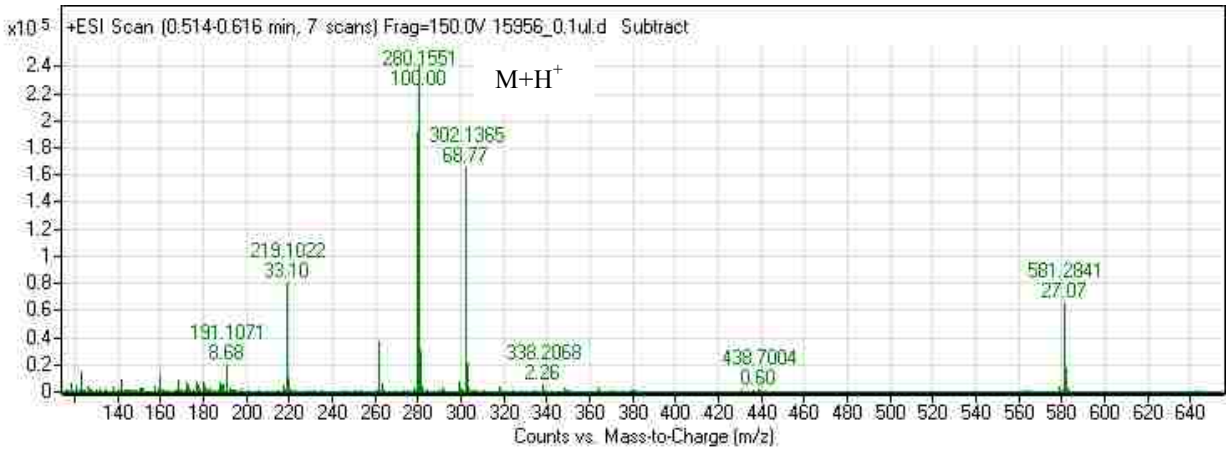

^{1}H NMR data for compound 2f

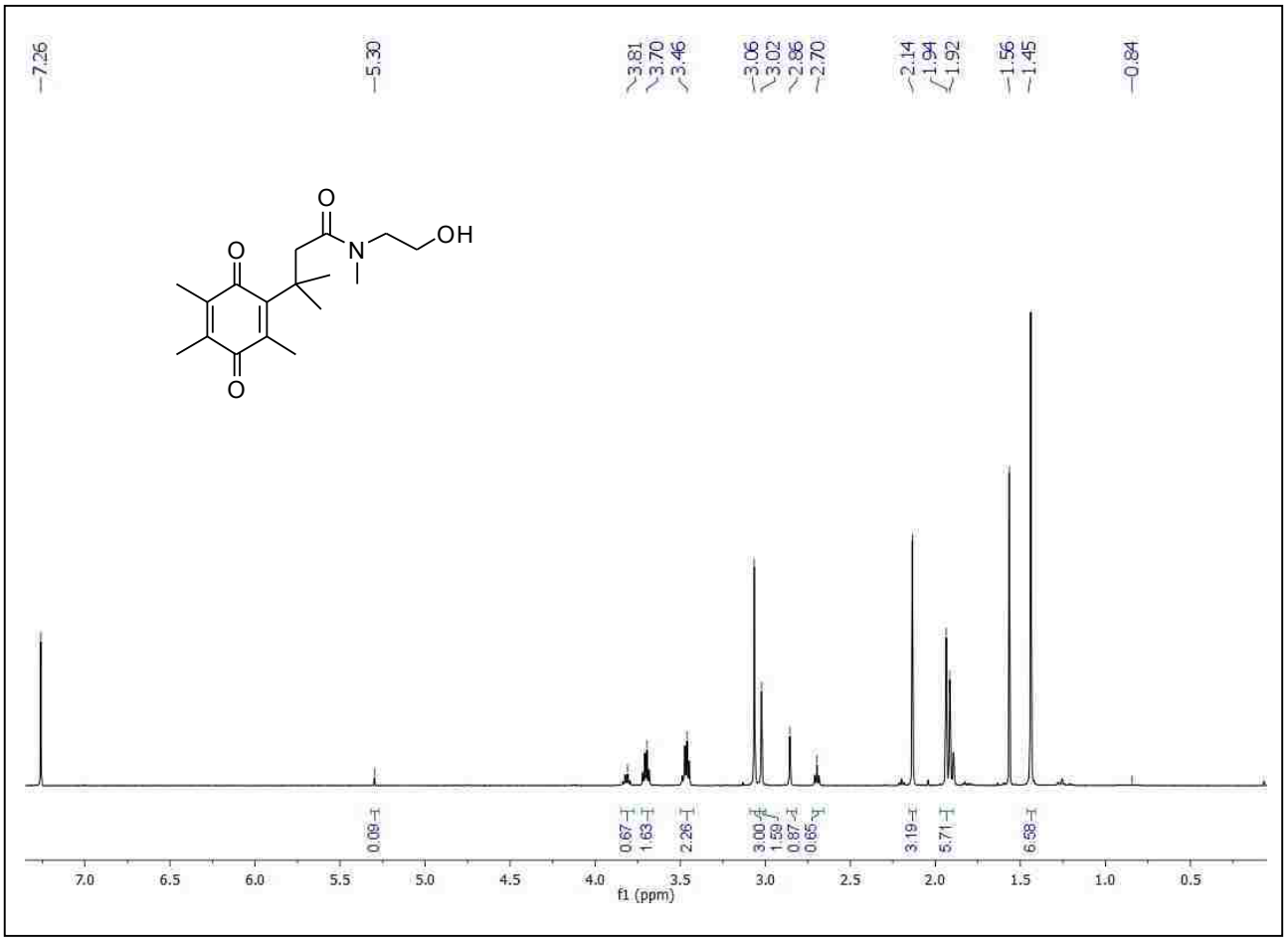

HR-ESI-ToF-MS data compound 2f

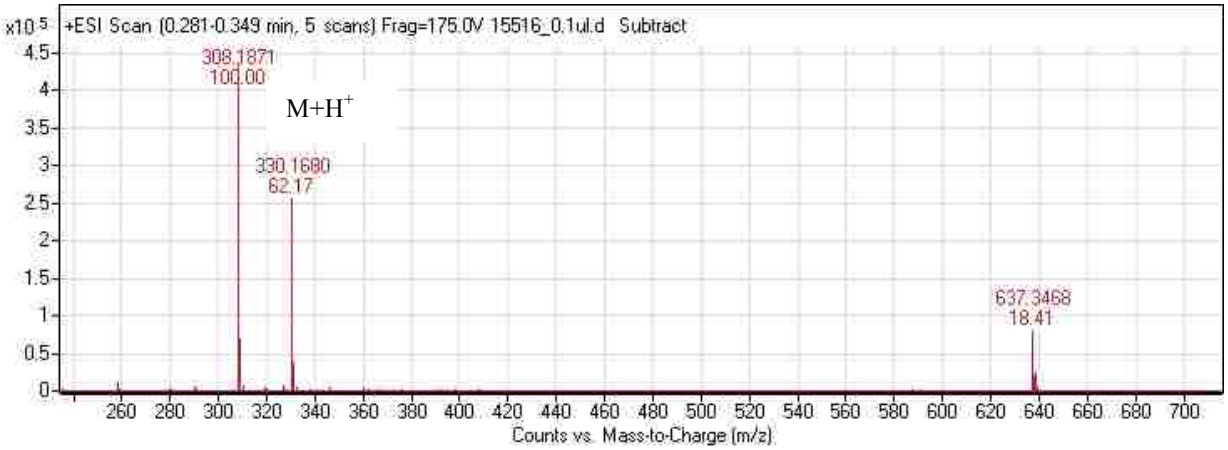

^{1}H NMR data for compound 7

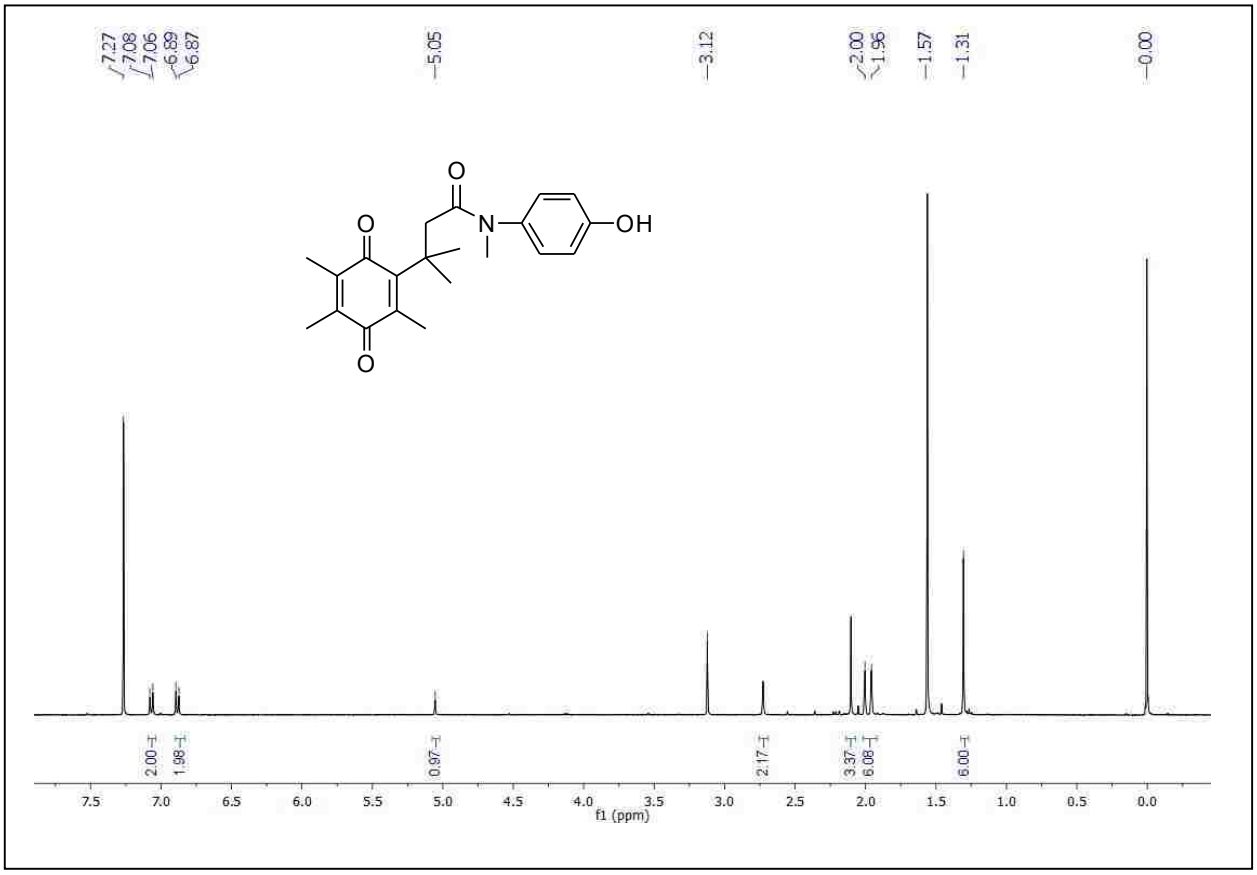

HR-ESI-ToF-MS data compound 7

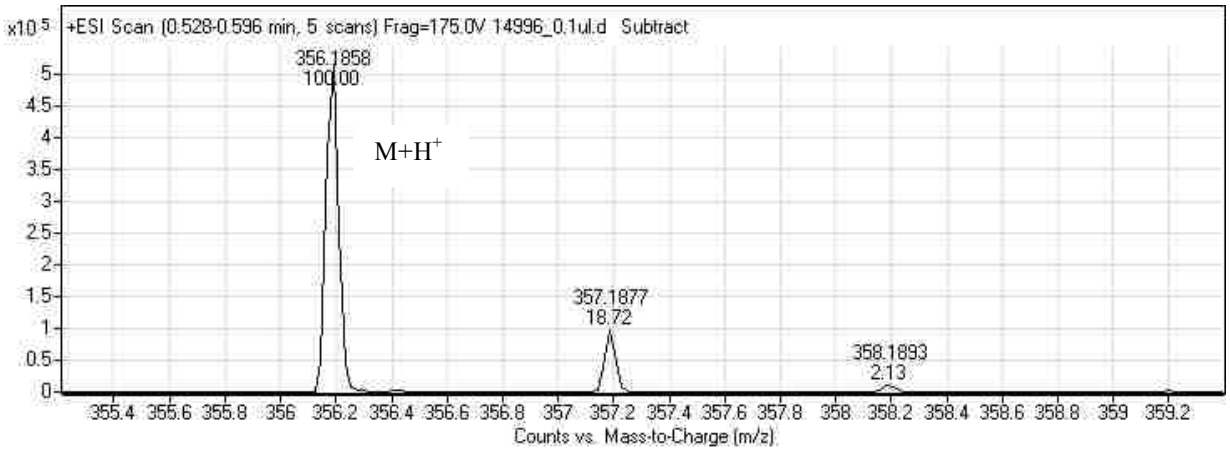

^{1}H NMR data for Internal Standard

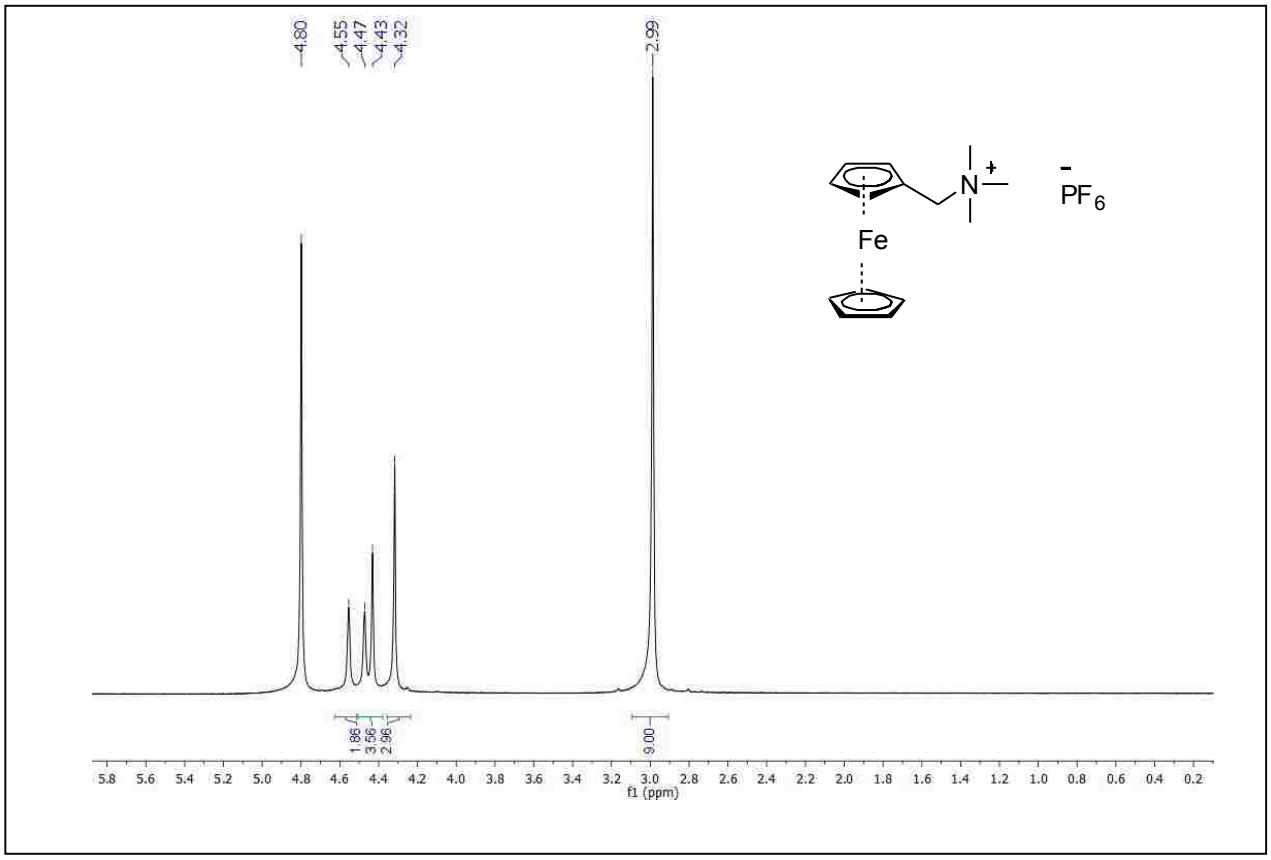

HR-ESI-ToF-MS data of Internal Standard

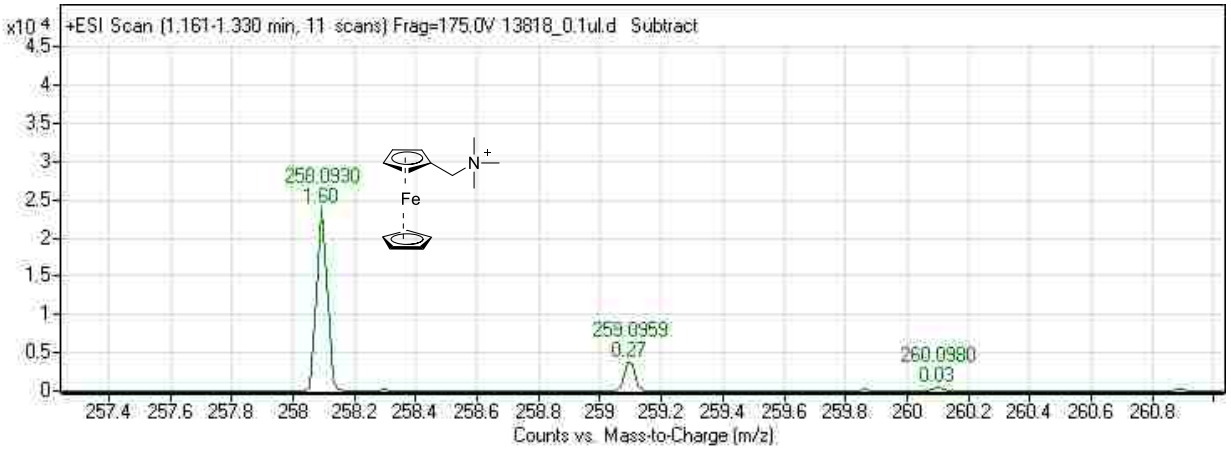

2.6 References

(1) Carrier, N. H. Redox-Active Liposome Delivery Agents with Highly Controllable Stimuli-Responsive Behavior. Ph.D. Dissertation, Louisiana State University, Baton Rouge, LA 2011.

(2) Carpino, L. A.; Triolo, S. A.; Berglund, R. A. Reductive lactonization of strategically methylated quinone propionic acid esters and amides. *The Journal of Organic Chemistry* **1989**, *54*, 3303-3310.

(3) Unruh, D. A.; Mauldin, C.; Pastine, S. J.; Rolandi, M.; Fréchet, J. M. J. Bifunctional Patterning of Mixed Monolayer Surfaces Using Scanning Probe Lithography for Multiplexed Directed Assembly. *Journal of the American Chemical Society* **2010**, *132*, 6890-6891.

CHAPTER 3
KINETIC STUDIES ON LACTONIZATION OF QUINONE PROPIONIC ACID AMIDE DERIVATIVES BY ^{1}H NMR FOR DEVELOPMENT OF REDOX-ACTIVE LIPOSOMES

3.1 Introduction

Liposomes are extremely versatile and malleable nanocarriers that attract great interest in drug delivery.[1] At present, the development of stimuli-responsive liposomal formulations that utilize endogenous triggers for cancer therapy is vast of interest.[2-5] Such systems have the ability to improve tumor selectivity and the activity of the anticancer agent compared to free drug, and hence other reduced harmful side effects.[2,6] However, the effectiveness of liposomal drugs not only depends on the properties of the encapsulated drug, but also on the pharmacokinetics, rate of drug release, and bio-distribution of the liposome carrier. Therefore, optimization of these carrier properties, especially the rate of drug release, is vital for chemotherapy.[1,7,8]

Liposomes that exhibit longer circulation life time, as well as therapeutically optimized drug release rates, are highly beneficial for *in vivo* therapeutic applications.[1] The relationship between circulation life time and antitumor activity was found to be directly proportional for various tumor models. In other words, extended circulation life times have revealed higher antitumor activity.[9,10] The same trend was observed with respect to rate of drug release from liposomes as anticancer agents which have shown greater stability and activity with prolonged exposure to cancerous cells.[1] Johnston and coworkers have demonstrated that vincristine, the cell cycle specific agent, has caused extensive antitumor activity with slower release rates for L1210, P388 (murine leukemia) and A431 (human squamous cell carcinoma) tumor models.[6] In addition, Drummond *et al*. have revealed a similar relationship against HT-29 (human colon carcinoma) and BT-474 (human breast carcinoma) cells with liposomal formulations of vinorelbine and

irinotecan, respectively. [1,11] Thus, it is important to optimize the drug releasing rate of liposomes in order to maximize the drug bioavailability, and hence, higher antitumor activity.

Inspired by the findings of redox-induced facile lactonization of trimethyl-lock quinones by Carpino and others,[12-14] the McCarley research group developed a new liposome system, where lipid (DOPE) head groups are capped with trimethyl-lock quinone propionic acid group.[15] Initial studies confirmed high stability, as well as stimulated payload release behavior, leading to the current work of optimization. Upon induction of a redox-stimulus, the quinone head group undergoes lactonization that leads to its cleavage from the DOPE lipid. Once the head group is released, naked lipid goes through a lamellar to inverted micelle hexagonal (L_α to H_{II}) phase transition, leading to release of the encapsulated contents.[15] Thus far, the McCarley research group has formulated four different liposome systems by varying the substituent at the 3′ position of the trimethyl-lock quinone propionic acid system (Q_H-DOPE, Q_{Me}-DOPE, Q_{Br} -DOPE, and Q_{nPr}-DOPE). Payload release studies of calcein entrapped in liposomes, using fluorescence spectroscopy, demonstrated the different liposomes to have unique release profiles.[8] The results indicate that the quinone head group plays an important role during the destabilization process, especially in the process of lactonization. Therefore, it is essential to identify the mechanism and kinetics of lactonization, such that liposome rupture can be modified to match the drug efficacy profiles and thereby improve therapeutic impact.

After the discovery of the trimethyl-lock ortho-hydroxyhydrocinnamic acid undergoes facile lactonization, research has progressed to identify its mechanism and rates of reaction.[16] Cohen and several other research groups extensively studied the lactonization process of ortho-hydroxyhydrocinnamic acids experimentally and figured out the mechanism as follows. The phenolic moiety of the ortho-hydroxyhydrocinnamic acid undergoes nucleophilic attack at the

propionic acid carbonyl to yield a tetrahedral intermediate in an equilibrium process. Then the intermediate proceeds via collapse to form the lactone via the slower rate determining step.[16-20] This process has been adapted for the quinone propionic acids here in[12-14] Scheme 3.1.

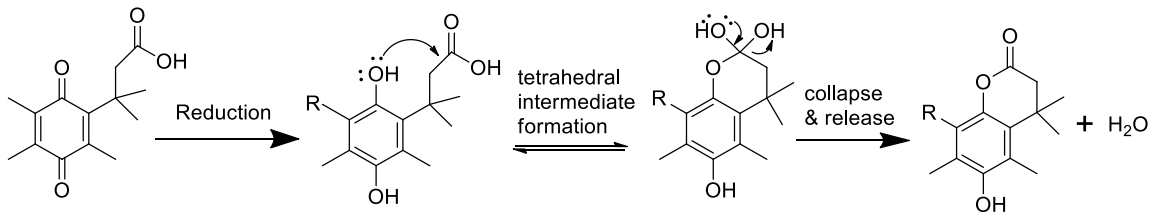

Scheme 3.1: General mechanism of trimethyl-lock quinone lactonization.

Currently, we are developing two major types of liposome formulations using the following parent lipid structures (Figure 3.2). Because lactonization plays a major role in the process of liposome destabilization, it is critical to find out the rate of cyclization of these structures upon reduction, so as to fully understand liposome contents release. In order to achieve this target, model compounds of different trimethyl-lock quinone propionic acid amide derivatives were synthesized by varying the amide structure (R_1, R_2) and the functional group at the 3′ position (R_3, Figure3.1: quinone-ethanolamine (R_3 = CH_3, Br, NPr, H, NMe, R_2 =H, R_1 = CH_2CH_2OH; Q-ETA), quinone-methylethanolamine (R_3 = CH_3, R_2 = CH_3, R_1= CH_2CH_2OH; Q-MeETA), quinone-methylaminophenol (R_3 = CH_3, R_2 =CH_3 =R_1 =C_6H_5OH; Q-NMeBnOH)). Synthesized derivatives mimic the parent lipid structure to a greater extent and follow the same mechanism with respect to reductive activation where they form lactone by releasing free amine to the reaction medium.

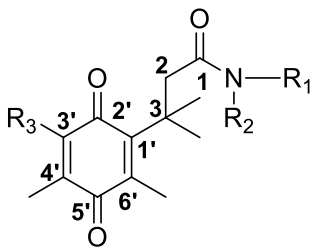

Figure 3.1: Amide derivative of trimethyl-lock quinone propionic acid.

Nuclear magnetic resonance (NMR) spectroscopy is a powerful tool to investigate compound behavior with respect to different perturbations.[12,21] Therefore, ^{1}H NMR experiments were carried out to investigate the lactonization behavior of the synthesized derivatives. The results described herein explain the effect of varying the 3′ quinone functionality, amide structure (R_1, R_2) as well as reaction conditions including temperature, solvent, and buffer toward the rate of lactonization.

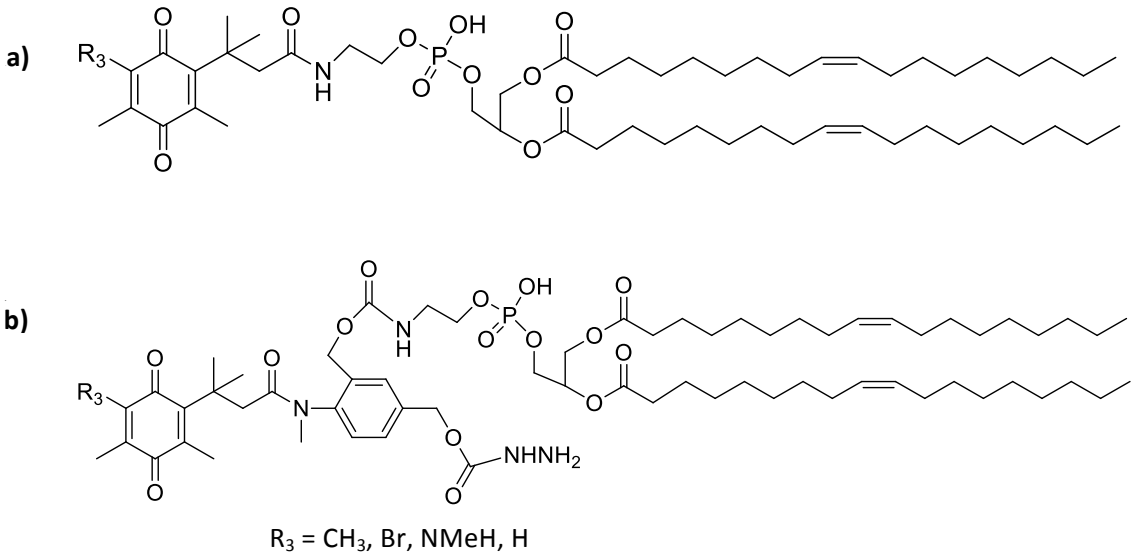

Figure 3.2: Parent lipid structures a) Q-DOPE b) Q-AQM-DOPE used for liposome formation.

3.2 Experimental Section

3.2.1 Materials

Deuterated solvents (D_2O, d_6-DMSO 98%), potassium dideuterium phosphate (KD_2PO_4), dipotassium deuterium phosphate (K_2DPO_4), potassium chloride (KCl), deuterated sodium hydroxide (NaOD), sodium hydroxide pellets (NaOH), methanol (MeOH), and sodium dithionite ($Na_2S_2O_4$) were purchased from Sigma Aldrich. Except sodium dithionite, all the other chemicals were used as received. Sodium dithionite was purified before use (Section 3.2.2). Previously synthesized ferrocene salt ($C_{18}H_{20}F_6FeNP$, Figure 3.3) was used as an internal standard for some ^1H NMR experiments.

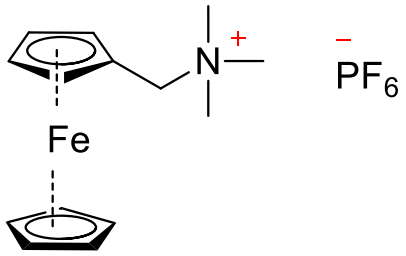

Figure 3.3: Ferrocene salt, internal standard used for ^1H NMR experiments.

3.2.2 Sodium Dithionite ($Na_2S_2O_4$) Purification

Commercially available sodium dithionite (6 g) was dissolved in 40 mL of degassed 0.1N NaOH solution under inert conditions. To this solution, 45 mL of degassed MeOH/ 0.1N NaOH (4:1) solution was slowly added through a syringe until crystals form from the solution. Once crystals appeared, the solution was drained and this sequence was repeated for a total of three times to gain purified dithionite crystals. Purified wet dithionite crystals were then vacuum dried for 24 hours and were stored under inert dry conditions.[22]

3.2.3 Deuterated Buffer Preparation

Potassium dideuterium phosphate (23.74 mg, 0.0333M), dipotassium deuterium phosphate (59.12 mg, 0.0666M), and potassium chloride (38.24 mg, 0.1 M) were dissolved in 5 mL of D_2O solution while adjusting to required pD (7.21 or 7.41) using deuterated sodium hydroxide to gain a 0.1 M phosphate buffer solution.

3.2.4 Instrumentation

3.2.4.1 Nuclear Magnetic Resonance Spectroscopy (NMR)

Kinetic experiments were conducted using either a Bruker AV Liquid 400 MHz or Bruker DPX 400MHz spectrometer. After addition of chemical reducing agent ($Na_2S_2O_4$), successive spectra were collected at 1 min 33 second or 2 min 29 second intervals, and each spectrum was set to acquire 16 or 32 scans with pre-scan delay. The spectra were normalized with respect to the three methyls (δ 2.85 ppm) of the ferrocene internal standard. The change in integrals of gemdimethyls was used as index to evaluate the kinetics.[23]

3.2.5 General Procedure for Sample Preparation

3.2.5.1 D_2O as Solvent

An internal standard solution was prepared by dissolving ferrocene salt in Figure 3.3 (0.02–0.03 g) in D_2O (3 mL). The quinone-amide compound (0–3 mg) was dissolved in this same internal standard solution (700 μL), and the initial ^{1}H NMR spectrum was recorded. A similar amount of the quinone-amide (0–3 mg) was dissolved in 500 μL of the internal standard solution. To this solution, an excess of sodium dithionite (5:1, $S_2O_4^{2-}$:quinone-amide) in 200 μL of internal standard was added, and successive ^{1}H NMR spectra were recorded. All the NMR solutions were degassed before spectral acquisition.

3.2.5.2 DMSO-D_2O as Solvent

Ferrocene salt in Figure 3.3 (2–3 mg) and the quinone-amide compound (0–4 mg) were dissolved in a 5:2 (v/v) mixture of DMSO and D_2O (700μL) and the initial ^{1}H NMR spectrum was recorded. A similar amount of ferrocene salt in Figure 3.3 (2–3 mg) and quinone-amide compound (0–4 mg) were dissolved in 500 μL of DMSO, and to this solution, an excess of sodium dithionite (5:1, $S_2O_4^{2-}$:quinone-amide) in 200 μL of D_2O was added. ^{1}H NMR spectra were recorded successively. All the NMR solutions were degassed before spectral acquisition.

3.3 Results and Discussion

3.3.1 Lactonization Behavior of Q-ETA Derivatives

3.3.1.1 Effect of Functional Group

To investigate the effect of quinone functionality at the 3′ position on the quinone on lactonization, five different quinone-ethanolamine (Q-ETA) derivatives were synthesized (Q_{Me}-ETA, Q_{Br}-ETA, Q_{NMe}-ETA, Q_H-ETA, Q_{NPr}-ETA) and were subjected to ^{1}H NMR experiments according to the procedure described in Section 3.2.5.1 in D_2O medium. Compounds showed different lactonization profiles after reduction, and the behavior of each derivative will be discussed in the following paragraphs.

In Figure 3.4 is shown the reduction and lactonization behavior of Q_{Me}-ETA upon addition of sodium dithionite (reducing agent). ^{1}H resonances of all the peaks were shifted downfield with respect to the initial spectrum (Figure 3.4 A) by 0.25 ppm and that spectrum was attributable to the corresponding tetrahedral intermediate (Figure 3.4 B). This outcome was expected, due to previous UV spectroscopic studies confirming the quinone is essentially instantly (100 ms) reduced to hydroquinone, and its rapid transformation to the tetrahedral intermediate[24]. In the successive spectra, the intensity of peaks indicated as **a′, b′, c′, d′, e′** and

g′ decreased, while that of the peak indicated as **h′** was increased with time. The intensity of the peak denoted as **f′** remained constant. The changed signals, **a′, b′, c′, d′,** and **e′** are associated with the time-dependent lactone formation, whereas remaining signals, **f′** and **h′** are associated with release of ethanolamine to the medium. The lactone precipitated from solution, resulting in a decrease of the corresponding signals in the spectrum. The process was completed approximately after 170 minutes (Figure 3.4 F) and was verified by the respective control experiment. The Figure 3.5 is shown the spectra for an authentic sample of Q_{Me}-lactone with ferrocene (top) and the lactonized product after completion of the reaction (bottom). Because lactone peaks did not show up in both spectra, insolubility of the lactone in D_2O medium can be confirmed.

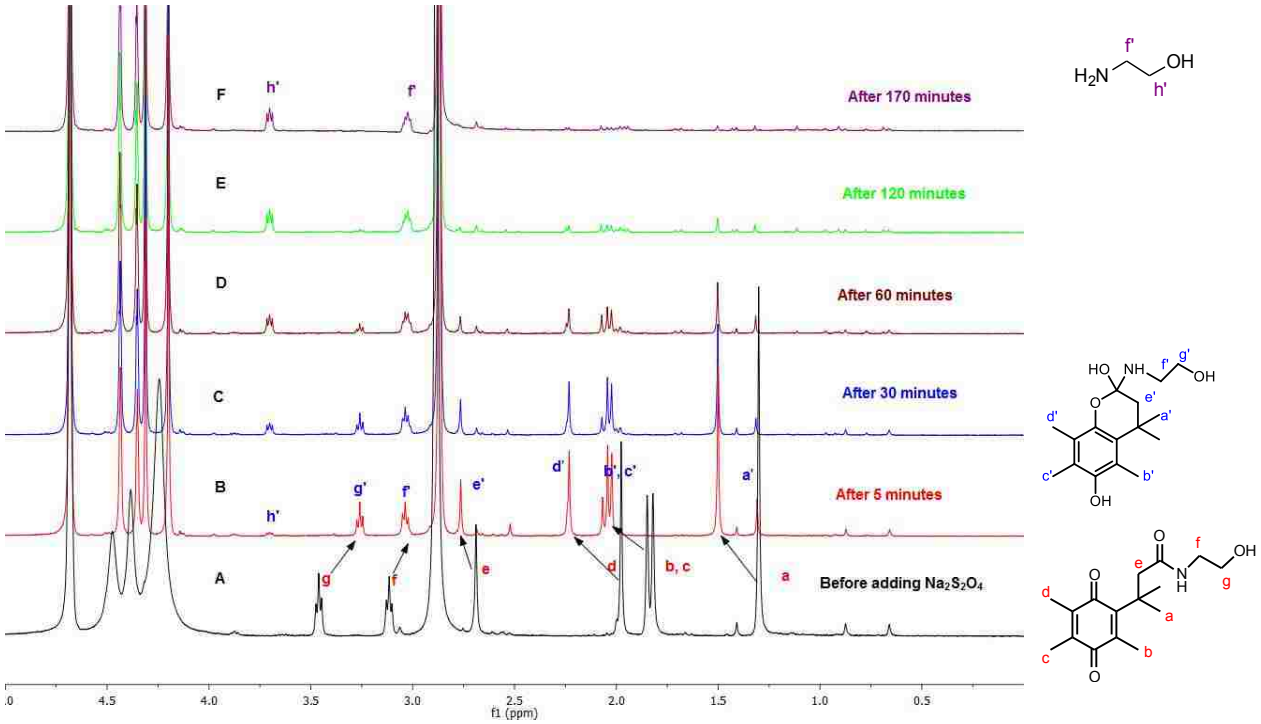

Figure 3.4: Time-dependent Q_{Me}-ETA (3.8×10^{-3} M) lactonization in pure D_2O by ^1H NMR. The signals at δ 2.85 ppm and 4.20–4.50 ppm are associated with the internal standard.

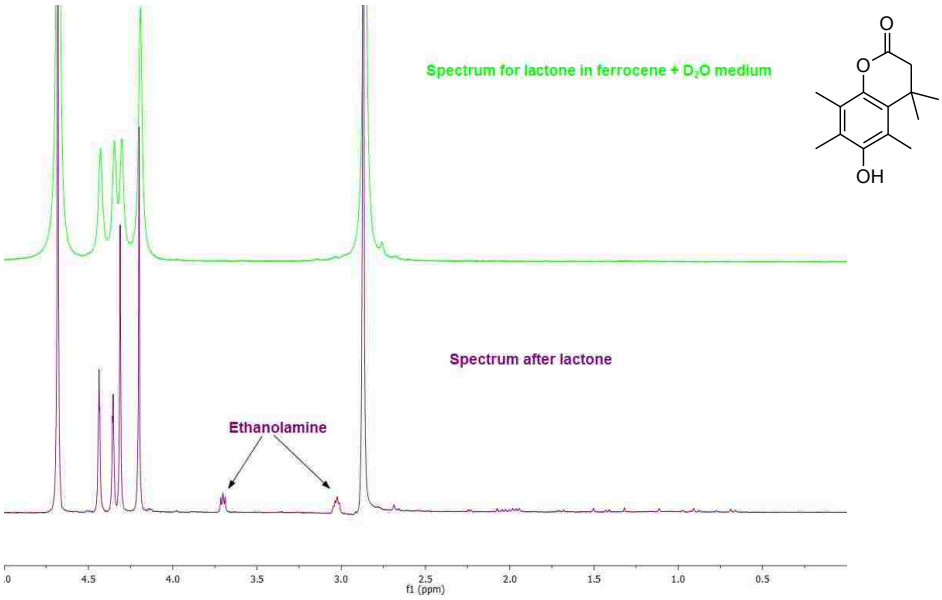

Figure 3.5: Confirmation of Q_{Me}-lactone (4.8×10^{-3} M) precipitation in pure D_2O by ^1H NMR. The signals at δ 2.85 ppm and 4.20–4.50 ppm are associated with the internal standard.

In order to evaluate the kinetics of the process, integration of the gemdimethyl signal at 1.46 ppm of successive spectra were collected, as its intensity is directly proportional to the remaining tetrahedral intermediate concentration [Q_{Me}-ETA_{Tet}] at any given time. The [Q_{Me}-ETA_{Tet}] with respect to time was calculated using respective integrals and initial Q_{Me}-ETA concentration. The plot of ln ([Q_{Me}-ETA_{Tet}]$_{t=t}$ / [Q_{Me}-ETA_{Tet}]$_{t=0}$]) versus time showed linear decay (Figure 3.6) where reaction followed the integrated rate law of first-order kinetics and can be explained by following mathematical Equations 3.1 and 3.2.[25,26]

$$[Q_{Me}\text{-}ETA_{Tet}]_{t=t} = [Q_{Me}\text{-}ETA_{Tet}]_{t=0}\, e^{-kt} \qquad \textbf{Equation 3.1}$$

$$\ln ([Q_{Me}\text{-}ETA_{Tet}]_{t=t} / [Q_{Me}\text{-}ETA_{Tet}]_{t=0}]) = -kt \qquad \textbf{Equation 3.2}$$

The rate constant (k) of the lactonization process was obtained as k = 0.023 min^{-1} and half life of the reaction was calculated from Equation 3.3[25,26] as $t_{½}$ = 30 minutes.

$$t_{½} = \ln 2 / k \qquad \textbf{Equation 3.3}$$

Reduction and lactonization of Q_{Br}-ETA (Figure 3.7) was rapid, and the reaction was complete within 5 minutes. Bromo-lactone was precipitated from the solution, while ethanolamine was released to the medium. This behavior was mainly due to the inductive electron withdrawing nature of the bromine functionality which facilitates faster reduction followed by more rapid lactonization. Using 1% remaining reactant and $t_{99\%}$ = 5 min, k is estimated to be ≥ 0.9 min^{-1}. Further studies on Q_{NMe}-ETA and Q_{NPr}-ETA derivatives (Figure 3.8 and 3.9) have exhibited almost same reduction and lactonizaton profile as Q_{Br}-ETA. The processes were completed within 3 minutes possibly due to the internal base catalysis behavior of nitrogen atom of NMe and NPr groups. Using 1% remaining reactant and $t_{99\%}$ = 3 min, k is estimated to be ≥ 1.5 min^{-1}. However, the resulting lactones were soluble in the D_2O medium due to the effect of hydrogen bonding and were able to be detected in consecutive spectra.

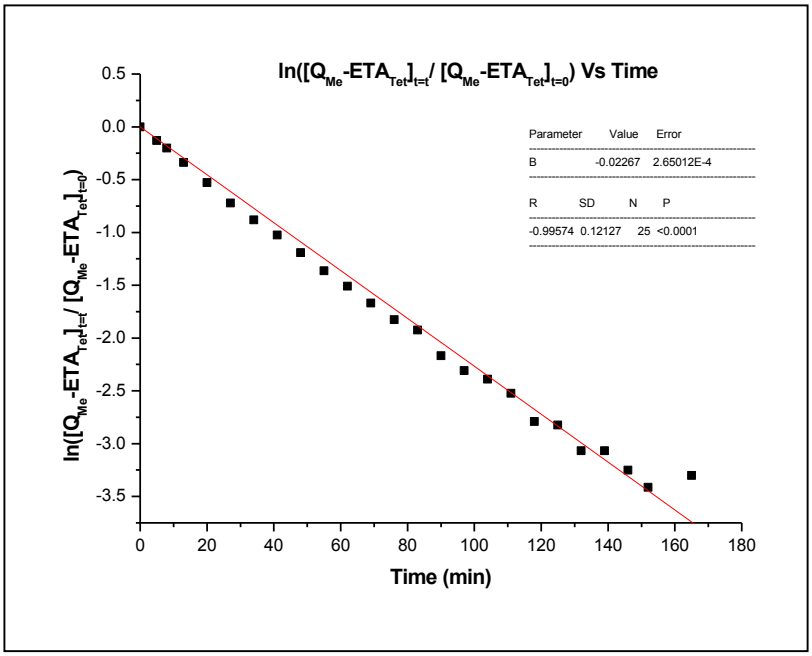

Figure 3.6: Kinetic evaluations of Q_{Me}-ETA lactonization in pure D_2O medium.

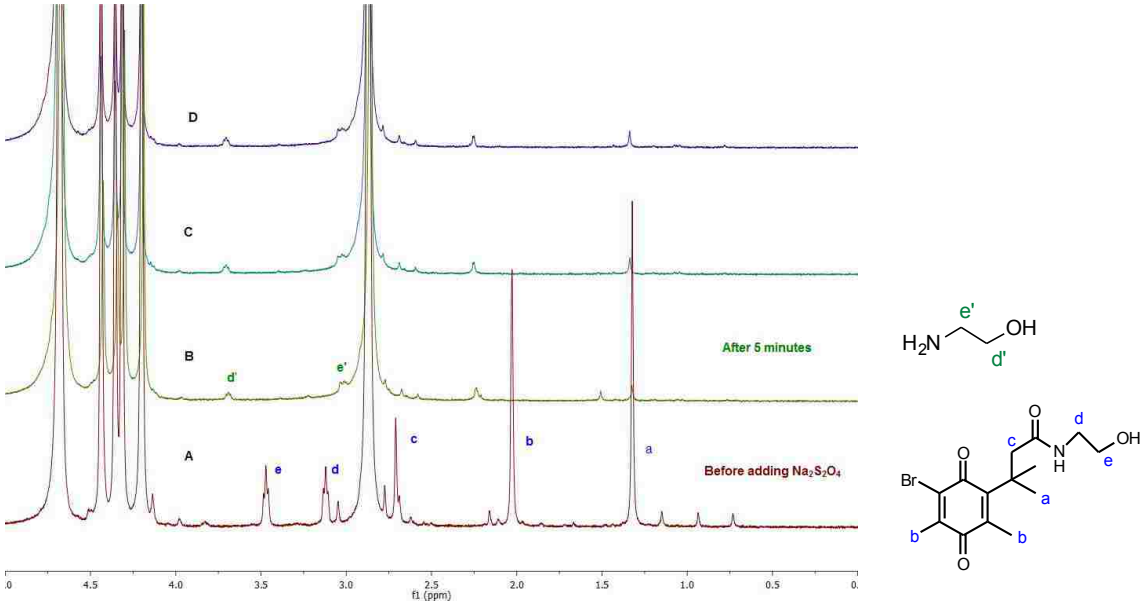

Figure 3.7: Time-dependent Q_{Br}-ETA (3.16×10^{-3} M) lactonization in pure D_2O by ^1H NMR. The signals at δ 2.85 ppm and 4.20–4.50 ppm associated with the internal standard.

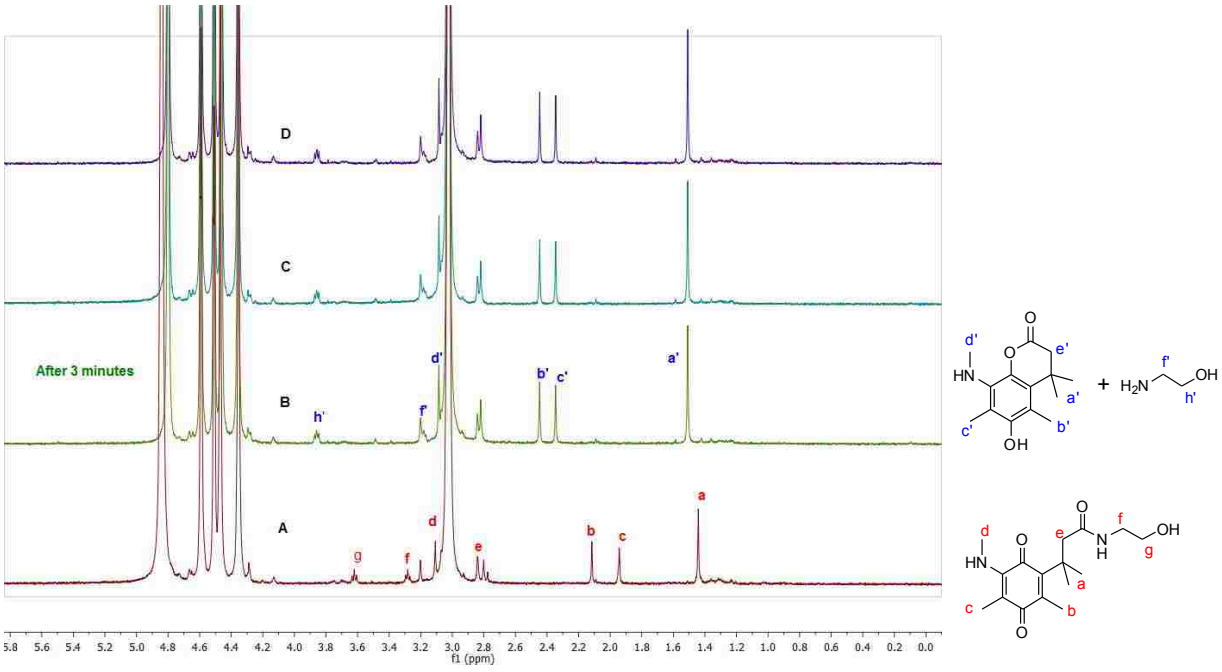

Figure 3.8: Time-dependent Q_{NMe}-ETA (3.80×10^{-3} M) lactonization in pure D_2O by ^1H NMR. The signals at δ 3.00 ppm and 4.30–4.60 ppm associated with the internal standard.

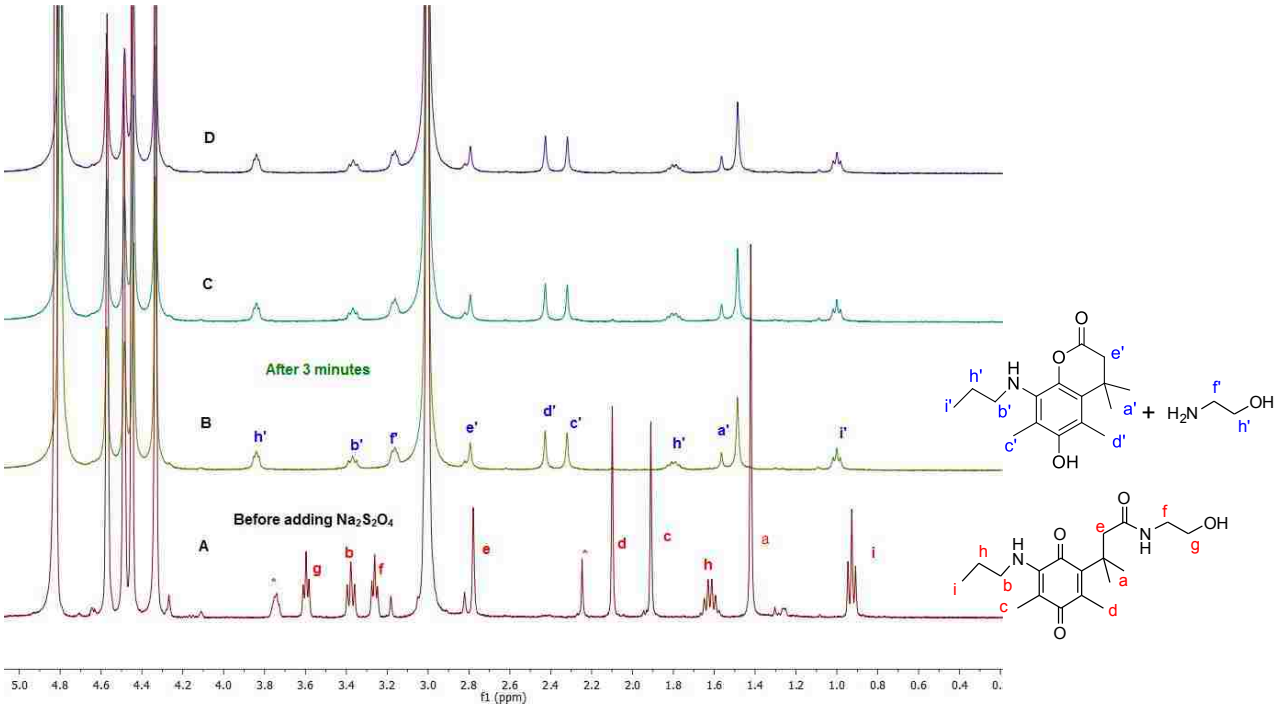

Figure 3.9: Time-dependent Q_{NPr}-ETA (3.02×10^{-3} M) lactonization in pure D_2O by ^1H NMR. The signals at δ 3.00 ppm and 4.30–4.60 ppm associated with the internal standard. The signals denoted as asterisks indicate the residual solvents that remain from the purification.

On the contrary, Q_H-ETA compound has shown a complicated spectrum in D_2O medium, where the peaks corresponding to methyls were split even before adding the reducing agent (Figure 3.10 A). This observation might be due to the formation of one or more degradation products, such as spirolactams in aqueous condition (Scheme 3.2).[27] Formation of spirolactam has been an extensively studied concept, and is more prominent in base-catalyzed soft reaction conditions.[27-29] Base mediated (D_2O) deprotonation of the amide nitrogen facilitates the negative charge formation on nitrogen, resulting a highly reactive nucleophilic species that can attack the quinone ring to form several products.[29] However, the formation of product **5** (Scheme 3.2) is thermodynamically less favorable, but it might be kinetically possible owing to the release of steric strain involved in the trimethyl lock system.[27] Therefore, more research is required to further ascertain the identity of the spirolactam products.

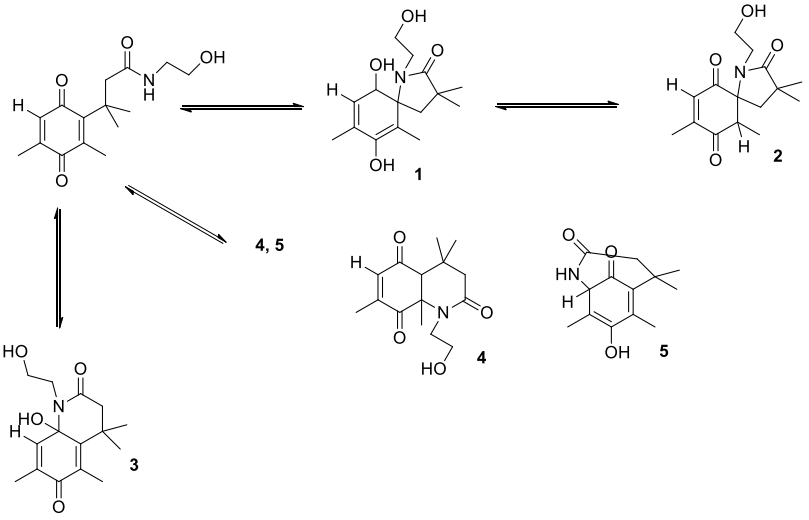

Scheme 3.2: Possible degradation routes of Q_H-ETA in aqueous condition in the absence of a reducing agent.

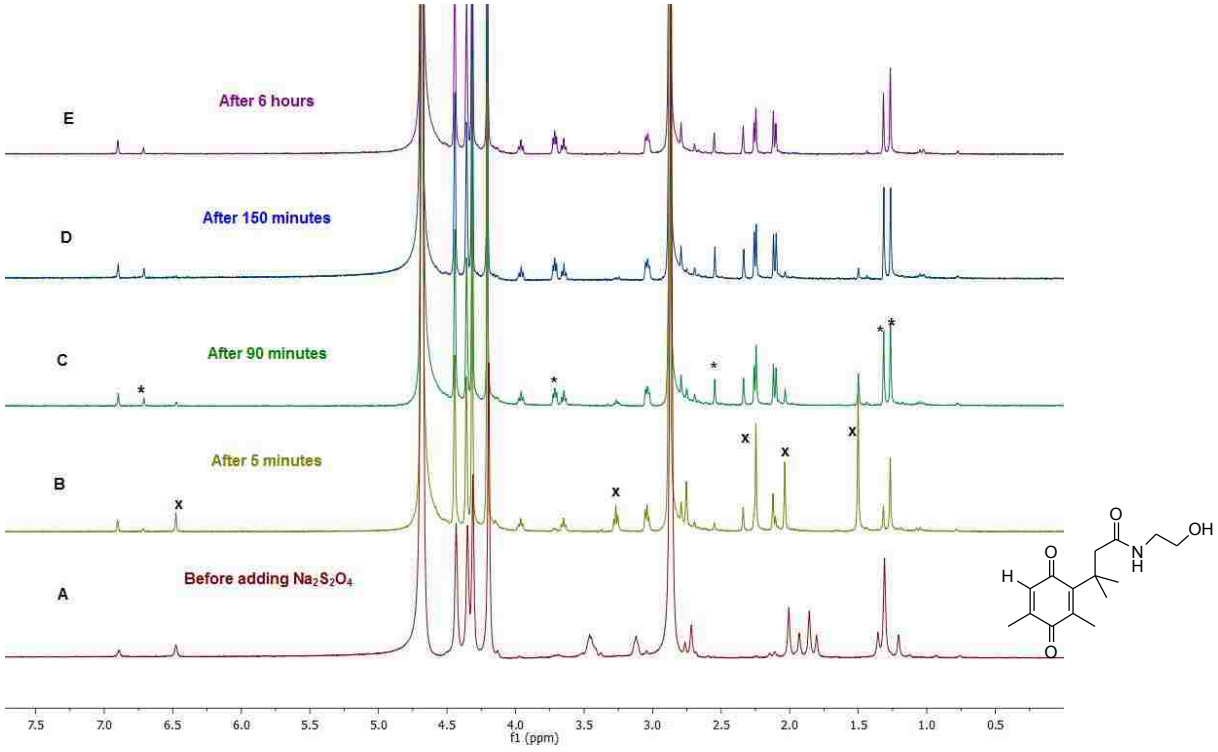

Figure 3.10: Time-dependent Q_H-ETA (4.7×10^{-3} M) lactonization in pure D_2O by ^1H NMR. The signals at δ 2.85 ppm and 4.20–4.50 ppm associated with the internal standard. Asterisk (*****) and (**x**) represent the increasing and decreasing signals respectively.

Upon introduction of the reducing agent, peaks were shifted downfield, and the spectrum was more complicated, indicating the formation of tetrahedral intermediate along with

spirolactam product (Figure 3.10 B). Peaks denoted by an asterisk (*) increased, while peaks symbolized as (**x**) were decreased with time. The others remained constant throughout the experimental period. However, no detectable precipitation of lactone occurred for 6 hours (Figure 3.10 C-E), revealing the much slower lactonization process in D_2O medium. Furthermore, the spectrum of pure Q_H-ETA in $CDCl_3$ was recorded to assess the possibility of spirolactam formation under organic conditions. The spectrum did not show any splitting as in the previous, thus confirming that degradation does not take place in an organic medium (Figure 3.11). The same trend was observed with the Q_H-COOH system, pointing out that the H functionality at the 3′ position is associated with spirolactam formation in D_2O medium (Figure 3.12).

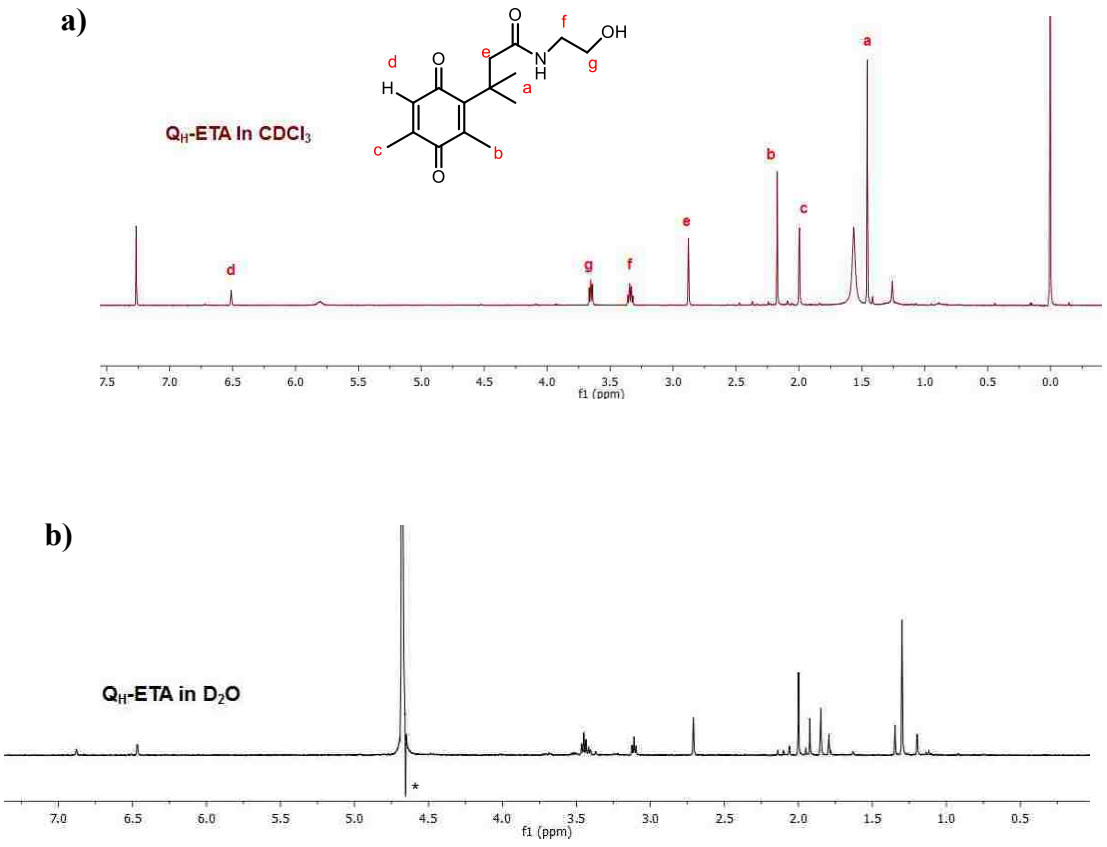

Figure 3.11: Spectral comparison of Q_H-ETA in (a) $CDCl_3$ and (b) D_2O medium. Asterisk (*) at 4.65ppm in spectrum (b) represents the noise peak.

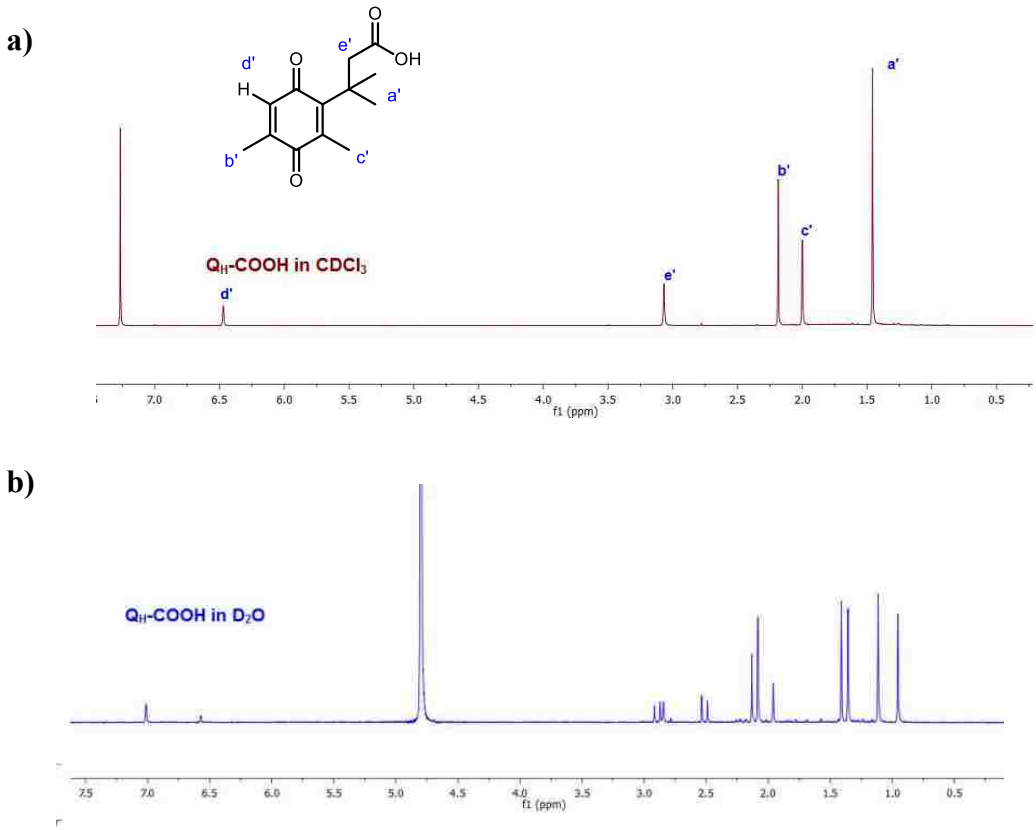

Figure 3.12: Spectral comparison of Q_H-COOH in (a) $CDCl_3$ and (b) D_2O medium.

3.3.1.2 Effect of Organic Solvents

As a majority of bulky quinone propionic amide derivatives do not dissolve in aqueous medium, it is important to understand how the presence of organic solvents affect their rate of reduction and lactonization. Thus, as an initial attempt, lactonization studies were conducted with Q_{Me}-ETA in a mixture of DMSO:D_2O (5:2) in order to compare the nature of the lactonization process with respect to aqueous conditions.

The rate of reduction was as fast as previous studies (compare Figure 3.13 A and B to Figure 3.4 A and B), but the cyclization was slower compared to the study in pure D_2O medium indicating that the tetrahedral intermediate is somewhat stable in organic medium (compare Figure 3.13 C through D to Figure 3.4 C through F). However, dramatic concentration reduction was observed after addition of the chemical reducing agent. This observation might be due to

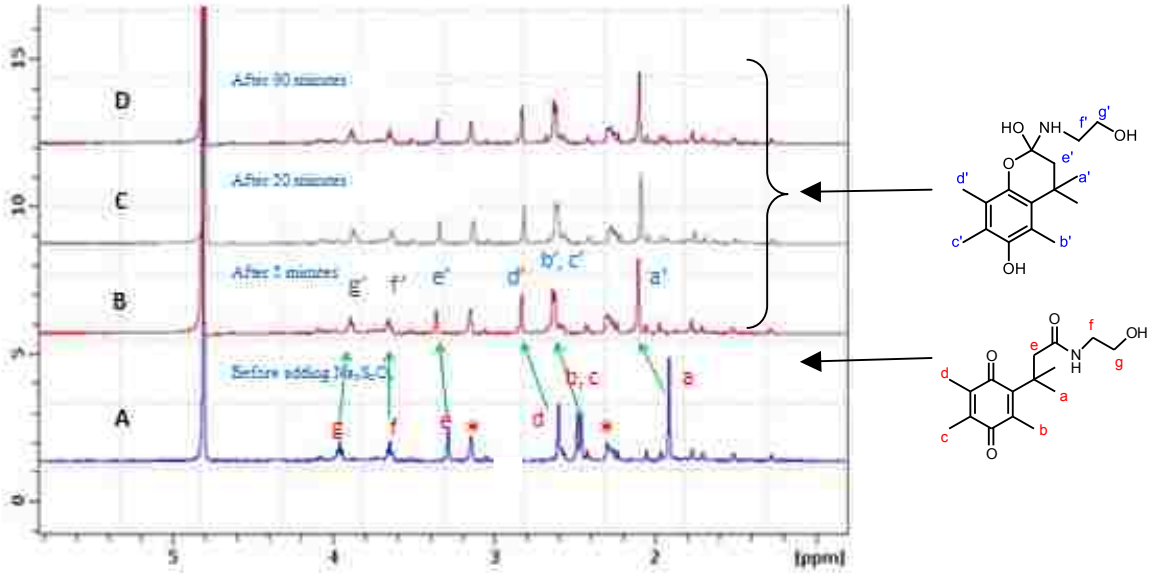

Figure 3.13: Time-dependent Q_{Me}-ETA lactonization in a 5:2 mixture of DMSO:D_2O by ^1H NMR in the absence of internal standard. (*) denotes the impurities from medium.

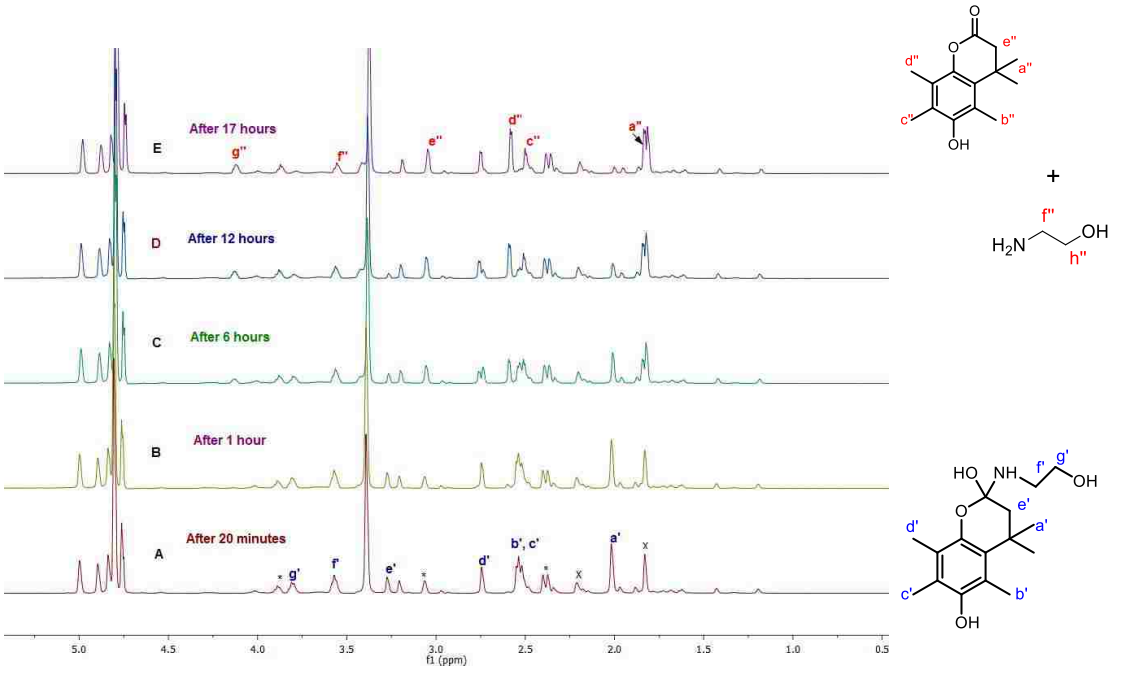

Figure 3.14: Time-dependent Q_{Me}-ETA (1.7×10^{-2} M) lactonization in a 5:2 mixture of DMSO: D_2O by ^1H NMR in the presence of internal standard. Both (*) & (x) denote the impurities from medium.

the salt precipitation from the medium leading to lower quinone to hydroquinone conversion. Both lactone and ethanolamine were soluble in the reaction medium, and the process was complete after approximately 17 hours (Figure 3.14 A-E). The rate constant (k) and half life ($t_{1/2}$) were found as 0.0026 min^{-1} and 2.7×10^2 minutes respectively (Figure 3.15). Lactonization was 9 times slower compared to the study in D_2O medium, and these findings are comparable with previous rate data that were obtained via cyclic voltammetry (CV)[30] and UV-visible spectroscopy by colleagues in the McCarley research group.

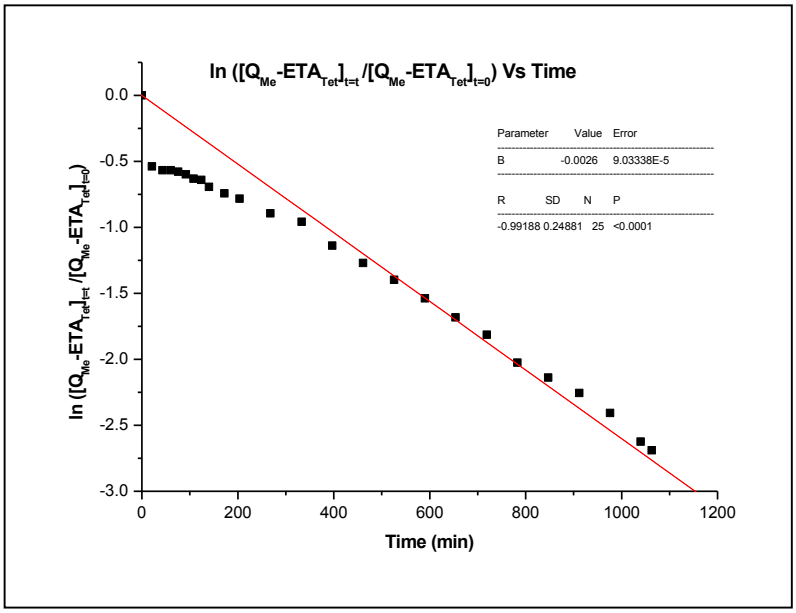

Figure 3.15: Kinetic evaluations of Q_{Me}-ETA lactonization in a 5:2 mixture of DMSO:D_2O.

3.3.1.3 Effect of Temperature

Because our main goal is to use our liposome system under biological conditions, it is important to investigate how the temperature affects the rate of lactonization. Therefore, temperature studies of Q_{Me}-ETA were performed at 10 °C, 25 °C and 35 °C in D_2O medium (Table 3.1). At 25 °C, the lactonization process was complete within 170 minutes. In theory, for

a given activated process, the rate of the reaction will increase with increasing temperature.[26] As anticipated at 35 °C, the reaction reached completion within 90 minutes, due to the increased rate of lactonization. Lowering the temperature of the system to 10 °C caused reaction to be incomplete even after 500 minutes. Raising the temperature from 25 °C to 35 °C accelerated the reaction rate by two fold, whereas lowering the temperature from 25 °C to 10 °C retarded the process roughly by four times. The rate constant (k) and half life ($t_{1/2}$) values are summarized in (Table 3.1), and the associated kinetic plots are presented in Figure 3.16. Furthermore, the activation energy for Q_{Me}-ETA lactonization in D_2O was calculated using the rate values, and it was found as 59.1 $kJmol^{-1}$.

Table 3.1: Kinetic results for Q_{Me}-ETA lactonization in D_2O medium at different temperatures. Only one replicate obtained in each case.

Temperature (°C)	**Rate constant k (min^{-1})**	**Half life $t_{1/2}$ (minutes)**
10 °C	0.0061	1.1×10^2
25 °C	0.023	30
35 °C	0.046	15

3.3.1.4 Effect of Buffer Conditions

In regards to liposome opening under physiological conditions, another avenue of study that of lactonization kinetics under buffered conditions. In a preliminary study by Cohen and Milstein, a faster intramolecular cyclization of trimethyl-lock system was observed under both acidic and basic buffered conditions. The catalysis was concurrent, but not concerted.[16,17] Amsberry *et al*. also observed the same trend under phosphate buffered conditions for model trimethyl-lock hydroxy amides.[31] Therefore, to probe this effect further, lactonization studies of Q_{Me}-ETA were conducted in 0.1 M deuterated phosphate buffer medium at 25 °C. Buffer solutions were prepared according the procedure described in Section 3.2.3 at a 7.20–7.45 pD

a)

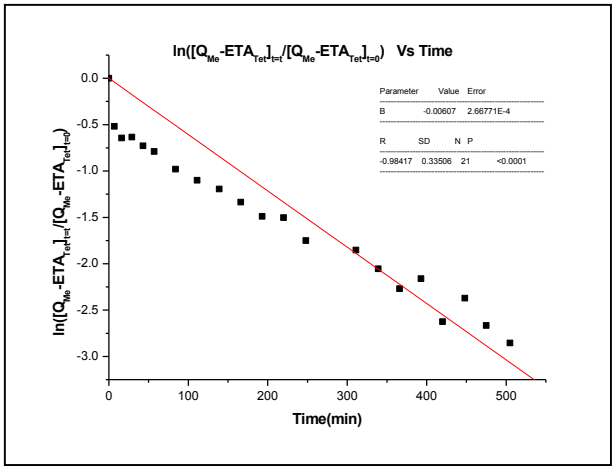

b)

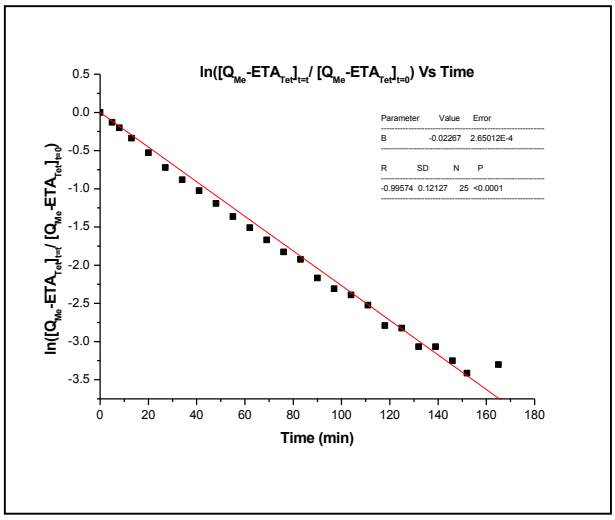

c)

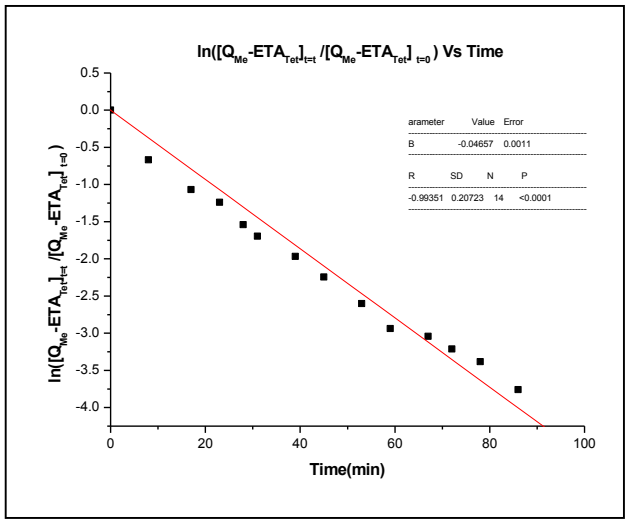

Figure 3.16: Kinetic evaluations of Q_{Me}-ETA lactonization in D_2O medium at a) 10 °C (3.6×10^{-3} M), b) 25°C (3.8×10^{-2} M), and c) 35 °C (4.3×10^{-2} M).

range, as it mimics the physiological nature to a good extent. Both studies at pD 7.41 and 7.21 reached completion after 35 to 45 minutes, with rate constants of 0.095 min^{-1}, and 0.075 min^{-1} respectively. Because the rate constants were not much different, statistical analysis (*t*-test) was conducted to find out if they differ significantly. The resulting *t* value confirmed the similarity of the rate constants at the 95 confidence level, and all results are summarized in Table 3.2 and related plots are presented in Figure 3.17 and 3.18. In addition, the presence of phosphate buffer results in more rapid cyclization kinetics, confirms the rate of cyclization is roughly four times that without buffer present (Table 3.1 and 3.2).

Table 3.2: Kinetic data for Q_{Me}-ETA lactonization in 0.1 M phosphate buffer conditions

pD	**Average Rate constant (*k*) (min^{-1})**	**Average Half life ($t_{1/2}$) (min)**	***t*-test Values**
7.41	0.081	8.6	calculated: 0.999
7.21	0.070	9.9	tabulated: 2.776

3.3.2 Lactonization Behavior of Q_{Me}-COOH

The lactonization behavior of Q_{Me}-COOH was studied in order to investigate the impact of amide presence versus free acid on the rate of lactonization. The kinetic experiment was initially performed at 25 °C in D_2O medium. The free acid (Q_{Me}-COOH) cyclized rapidly compared to its ethanolamine analog (Q_{Me}-ETA), indicating that the amide structure has a significant impact on the process. The process for Q_{Me}-COOH reached completion within 5 minutes, proving the acid autocatalysis ability of Q_{Me}-COOH. Lactone precipitated from the solution, and signals for the lactone were not present in the ^1H NMR spectrum (Figure 3.19). A lower end estimation of *k* is roughly; 0.9 min^{-1}, using 1% remaining reactant and $t_{99\%}$ = 5 min. This observation was supported by the preliminary research done by Cohen and coworkers that came to the same conclusion with respect to their orthohydroxyhydrocinnamic acid compounds.[16,17]

a)

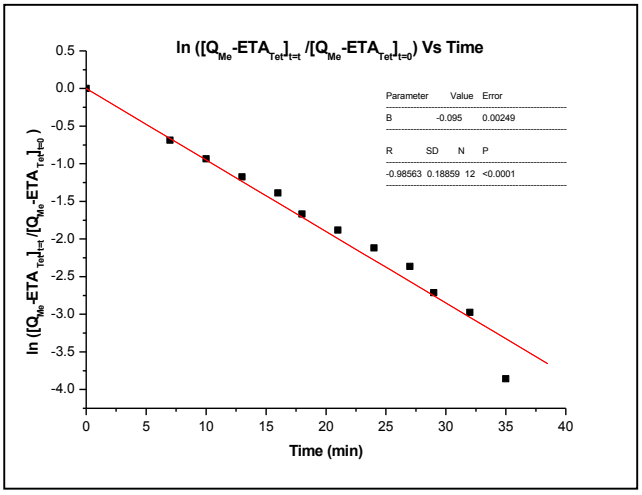

b)

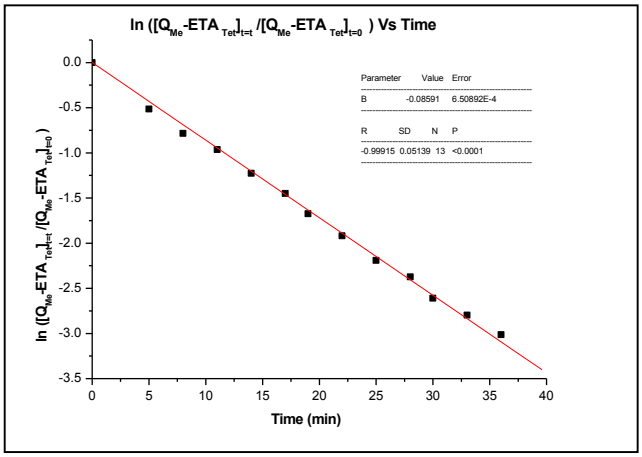

c)

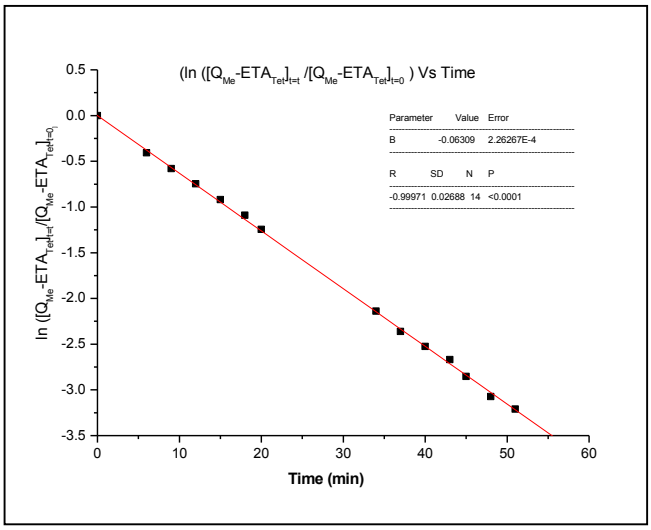

Figure 3.17: Kinetic evaluation of Q_{Me}-ETA lactonization in 0.1 M, pD 7.41 phosphate buffer medium; three replicates are shown.

a)

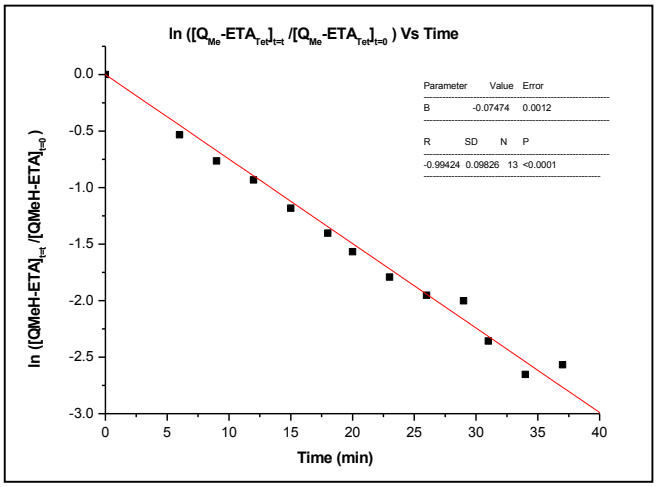

b)

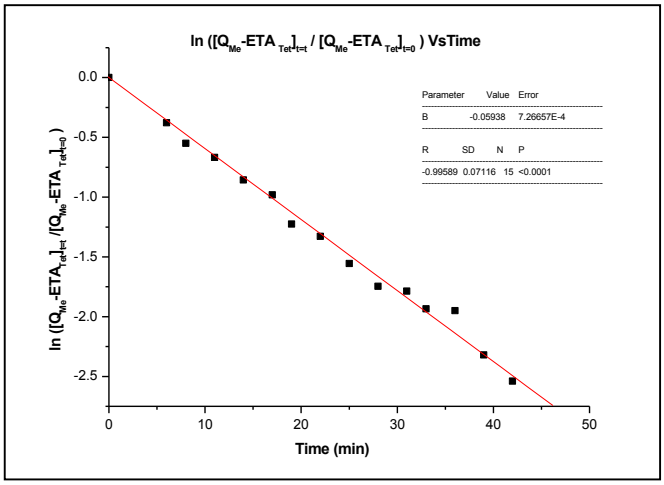

c)

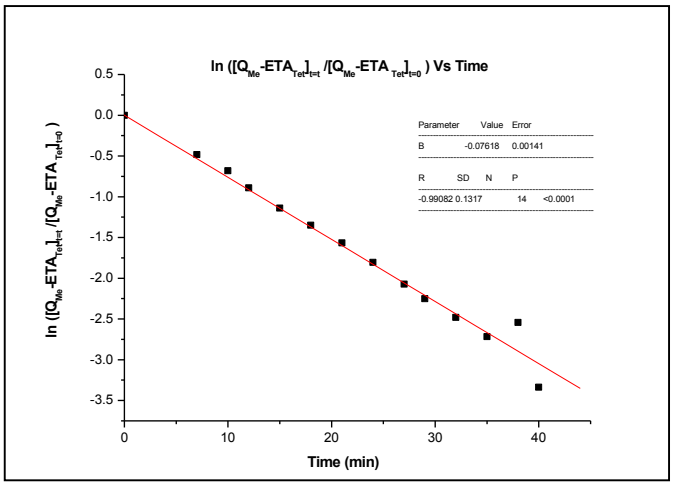

Figure 3.18: Kinetic evaluation of Q_{Me}-ETA lactonization in 0.1 M, pD 7.21 phosphate buffer medium; three replicates are shown.

Moreover, lactonization of Q_{Me}-COOH was studied in 0.1 M phosphate buffer at pD 7.41, and the reaction was completed in 3 minutes as anticipated (Figure 3 20); a lower end estimation of *k* is 1.5 min^{-1} using 1% remaining reactant and $t_{99\%}$ = 3 minutes.

3.3.3 Lactonization Behavior of Other Q_{Me}-Amide Derivatives

To further examine how the amide structure affects the rate of lactonization, studies were undertaken wherein the quinone structure was held constant, while the type of amide structure was varied. Q_{Me} was selected as the parent quinone structure, as it would be capable of providing measurable rate values.

As an initial attempt, a kinetic study of Q_{Me}-*N*-methylaminophenol (Q_{Me}-NMeBnOH, Figure 3.21 A) was conducted to determine the impact of aromatic amide on the rate of lactonization. The use of Q_{Me}-aminophenol was avoided because of its capability of forming spirolactam structures that have previously been observed by several research groups.[27-29]

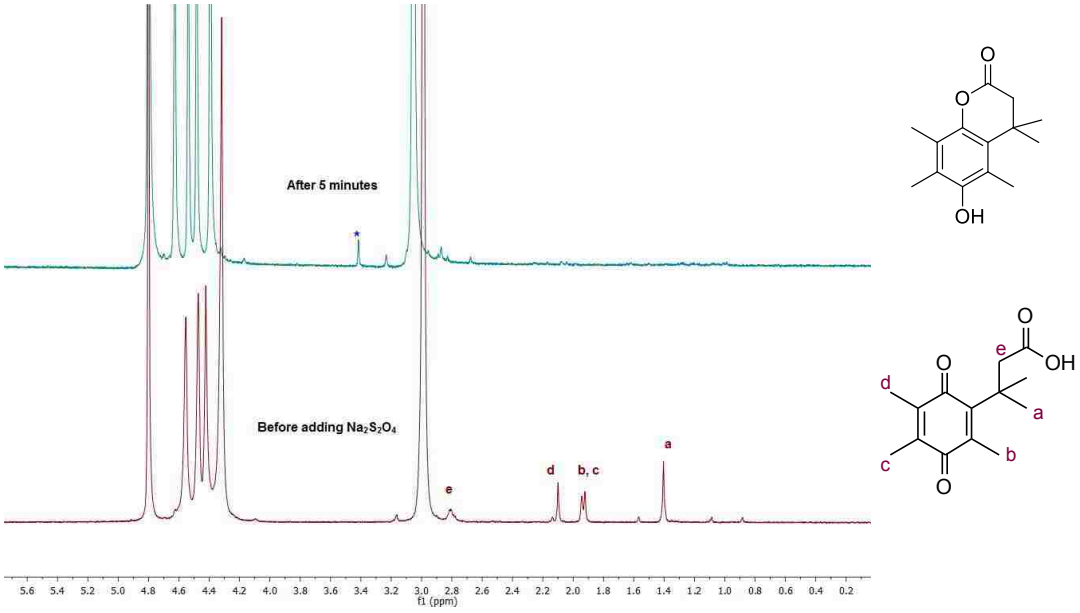

Figure 3.19: Time-dependent Q_{Me}-COOH (4.3×10^{-3} M) lactonization in D_2O medium by ^1H NMR. The signals at δ 3.00 ppm and 4.30–4.60 ppm associated with the internal standard.

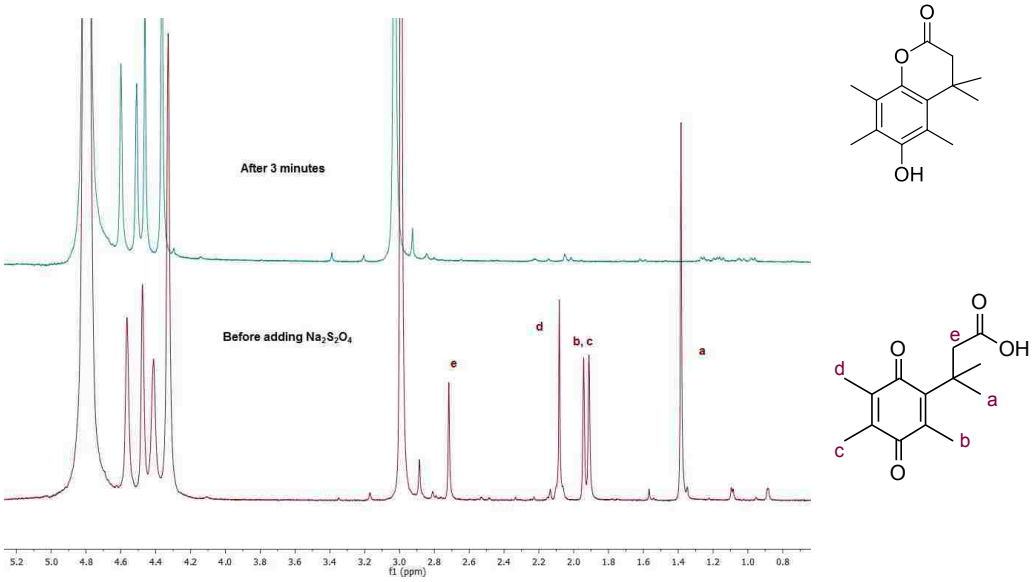

Figure 3.20: Time dependent Q_{Me}-COOH (4.7×10^{-3} M) lactonization in 0.1 M phosphate buffer at pD 7.41 by ^{1}H NMR. The signals at δ 3.00 ppm and 4.30–4.60 ppm associated with the internal standard.

The experiment was conducted in DMSO:D_2O (5:2) medium due to the poor solubility of Q_{Me}-NMeBnOH in pure D_2O; the procedure described in Section 3.2.3.2 was used. Successive spectra were collected for 60 minutes. Formation of the tetrahedral intermediate was confirmed after addition of the reducing agent, and it was stable for more than one hour, as noted by the lack of spectral changes (Figures 3.21 B, C). This confirmed the stability of the tetrahedral intermediate in the organic/aqueous medium. After 12 hours, additional peaks were detected but the cyclization process was not complete (Figure 3.21 D). However, observation after 69 hours verified completion of the process (Figure 3.21 E) where (*N*-methylamino)phenol and lactone were released to the medium, as was confirmed by the related control experiment (Figures 3.21 E, F). These specific observations confirmed the much slower rate of lactonization for Q_{Me}-NMeBnOH, revealing the tunability of the process through the variation of the amide structure.

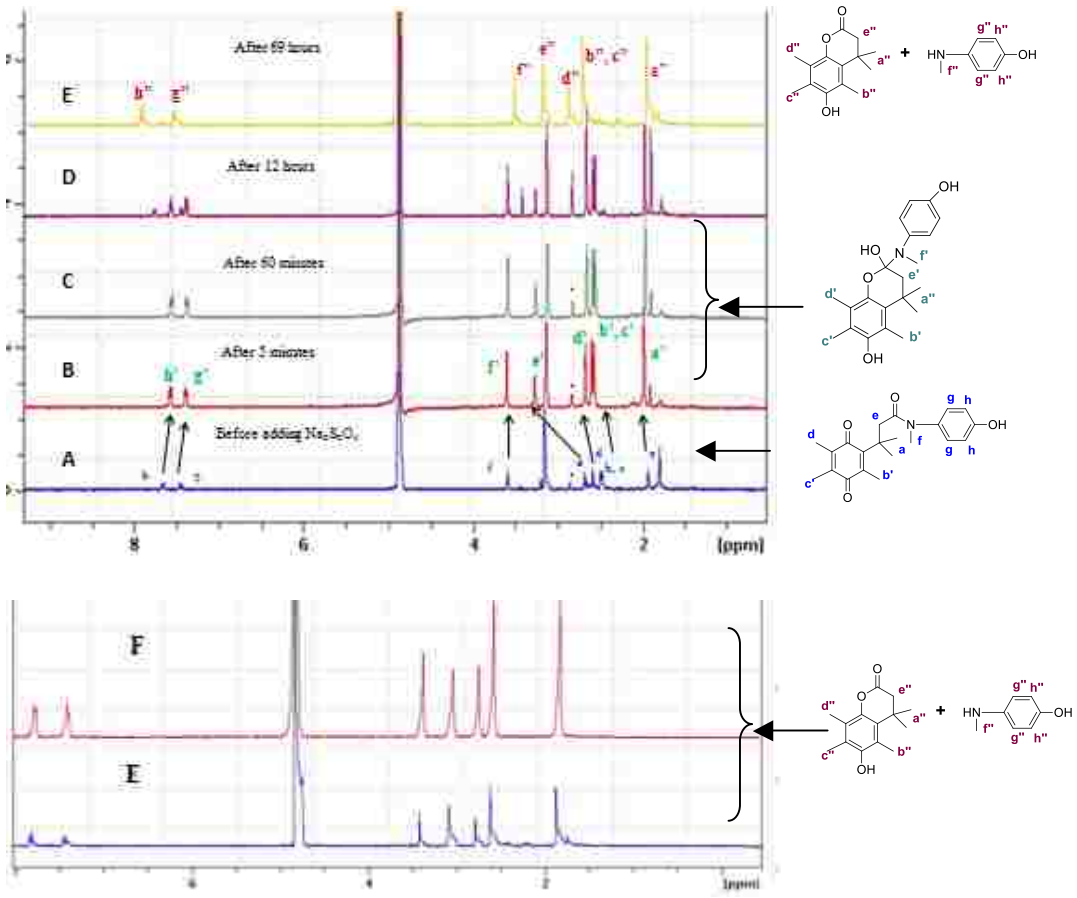

Figure 3.21: Time-dependent, Q_{Me}-NMeBnOH (4.1×10^{-3} M) lactonization in a 5:2 mixture of DMSO:D2O medium by ^{1}H NMR in the absence of internal standard.

To further assess the lactonization behavior of Q-amides through fluorescence detection, a kinetic study of Q_{Me}-NN (Scheme 3.3) was performed in DMSO:D_2O (5:2) medium. After introducing sodium dithionite, some of the initial peaks shifted downfield, while most of the peaks remained as in the previous spectrum (Figure 3.22 A and B). Successive spectra were collected for only 1 hour, and no significant changes were detected (Figure3.22 C). After nearly 12 hours, a decrease in intensity of the gem-dimethyl peak was observed, while some additional peaks appeared in the spectrum, but changes were minor (Figure 3.22 D). However, after 24 hours, the changes were significant, but the process was incomplete (Figure3.20 E). The

lactonization was much slower, and formation of relevant *NN* identified by fluorescence detection (Scheme 3.3).

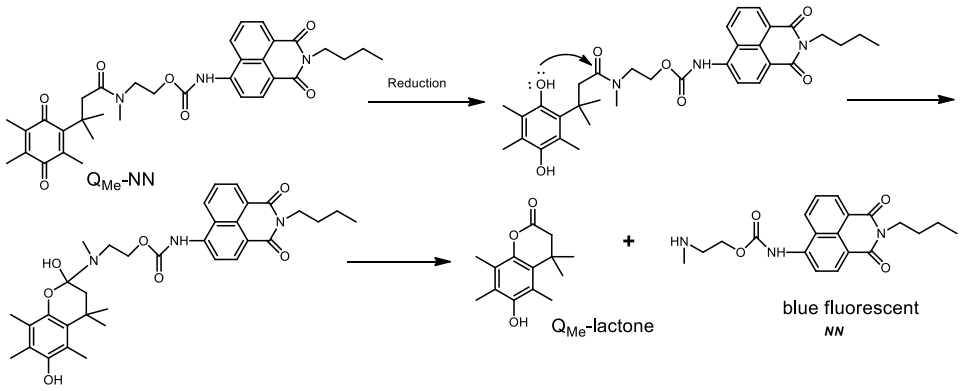

Scheme 3.3: Mechanism of Q_{Me}-NN disconnection after reduction.

From these results, it is clear that the tertiary amide structures do affect their rate of lactonization compared to simple analogues. Since both Q_{Me}-NN and Q_{Me}-NMeBnOH possesses *N*-methyl group at the amide part (Figures 3.21 and 3.22), our next concern was to study the impact from *N*-methyl functionality on this process. The Q_{Me}-methylethanolamine (Q_{Me}-MeETA) was used to study the lactonization kinetics where it showed spectral changes in different solvent conditions (Figure 3.23). The changes were significant and might be attributable for corresponding stereoisomers. However, kinetics evaluation was performed in D_2O medium due to the slower process in organic conditions which was evident from previous studies. Lactone precipitated from the solution, while methylethanolamine was released to the medium (Figure 3.24 A-E). Successive spectra were collected for 2 hours, and initial concentration changes were used for the kinetic evaluations (Figure 3.25). The rate constant (k) and $t_{1/2}$ were 0.013 min^{-1} and 53 nearly minutes, respectively, and the reaction rate constant was two times less compared to that of the Q_{Me}-ETA lactonization.

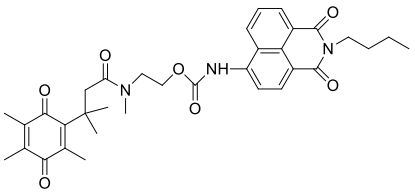

a)

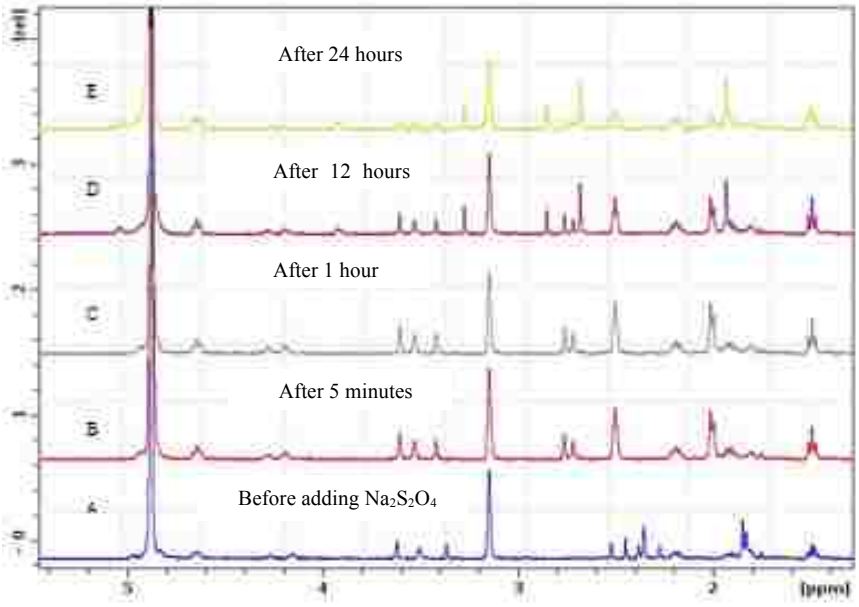

b)

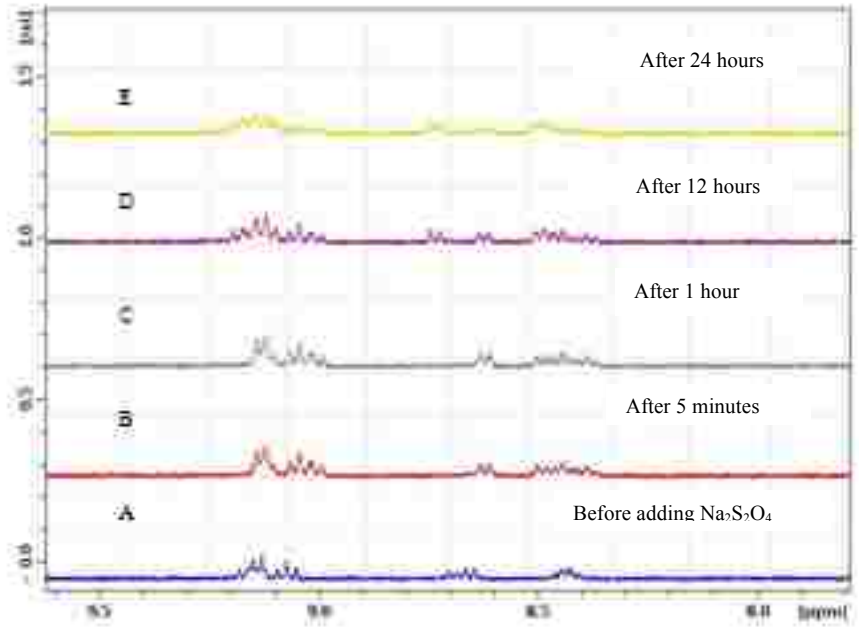

Figure 3.22: Time-dependent Q_{Me}-NN (2.4×10^{-3} M) lactonization in a 5:2 mixture of DMSO: D_2O medium by a) ^1H NMR region of 0.00– 5.50 ppm b) region of 7.50–9.75 ppm.

A)

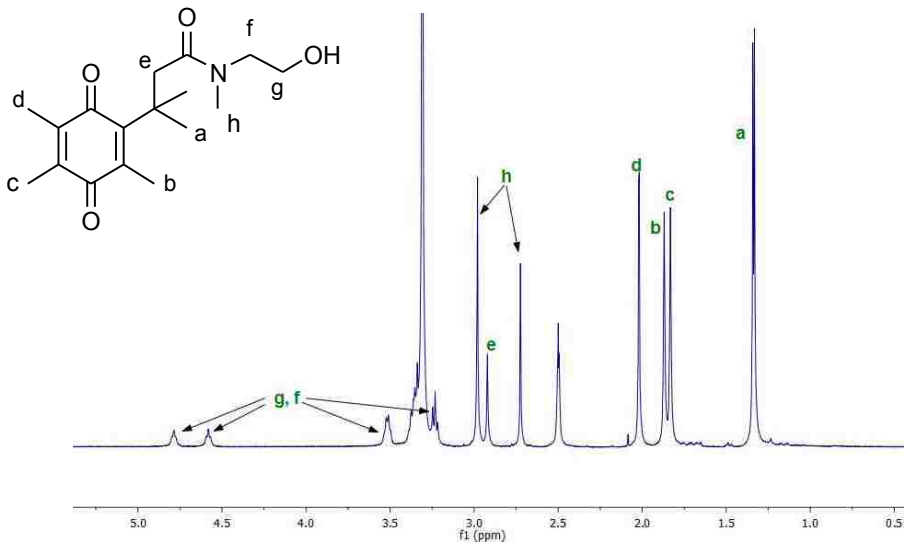

B)

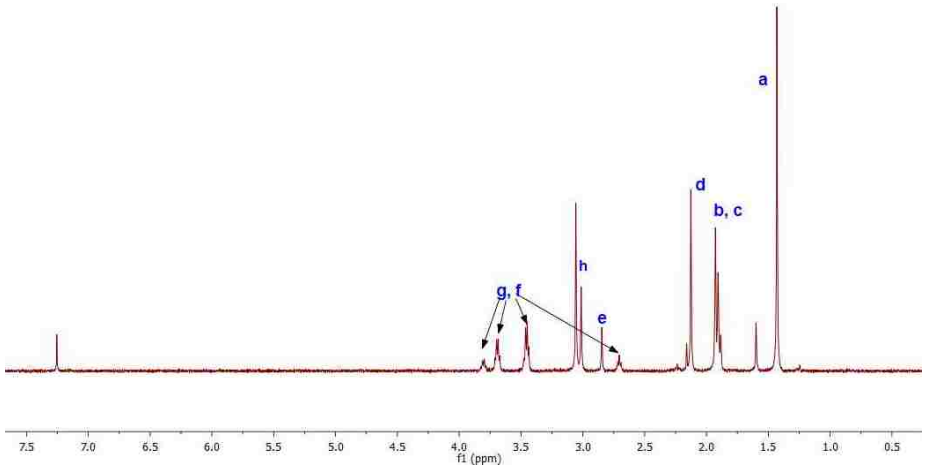

C)

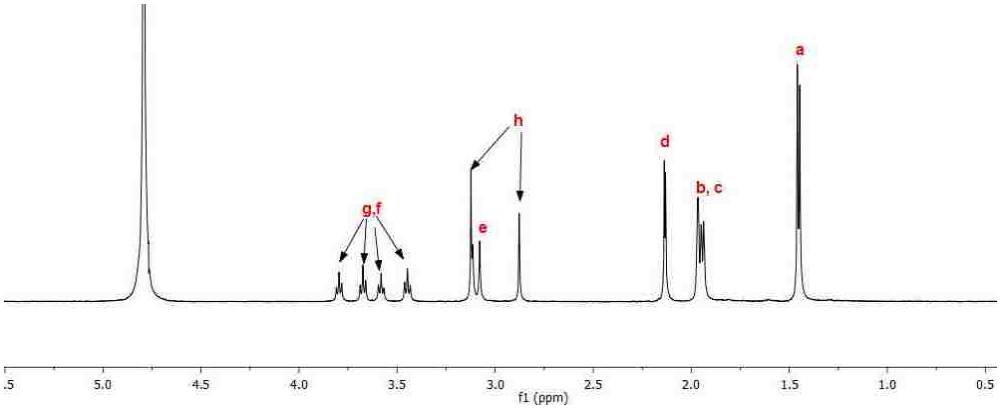

Figure 3.23: Spectral variations of Q_{Me}-MeETA in different solvents A) DMSO, B) $CDCl_3$, and C) D_2O.

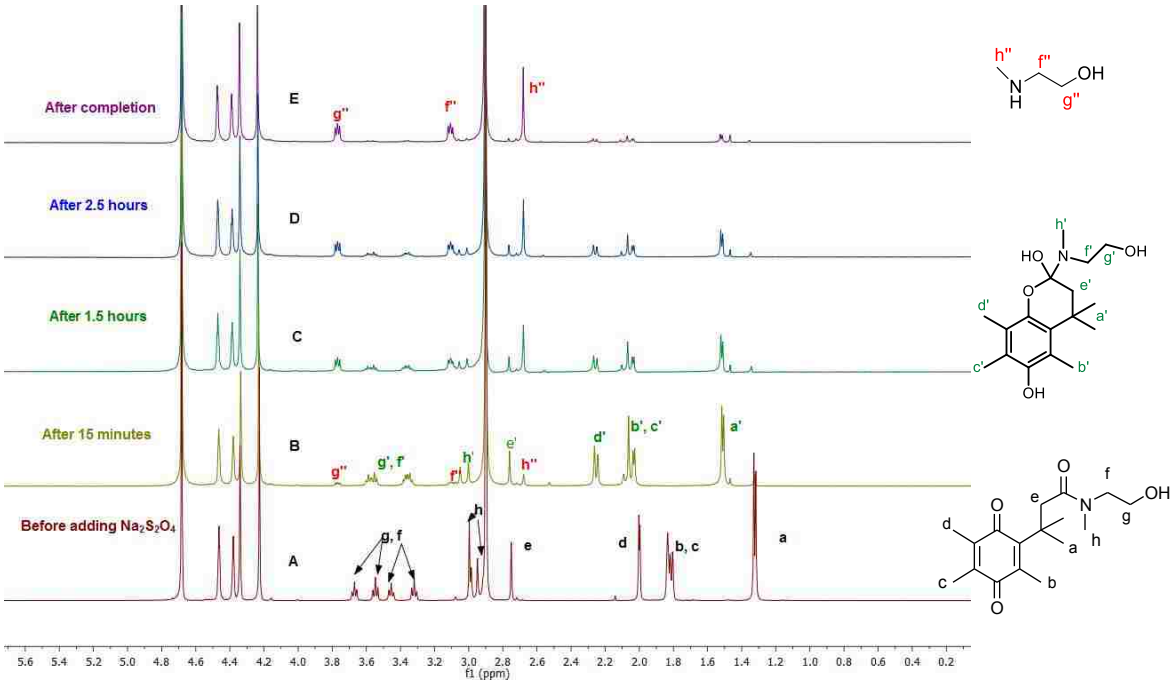

Figure 3.24: Time-dependent Q_{Me}-NMeETA (1.3×10^{-3} M) lactonization in pure D_2O medium by ^1H NMR. The signals at δ 2.90 ppm and 4.20–4.45 ppm associated with the internal standard.

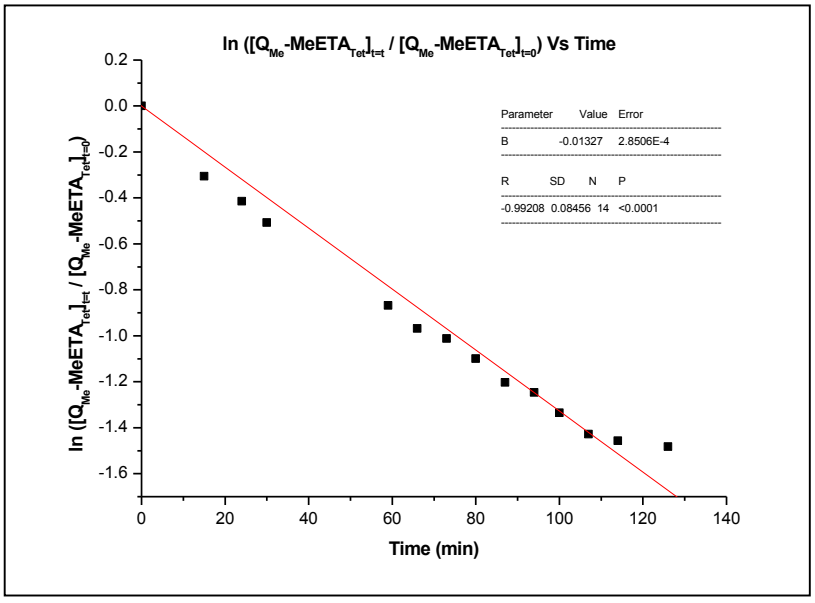

Figure 3.25: Kinetic evaluation of Q_{Me}-MeETA (1.3×10^{-3} M) lactonization in pure D_2O medium.

3.4 Conclusion

The reduction and lactonization behavior of eight different trimethyl-lock quinone propionic acid derivatives were investigated by ^{1}H NMR spectroscopy; the outcomes are summarized in Table 3.3. In all amides except Br, NPr, and NMe on quinone ring, upon addition of reducing agent, tetrahedral intermediate was formed, as noted by peaks shifted down field with respect to their original spectra. Lactonization profiles of Q-ETA compounds revealed different lifetimes, indicating that 3′ quinone substitution can be utilized to tune the rate of lactonization. In D_2O, upon addition of the reducing agent ($Na_2S_2O_4$), Q_{Br}-ETA, Q_{NMe}-ETA, and Q_{NPr}-ETA lactonized rapidly, while Q_H-ETA showed a much slower intramolecular cyclization. The rapid lactonization behavior for Q_{Br}-ETA can be attributed to the electron withdrawing nature of bromine, while for the others, the internal base catalysis behavior of *N*-propylamino and *N*-methylamino nitrogen atom accelerated the cyclization.[8] The rate for Q_{Me}-ETA was moderate and the rate constant (k) and half life ($t_{1/2}$) were calculated successfully.

The rate of lactonization of Q_{Me}-ETA was found to vary with temperature, buffer, and solvent conditions. The existence of buffer conditions and increasing temperature accelerated cyclization, whereas the presence of organic solvent made the lactonization slower, caused by enhanced stability of the tetrahedral intermediate. The Q_{Me}-COOH cyclization was much faster compared to the Q_{Me}-ETA derivative, due to its autocatalysis behavior. Inclusion of secondary amide structures with the NMe functionality shows that the cyclization process was retarded compared to simple amide structures.

These findings are supported by previous electrochemical and liposome payload release studies.[8,30] Careful selection of quinone-amide structures and experimental conditions can be utilized to optimize the liposome system for future applications.

Table 3.3: Summary of kinetic Evaluation.

Quinone-Amide	Solvent	k (min^{-1})	$t_{½}$(min)
Q_{Me}-ETA	D_2O	0.023	30
Q_{Br}-ETA	D_2O	≥ 0.9	-
Q_{NMe}-ETA	D_2O	≥ 1.5	-
Q_{NPr}-ETA	D_2O	≥ 1.5	-
Q_{H}-ETA	D_2O	Infeasible calculation	-
Q_{Me}-ETA	DMSO:D_2O (5:2)	0.0026	2.7×10^2
Q_{Me}-ETA (10 °C)	D_2O	0.0061	1.1×10^2
Q_{Me}-ETA (35 °C)	D_2O	0.046	15
Q_{Me}-ETA	(0.1 M Phosphate buffer, pD 7.85)	0.081	8.6
Q_{Me}-ETA	(0.1 M Phosphate buffer, pH 7.64)	0.070	9.9
Q_{Me}-COOH	D_2O	≥ 0.9	-
Q_{Me}-COOH	(0.1 M Phosphate buffer pH 7.85)	≥ 1.3	-
Q_{Me}-NMeBnOH	DMSO:D_2O (5:2)	Much slower process	-
Q_{Me}-NN	DMSO:D_2O (5:2)	Much slower process	-
Q_{Me}-NMeETA	D_2O	0.013	53

***Note:** All reactions were conducted in 25 ° C except as noted.

3.5 References

(1) Drummond, D. C.; Noble, C. O.; Hayes, M. E.; Park, J. W.; Kirpotin, D. B. Pharmacokinetics and in vivo drug release rates in liposomal nanocarrier development. *Journal of Pharmaceutical Sciences* **2008**, *97*, 4696-4740.

(2) Blanche, E. A.; Maskell, L.; Colucci, M. A.; Whatmore, J. L.; Moody, C. J. Synthesis of potential prodrug systems for reductive activation. Prodrugs for anti-angiogenic isoflavones and VEGF receptor tyrosine kinase inhibitory oxindoles. *Tetrahedron* **2009**, *65*, 4894-4903.

(3) Andresen, T. L.; Jensen, S. S.; Kaasgaard, T.; Jorgensen, K. Triggered activation and release of liposomal prodrugs and drugs in cancer tissue by secretory phospholipase A2. *Current Drug Delivery* **2005**, *2*, 353-362.

(4) Budker, V.; Gurevich, V.; Hagstrom, J. E.; Bortzov, F.; Wolff, J. A. pH-sensitive, cationic liposomes: A new synthetic virus-like vector. *Nature Biotechnology* **1996**, *14*, 760-764.

(5) Sawant, R. R.; Torchilin, V. P. Liposomes as 'smart' pharmaceutical nanocarriers. *Soft Matter* **2010**, *6*, 4026-4044.

(6) Johnston, M. J. W.; Semple, S. C.; Klimuk, S. K.; Edwards, K.; Eisenhardt, M. L.; Leng, E. C.; Karlsson, G.; Yanko, D.; Cullis, P. R. Therapeutically optimized rates of drug release can be achieved by varying the drug-to-lipid ratio in liposomal vincristine formulations. *Biochimica et Biophysica Acta (BBA) - Biomembranes* **2006**, *1758*, 55-64.

(7) Kaasgaard, T.; Andresen, T. L. Liposomal cancer therapy: exploiting tumor characteristics. *Expert Opinion on Drug Delivery* **2010**, *7*, 225-243.

(8) Carrier, N. H. Redox-Active Liposome Delivery Agents with Highly Controllable Stimuli-Responsive Behavior. Ph.D Dissertation, Louisiana State University, Baton Rouge, LA. 2011.

(9) Gabizon, A.; Shmeeda, H.; Barenholz, Y. Pharmacokinetics of Pegylated Liposomal Doxorubicin: Review of Animal and Human Studies. *Clinical Pharmacokinetics* **2003**, *42*, 419-436.

(10) Georgiadis, M. S.; Russel, E. K.; F, G. A. Paclitaxel cCytotoxicity against human lung cancer cell lines increase with prolonged exposure durations. *Clinical Cancer Research* **1997**, *3*, 449-454.

(11) Drummond, D. C.; Noble, C. O.; Guo, Z.; Hong, K.; Park, J. W.; Kirpotin, D. B. Development of a Highly Active Nanoliposomal Irinotecan Using a Novel Intraliposomal Stabilization Strategy. *Cancer research* **2006**, *66*, 3271-3277.

(12) Carpino, L. A.; Triolo, S. A.; Berglund, R. A. Reductive lactonization of strategically methylated quinone propionic acid esters and amides. *The Journal of Organic Chemistry* **1989**, *54*, 3303-3310.

(13) Berglund, R. A. Bioreductive Heterosubstituted Quinne Antitumor Drug Delivery Agents. Ph.D. Dissertation, University of Massachusetts, 1987.

(14) Triolo, S. A. Quinone Amides Potentially Capable of Selective Delivery of Antitumor Drugs by Redox Control. Ph.D. Dissertation, University of Massachusetts, 1986.

(15) Ong, W.; Yang, Y.; Cruciano, A. C.; McCarley, R. L. Redox-Triggered Contents Release from Liposomes. *Journal of the American Chemical Society* **2008**, *130*, 14739-14744.

(16) Milstien, S.; Cohen, L. A. Rate Acceleration by Stereopopulation Control: Models for Enzyme Action. *Proceedings of the National Academy of Sciences* **1970**, *67*, 1143-1147.

(17) Milstien, S.; Cohen, L. A. Stereopopulation control. I. Rate enhancement in the lactonizations of o-hydroxyhydrocinnamic acids. *Journal of the American Chemical Society* **1972**, *94*, 9158-9165.

(18) King, M. M.; Cohen, L. A. Stereopopulation control. VII. Rate enhancement in the lactonization of 3-(o-hydroxyphenyl)propionic acids: dependence on the size of aromatic ring substituents. *Journal of the American Chemical Society* **1983**, *105*, 2752-2760.

(19) Hillery, P. S.; Cohen, L. A. Stereopopulation control. 9. Rate and equilibrium enhancement in the lactonization of (o-hydroxyphenyl)acetic acids. *The Journal of Organic Chemistry* **1983**, *48*, 3465-3471.

(20) Caswell, M.; Schmir, G. L. Formation and hydrolysis of lactones of phenolic acids. *Journal of the American Chemical Society* **1980**, *102*, 4815-4821.

(21) Nunez, O.; Campo, F. D. Direct Determintion of the Rate of Breakdown of a Breakdown of a stable tetrahedral intermediate by Dynamic NMR. *Acta Cientifica Venezolana* **1989**, *40*, 301-302.

(22) McKenna, C. E.; Gutheil, W. G.; Song, W. A method for preparing analytically pure sodium dithionite. Dithionite quality and observed nitrogenase-specific activities. *Biochimica Biophysica Acta* **1991**, *1075*, 109-117.

(23) Ong, W.; McCarley, R. L. Redox-driven shaving of dendrimers. *Chemical Communications* **2005**, 4699-4701.

(24) Balamayuran, S.; McCarley, R. L.; Manuscript in Preparation.

(25) Atkins, P. W. *Physical Chemistry Atkins*; 6th edition.; Oxford University Press, **1998**, pages 767-769.

(26) Wright, M. R. *An introduction to chemical kinetics*; Jhon Wiley & Sons Ltd, **2004**, pages 58-93.

(27) Wolfe, J. L.; Vander Velde, D.; Borchardt, R. T. Facilitated intramolecular conjugate addition of N-(p-methoxyphenyl)-3-(3',6'-dioxo-2',4'-dimethylcyclohexa-1',4'-dienyl)-3,3-

dimethylpropionamide. 1. Product characterization. *The Journal of Organic Chemistry* **1992**, *57*, 6138-6142.

(28) Liu, S.; Wang, B.; Nicolaou, M. G.; Borchardt, R. T. "Trimethyl lock" facilitated spirocyclizations: A structural analysis. *Journal of Chemical Crystallography* **1996**, *26*, 209-214.

(29) Nicolaou, M. G.; Wolfe, J. L.; Schowen, R. L.; Borchardt, R. T. Facilitated Intramolecular Conjugate Addition of Amides of 3-(3‘,6‘-Dioxo-2‘,4‘-dimethyl-1‘,4‘-cyclohexadienyl)-3,3-dimethylpropionic Acid. 2. Kinetics of Degradation. *The Journal of Organic Chemistry* **1996**, *61*, 6633-6638.

(30) Mendoza, M. F. Characterization of Triggerable Quinones for the Development of Enzyme-Responsive Liposomes. Dissertation, Lousiana State University, Baton Rouge, LA. 2012.

(31) Amsberry, K. L.; Borchardt, R. T. The lactonization of 2'-hydroxyhydrocinnamic acid amides: a potential prodrug for amines. *The Journal of Organic Chemistry* **1990**, *55*, 5867-5877.

CHAPTER 4
CONCLUSIONS AND OUTLOOK

4.1 Summary

The overall goal of this research was to investigate the kinetics of reduction and lactonization of trimethyl-lock quinone propionic acids and their amide derivatives, in order to optimize our recently developed redox-active liposome drug delivery system.[1-3] Upon interaction with a redox stimulus, trimethyl-lock quinone head groups undergo intramolecular lactonization to initiate liposomal disintegration. Thus, evaluation of lactonization kinetics with respect to diverse quinone-amide structures and experimental conditions is important, because the outcomes can be used to tailor the liposomal payload release.

Seven different trimethyl-lock quinone propionic acid derivatives were synthesized by varying either the amide structure or the 3′ functionality of the quinone head group: Q_{Me}-ETA, Q_{Br}-ETA, Q_{NMe}-ETA, Q_{NPr}-ETA, Q_{H}-ETA, Q_{Me}-MeETA, and Q_{Me}-NMeBnOH. The synthesis of quinone-amide followed a similar procedure where they were prepared from corresponding *N*-hydroxysuccinimide derivative and were obtained in good yield. These quinone-amides were then subjected to chemical reduction, and their lactonization behavior was followed by ^{1}H NMR spectroscopy. The gem-dimethyl integrals were used to evaluate the kinetics, and it was found that lactonization was much slower compared to the reduction. Lactonization occurred through tetrahedral intermediate collapse and followed first order kinetics. Initially, lactonization behavior of different Q-ETA compounds were studied in D_2O; from fastest to slowest, the average lifetime values for complete lactonization are as follows: Q_{NMe}-ETA (3 min), Q_{NPr}-ETA (3 min), Q_{Br}-ETA (5 min), Q_{Me}-ETA (170 min) and Q_{H}-ETA (> 6 hours). From these results, it is evident that the 3′ functionality of the quinone ring does affect the lactonization and these can be selectively incorporated to liposome systems to control their payload release.

Because Q_{Me}-ETA has shown measurable lactonization profile, its rate constant *k*: 0.023 min^{-1} and $t_{1/2}$ of 30 were calculated and employed for further studies. In organic/aqueous medium (DMSO:D_2O), it was found that the tetrahedral intermediate was somewhat stable after its formation from reduction, resulting in a 9 times slower lactonization when compared to 100% aqueous conditions. Increasing the experimental temperature enhanced the rate of lactonization (at 35 °C, k = 0.046 min^{-1} and $t_{1/2}$ = 15) whereas lowering the temperature created hostile conditions for the process and the reaction continued for an extended period of time (at 10 °C, k = 0.0061 min^{-1} and $t_{1/2}$ = 1.1×10^2). Experiments in buffer environment also exhibited accelerated lactonization. However, alteration of buffer pD from 7.21 to 7.41 did not significantly influence the lactonization rate constant.

After identifying the behavior of Q-ETA derivatives, research was focused toward the investigation of the cyclization nature of other quinone propionic amide derivatives: Q_{Me}-MeETA, Q_{Me}-NMeBnOH and Q_{Me}-NN. Interestingly, in organic medium (DMSO:D_2O = 5:2), the tetrahedral intermediate of both Q_{Me}-NMeBnOH and Q_{Me}-NN were stable for more than 1 hour, resulting in an extremely slower lactonization where the process took more than 24 hours to complete. Finally, to assess the effect of the secondary amide functionality in the amide structure, kinetic study on Q_{Me}-MeETA was performed in D_2O medium, and it was observed that the rate constant for lactonization was 2 times slower when compared to the Q_{Me}-ETA derivative.

4.2 Conclusion

The results presented in this thesis demonstrate the capability of tuning the lactonization process of trimethyl-lock quinone propionic acid derivatives upon interaction with a redox stimulus. Synthesis of quinone-amide derivatives followed a common methodology and products were obtained in good yield. With the addition of different substituents onto the 3′

position of the quinone head group, lactonization rates were significantly varied, which was in agreement with previously studied liposome payload release profiles.[2] The rate of lactonization was influenced by changes in temperature, buffer, and solvent conditions. Tertiary quinone-amide structures exhibited slower rates of lactonization while the opposite was observed with secondary structures. Inclusion of the NMe functionality to the amide structure, slows down the lactonization process significantly. Modification of trimethyl-lock quinone based liposomes through of tertiary amide structures enables to have slower payload release profiles which is highly important in chemotherapy.

4.3 Outlook

A growing number of stimuli-responsive liposomal formulations that can selectively deliver chemotherapeutics to the tumor site by taking advantage of over-expressed tumor reductive enzymes are becoming of great interest in modern drug delivery.[4-6] To that end, redox-responsive, quinone trimethyl-lock liposome (Q-DOPE) system has been developed where the liposomal destruction is initiated upon reduction and lactonization of the quinone head group.[1-3]

According to the literature, most of the chemotherapeutic agents exhibit their maximum antitumor activity, when they are distributed slower to intermediate rates within the tumor site.[7,8] Thus, details provided in this thesis could be useful to design new Q-DOPE liposomes and quinone based prodrugs by incorporating proper trimethyl-lock quinone head group as well as modified amide structures in order to attain slower to medium rate of drug release. In 1982, Cohen and Michael have shown that replacement of the methyl group at the 6′ position of the benzene ring with varying functionalities resulted in significant changes of lactonization rates for their 4,4–dimethyl–6–hydroxyhydrocoumarrins compounds.[9] Moreover, Jung and Piizzi pointed out the feasibility of lactonization of Potassium ω-Bromoalkanoate with bulky gem-dialkyl

groups.[10] Thus, it is important to investigate the feasibility of lactonization of quinone-amides having different gemdialkyls as well as different functional groups at 6′ position in order to develop new liposome formulations having enhanced pharmacokinetics. Furthermore, the results of this study can be used to develop other stimuli-sensitive trimethyl-lock systems (sensors, microfludic channels etc) to obtain an efficient cargo delivery.

4.4 References

(1) Ong, W.; Yang, Y.; Cruciano, A. C.; McCarley, R. L. Redox-Triggered Contents Release from Liposomes. *Journal of the American Chemical Society* **2008**, *130*, 14739-14744.

(2) Carrier, N. H. Redox-Active Liposome Delivery Agents with Highly Controllable Stimuli-Responsive Behavior. Ph.D Dissertation, Louisiana State University, Baton Rouge, LA. 2011.

(3) Forsythe, J. Kinetics and Mechanisms of Release by Redox-Active Liposomes in Drug Delivery. Ph.D Dissertation, Louisiana State University, Baton Rouge, LA. 2011.

(4) Blanche, E. A.; Maskell, L.; Colucci, M. A.; Whatmore, J. L.; Moody, C. J. Synthesis of potential prodrug systems for reductive activation. Prodrugs for anti-angiogenic isoflavones and VEGF receptor tyrosine kinase inhibitory oxindoles. *Tetrahedron* **2009**, *65*, 4894-4903.

(5) Andresen, T. L.; Jensen, S. S.; Kaasgaard, T.; Jorgensen, K. Triggered activation and release of liposomal prodrugs and drugs in cancer tissue by secretory phospholipase A2. *Current Drug Delivery* **2005**, *2*, 353-362.

(6) Terada, T.; Iwai, M.; Kawakami, S.; Yamashita, F.; Hashida, M. Novel PEG-matrix metalloproteinase-2 cleavable peptide-lipid containing galactosylated liposomes for hepatocellular carcinoma-selective targeting. *Journal of Controlled Release* **2006**, *111*, 333-342.

(7) Johnston, M. J. W.; Semple, S. C.; Klimuk, S. K.; Edwards, K.; Eisenhardt, M. L.; Leng, E. C.; Karlsson, G.; Yanko, D.; Cullis, P. R. Therapeutically optimized rates of drug release can be achieved by varying the drug-to-lipid ratio in liposomal vincristine formulations. *Biochimica et Biophysica Acta (BBA) - Biomembranes* **2006**, *1758*, 55-64.

(8) Georgiadis, M. S.; Russel, E. K.; F, G. A. Paclitaxel cCytotoxicity against human lung cancer cell lines increase with prolonged exposure durations. *Clinical Cancer Research* **1997**, *3*, 449-454.

(9) King, M. M.; Cohen, L. A. Stereopopulation control. VII. Rate enhancement in the lactonization of 3-(o-hydroxyphenyl)propionic acids: dependence on the size of aromatic ring substituents. *Journal of the American Chemical Society* **1983**, *105*, 2752-2760.

(10) Jung, M. E.; Piizzi, G. gem-Disubstituent Effect: Theoretical Basis and Synthetic Applications. *Chemical Reviews* **2005**, *105*, 1735-1766.

VITA

Karannagoda Liyanage Iresha Sampathi Perera was born in Colombo, Sri Lanka. She had her primary and secondary education at Anula Vidyalaya, Colombo. She entered the University of Colombo in year 2004 and was selected for a special degree in chemistry in 2006. She received her Bachelor of Science degree in chemistry in 2008 with Honors. After working for one year as a teaching assistant at the Department of Chemistry of University of Colombo, she enrolled in the master's programme in the Department of Chemistry at Louisiana State University in fall 2009. In summer 2010 she joined the laboratory of Prof. Robin L. McCarley. The Master of Science degree will be conferred at the summer 2012 commencement.